# Portrait of blood-derived extracellular vesicles in patients with Parkinson's disease

Jérôme Lamontagne-Proulx, MSc[1], Isabelle St-Amour, PhD[1], Richard Labib, PhD[2], Jérémie Pilon, BSc[2], Hélèna L. Denis, MSc[1], Nathalie Cloutier, PhD[1], Florence Roux-Dalvai, MSc[1], Antony T. Vincent, MSc[3], Sarah L. Mason, PhD[4], Anne-Claire Duchez, PhD[1], Arnaud Droit, PhD[1,5], Steve Lacroix, PhD[1,5], Nicolas Dupré, MD[1,6], Mélanie Langlois, MD[1,6], Sylvain Chouinard, MD[7], Michel Panisset, MD[7], Roger A. Barker, MBBS, PhD[4], Eric Boilard, PhD[1,8*], Francesca Cicchetti, PhD[1,9*]

[1]Centre de recherche du CHU de Québec, Québec, QC, Canada; [2]Département de mathématiques et génie industriel, École Polytechnique de Montréal, Montréal, QC, Canada; [3]Institut de Biologie Intégrative et des Systèmes, Université Laval, Québec, QC, Canada; [4]Department of Clinical Neurosciences, John van Geest Centre for Brain Repair, University of Cambridge, Cambridge, United Kingdom; [5]Département de médecine moléculaire, Université Laval, Québec, QC, Canada; [6]Département de médecine, Université Laval, Québec, QC, Canada; Département de neurosciences, Hôpital de l'Enfant-Jésus, Québec, QC, Canada; [7]Centre Hospitalier de l'Université de Montréal and Centre de recherche du Centre Hospitalier de l'Université de Montréal, Hôpital Notre-Dame, Département de médicine, Université de Montréal, Montréal, QC, Canada; [8]Département de microbiologie-infectiologie et d'immunologie, Université Laval, Québec, QC, Canada; [9]Département de psychiatrie & neurosciences, Université Laval, Québec, QC, Canada

**Correspondence to either:**

Francesca Cicchetti, Ph.D.
Centre de Recherche du CHU de Québec
Axe Neurosciences, T2-07
2705, Boulevard Laurier
Québec, QC, G1V 4G2, Canada
Tel #: (418) 656-4141 ext. 48853
Fax #: (418) 654-2753
E-mail: Francesca.Cicchetti@crchul.ulaval.ca

Eric Boilard, Ph.D.
Centre de Recherche du CHU de Québec
Infectious and immune diseases, T1-49
2705, Boulevard Laurier
Québec, QC, G1V 4G2, Canada
Tel #: (418) 656-4141 ext. 46175
Fax #: (418) 654-2765
E-mail: Eric.Boilard@crchudequebec.ulaval.ca

**Financial disclosure**: F.C., E.B., S.L. and I.S.-A. have filed a patent on the use of EEV as a biomarker in PD. J.L.P., R.L., J.P., H.L.D., N.C., F.R.-D., A.T.V., S.L.M., A-C.D., A.D., S.L., N.D., M.L., S.C. and R.A.B. declare no conflicts of interest.

**Funding sources**: The study was funded by The Michael J. Fox foundation and the Parkinson Society Canada to F.C. as main PI who is also a recipient of a Researcher Chair from the Fonds de Recherche du Québec en santé (FRQS) providing salary support and operating funds. I.S.-A. was supported by a CIHR-Huntington Society of Canada postdoctoral fellowship. R.B. and J.P. are supported by the Natural Science and Engineering Research Council of Canada (NSERC). R.A.B. and S.L.M. are supported by a National Institute for Health Research (NIHR) award of a Biomedical Research Center to the University of Cambridge and Addenbrooke's Hospital. RAB is an NIHR Senior Investigator. HLD hold a Desjardins scholarship from the Fondation du CHU de Québec. A.-C.D. is supported by the Fonds de Recherche des maladies Rhumatismales de l'Université Laval and the Canadian Arthritis Network. E.B. is supported by the Canadian Institutes of Health Research. N.D. MD-MSc are also funded by CIHR and by Canadian Consortium on Neurodegeneration in Aging (CCNA).

**ABSTRACT**

The production of extracellular vesicles (EV) is a ubiquitous feature of eukaryotic cells but pathological events can affect their formation and constituents. We sought to characterize the nature, profile and protein signature of EV in the plasma of Parkinson's disease (PD) patients and how they correlate to clinical measures of the disease. EVs were initially collected from cohorts of PD (n=60; Controls, n=37) and Huntington's disease (HD) patients (Pre-manifest, n=11; manifest, n=52; Controls, n=55) – for comparative purposes in patients with another chronic neurodegenerative condition – and exhaustively analyzed using flow cytometry, electron microscopy and proteomics. We then collected 42 samples from an additional independent cohort of PD patients to confirm our initial results. Through a series of iterative steps, we optimized an approach for defining the EV signature in PD. We found that the number of EV derived specifically from erythrocytes segregated with UPDRS scores corresponding to different disease stages. Proteomic analysis further revealed that there is a specific signature of proteins that could reliably differentiate control subjects from mild and moderate PD patients. Taken together, we have developed an EV blood-based assay that has the potential to be used as a biomarker for PD.

**Key words:** Blood cells; Erythrocytes; Extracellular vesicles; Alpha-synuclein

**HIGHLIGHTS:**

- Optimization of methodology to identify extracellular vesicles (EV) using FACS
- Demonstration of minimal test-retest variability intra-patient using FACS
- Development of a new approach to uncover the entire proteome of EV
- Segregation of Parkinson's disease patients with EV from erythrocytes (EEV) count
- EEV protein signature differentiates control from Parkinson's disease patients

**ABREVATIONS**

EV: Extracellular vesicles,

EEV: Extracellular vesicles derived from erythrocytes

LEDD: levodopa equivalent daily dose

UPDRS: Unified Parkinson Disease Rating Scale

**INTRODUCTION**

The last few years of research has seen our understanding of Parkinson's disease (PD) change dramatically. One of the major breakthroughs has been the realization that PD is a heterogeneous disorder, which brings with it challenges for the development and identification of useful biomarkers for diagnosis and disease progression, as well as the ability to track the successful translation of novel treatments to the clinic. This new understanding of the different clinical profiles seen in populations of PD patients has begun to translate into a redefinition of PD, as is evidenced by new diagnostic criteria released by the International PD and Movement Disorder Society (MDS) (Berg et al., 2014). This task force has also pointed out the importance of identifying reliable biomarkers for clinico-pathological diagnoses. Indeed, the development of a biomarker that could serve as a diagnostic tool, and/or a dependable predictor of disease course and evolution (and thus stratify populations of patients) as well as to assess treatment efficacy is of critical importance and urgently needed.

The search for such biomarkers has recently included the investigation of extracellular vesicles (EV); small entities that carry critical intracellular molecules and which mediate cell-to-cell communication in both physiological and disease conditions (Quek and Hill, 2017). EV are composed of membrane proteins and lipids, as well as cytoplasmic components of the cell from which they originate, such as mRNA and miRNA, organelles or infectious particles (e.g. prions, virus) (Porro et al., 2015). Their protein cargo, cell signature and availability in bodily fluids make EV very attractive candidate biomarkers and have already been studied in the blood, cerebrospinal fluid (CSF), urine and brains of patients with PD (see **Figure S1**) (Abd-Elhadi et al., 2015; Alvarez-Erviti et al., 2011; Araki et al., 2016; Barbour et al., 2008; Bartels et al., 2011; Danzer et al., 2012; El-Agnaf et al., 2006; Emmanouilidou et al., 2010; Fauvet et al., 2012; Fraser et al., 2013; Grey et al., 2015; Helferich et al., 2015; Ho et al., 2014; Kong et al., 2014; Kunadt et al., 2015; Melachroinou et al., 2013; Nakai et al., 2007; Nikam et al., 2009; Pretorius et al., 2014; Renella et al., 2014; Shi et al., 2014; Stuendl et al., 2016; Sudha et al., 2003; Tomlinson et al., 2015; Tsunemi et al., 2014; Wang et al., 2015). For example, EVs derived from the CSF contain α-synuclein (α-syn), its associated pathogenic species as well as the LRRK2 protein (Fraser et al., 2013). However, routinely collecting CSF presents a challenge given the invasive nature needed to collect it while plasma is a very accessible fluid that further allows real time monitoring, and which has consequently been more extensively studied from a biomarker perspective.

One of the reasons that EVs have become attractive for biomarker development relates to advances in

their isolation involving ultracentrifugation, centrifugation by density gradient, size exclusion using membranes and columns, polymeric precipitation, capture by immune-affinity and microfluidic approaches (Shevchenko et al., 1996). However, the bulk of the already published work on EV in bio-fluids relies on using a series of differential centrifugations with or without size filtration, for example gradient techniques that concentrate and purify EV (Konoshenko et al., 2018; Willis et al., 2017). Techniques utilizing solely the ultracentrifugation to perform EV counts are biased because they favor aggregations of vesicles while co-isolating a number of contaminants, such as proteins (Linares et al., 2015). Techniques to isolate EV have therefore recently been developed with the goal of maintaining the integrity and purity of the isolated entities (Konoshenko et al., 2018). We sought to use these advances to develop new approaches that would allow for the optimal analysis of EV in blood, and therefore shed light on a more accurate picture of these elements in PD with the hope that this could be used for biomarker development. This work initially involved optimizing the FACS analysis by stringent controls to unequivocally identify EVs and their cell origin, performing test-retest experiments to validate consistency of results over time in the same patient and finally, using hemoglobin removal to uncover the entire proteome of EV analyzed. This having been done, we then sought to characterize the nature and profile of EV in the plasma of patients, and how they correlate to clinical measures of disease state as well as defining the protein content in the subpopulations of EV. Finally we sought to validate this whole approach using a second independent cohort of patients with PD.

## MATERIALS AND METHODS

### Ethics statement and participant recruitment

Institutional review boards approved this study (CHU de Québec, #A13-2-1096; CHUM, #14.228; Cambridge Central Regional Ethics Committee, REC #03/303 & #08/H0306/26; and Cambridge University Hospitals Foundation Trust Research and Development department, R&D #A085170 & #A091246) in accordance with the Declaration of Helsinki, and written informed consents were obtained from all participants.

Blood samples were initially collected from 2 cohorts of patients with a total of 60 PD [one in Cambridge UK; one in Quebec Canada] as well as 37 age- and sex-matched healthy Controls (**Table 1**). For comparison, blood samples were also collected from a cohort of 52 Huntington's disease (HD) individuals [collected in Montreal, Canada] along with 55 age- and sex-matched healthy Controls (**Table S1**). Subsequently, an additional and independent cohort of 42 PD patients was collected to corroborate the

results related to EEV counts obtained from these first cohorts of patients (**Table S2**). In the case of PD patients, the UK Parkinson's Disease Society Brain diagnostic criteria were used, which gives a diagnostic accuracy of 98.6% when applied by movement disorder specialists (Hughes et al., 2002; Massano and Bhatia, 2012). The patients, at the time of bleeding, also underwent clinical evaluation which included the Unified Parkinson Disease Rating Scale (UPDRS), Hoehn and Yahr (H&Y) scale, the Mini Mental State Examination (MMSE), the Addenbrooke's Cognitive Examination (ACE) and the Beck Depression Inventory (BDI). UPDRS was obtained from the UK and Montreal cohorts but not the Quebec cohort for logistical reasons. In the case of the HD patients, their Unified Huntington Disease Rating Scale (UHDRS), Total Functional capacity (TFC) and calculated values for burden of disease (BDS) were all collected at the time of venepuncture and their diagnosis was confirmed by genetic testing. Participants were further asked to fill out a questionnaire related to health issues and medication and a full blood count was performed in all patients on the day of blood sampling. Comorbidities were determined from medical information reported by the participant or caregiver. Cancer refers to a participant having suffered from any cancer in the past. Medications were converted into levodopa equivalent daily dose (LEDD) using common calculator tools. It should be noted that blood sampling was conducted by the exact same team of investigators, following identical procedures in both UK and Canada.

For the test-retest experiments, collection of blood samples was performed on 25 healthy individuals with 2 samples per subject, taken after a 2-hour interval. This cohort included 11 men and 14 women with a mean age of 29 ± 5 years with no clinical reports of co-morbidities or medication intake. Note that fasting was not required prior to blood samplings in any of the cohorts that were recruited for this study. Calculation of % CVs of concentration measurements of EEVs was performed using GraphPad PRISM® Version 6.0 (GraphPad Software, LaJolla, CA).

**Preparation of platelet-free plasma and EV labeling**

Citrated blood was centrifuged twice for 15 minutes at 2500g at room temperature. Platelet-free plasma (PFP) was harvested and stored at -80°C within 2 hours of sampling following previously published guidelines (Lacroix et al., 2012). For specific details on EV labeling, please refer to the supplementary material.

In all cases, the control samples came from healthy participants and the blood was collected at exactly the same time of day as for the PD and HD patients in the UK and Canadian clinics. Every blood sample

was processed immediately to avoid release of non-physiological EV. For analyses relating to EV in plasma, all blood samples were centrifuged twice at 2500g to enable PFP recovery. The plasma was fractionated into 3 aliquots per individual and frozen immediately following processing (maximum of 2 hours following blood collection). Blood samples from Controls and PD were collected in parallel and laboratory analyses were blinded to participant status.

**Flow cytometry quantification**

For EV quantification, we used a FACS Canto II Special Order Research Product equipped with a forward scatter (FSC) coupled to a photomultiplier tube (FSC-PMT) and a small particle option. Flow cytometer performance tracking was carried out daily using the BD cytometer setup and tracking beads (BD Biosciences, San Jose, CA, USA). The size of the EV was determined using fluorescent silica beads of 100, 500 and 1000nm (**Figure S2**). The settings for the EV detection were determined as previously described using a threshold of 200 for SSC (also see **Figure S2**) (Rousseau et al., 2015). For specific details on plasma-related EV quantification, please refer to the supplementary material.

**Production and purification of EEV**

Blood was collected in heparin tubes and centrifuged for 10 minutes at 282g at room temperature. Blood cells were washed first in PBS-2%FBS, then with 0.9% sodium chloride solution and centrifuged for 10 minutes at 750g. To avoid leukocyte and/or platelet contamination, the buffy coat and upper fraction of erythrocytes were removed. To preserve erythrocytes, two volumes of glycerolyte 57 solution (57% glycerol, 142mM sodium lactate, 1mM KCl, 25mM sodium phosphate pH 6.8) were added to the pellet and stored at -80°C. For the *in vitro* generation of EEV, red blood cells were thawed and EV production was induced as previously described (Minetti et al., 2004). For specific details on EEV purification, please refer to supplementary material.

**C-reactive protein, free hemoglobin and α-synuclein quantification**

The concentrations of C-reactive protein (CRP) and free hemoglobin were determined in the PFP of all donors using the RayBio Human CRP ELISA Kit (RayBiotech, Norcross, GA, USA) and the Hemoglobin Human ELISA kit (Abcam, Toronto, ON, Canada). To quantify α-syn within erythrocytes and EEV, we used the human α-Syn ELISA kit (ThermoFisher Scientific, Waltham, MA, USA). Absorbance values were measured at 450nm using a multi-detection microplate reader (Synergy HT; BioTek; Winooski, VT, USA). All ELISA tests were performed according to the manufacturer's instructions.

**Scanning electron microscopy**

For the visualization by scanning electron microscopy, EEV were prepared as previously described (Duchez et al., 2015). For specific details on EEV preparation, please refer to supplementary material.

**Transmission electron microscopy**

For transmission electron microscopy, EEV were prepared and observed as previously described (Duchez et al., 2015). For specific details on EEV preparation and labelling, please refer to supplementary material.

**Mass spectrometry analysis and label free protein quantification**

The initial proteomic analyses were performed on 3 pools of 3 blood samples of each group. Following this, we undertook a completely new set of analyses to develop a method allowing us to isolate hemoglobin and better investigate the EEV proteome. For this, EVs from an additional 4 individuals per group (Control, mild PD and moderate PD) were prepared as described above. For each individual, 25µg of the protein sample, according to Bradford protein assay, was migrated onto an electrophoresis gel 4-12% Bis-Tris to separate hemoglobin from higher proteins. Following gel staining using Sypro Ruby (Thermo Fischer Scientific), the 12kDa band corresponding to the hemoglobin size was cut out and the remaining part of the gel further fractioned into 7 slices, exposed to trypsin digestion and peptide extraction on a MassPrep liquid handling robot (Waters, Milford, USA) according to the manufacturer's specifications and the protocol of Shevchenko et al. with the modifications suggested by Havlis et al. (Havlis et al., 2003; Shevchenko et al., 1996). For specific details on protein analysis purification, please refer to supplementary material. Spectra of peptides were searched against a human protein database (Uniprot Complete Proteome, taxonomy Homo sapiens – 83512 sequences) using the Andromeda search engine included in MaxQuant software version 1.5.5.1. (Cox and Mann, 2008). MaxQuant was also used to validate proteins and peptides at a 1% False Discovery Rate using a target/decoy database search as well as to undertake a Label Free Quantification of the identified proteins using the 'match between runs' option.

**Statistical analyses**

All statistical analyses were performed by a qualified statistician and details pertaining to these analyses for each experiment are provided in the supplementary material.

## RESULTS

### Optimizing EV detection and the demonstration of reproducibility

While we performed EV analyses in plasma, we ensured that reproducibility of EV identification and labeling was robust. For this, we undertook a series of control experiments to properly set the EV gate and fluorescent silica beads of 100nm (*Red*), 500nm (*Blue*) and 1000nm (*Yellow*) were acquired on a flow cytometer Canto II modified with a FSC-PMT small particle option (**Figure S2A-C**). The acquisition was performed at low speed at an approximated rate of 10µl/ml. The established EV gate was used for all experiments. Serial dilutions of EEV (1, 2, 4 and 10) were also undertaken to confirm the linearity of the quantification. FSC-PMT/SSC gates of PFP stained with annexin V fluorescent conjugate (a ligand of phosphatidylserine) and respective fluorochrome-conjugated antibodies directed against erythrocyte (CD235a+), endothelial (CD31+/CD41-), platelet (CD41+) and leukocyte (CD14+CD45+, monocytes; CD15+CD45+, granulocytes)-derived EVs were carefully established.

We further completed numerous controls to ensure specific EV labeling. We first determined that treatment with the ion chelator EDTA inhibited the binding of annexin V to phosphatidylserine. We observed minimal background using antibodies in the absence of PFP. Subsequently, EV sensitivity to 0.5% triton was assessed. Under these conditions, the membrane of the EVs is dissolved while protein aggregates are left intact (György et al., 2011). Results show that vast majority of EVs positive for their own fluorochrome-conjugated antibodies were eliminated by detergent (**Figure S2D-F**). Finally**,** we conducted a test-retest assay where two PFP samples per subject were collected approximately 2 hours apart in 25 healthy individuals. All samples were tested in duplicate and minimal inter-sample variability was observed (16% ± 7%) (**Figure S2G**).

In addition to full blood count, and as a precautionary measure, hematocrit, mean corpuscular hemoglobin and mean corpuscular volumes were evaluated and showed similar values between groups (**Figure S3A**). C-reactive protein quantifications were also obtained for all participants and revealed no differences between groups (**Figure S3B**). We did, however, observe a significant increase in EEV concentration in the PFP of individuals with diabetes and those suffering, or having suffered, from cancer (data not shown) and thus these participants were excluded from our analyses. PFP samples with elevated free hemoglobin (>45 000ng/ml), potentially due to hemolysis during blood sampling, were also excluded from further EEV-related analyses (**Figure S3C**), which account for the small discrepancies

between the total number of participants initially recruited and those reported in each analysis.

**Increase in erythrocyte-derived EV in PD patients is not a diagnostic tool**

Once all the controls established and verified, we collected and carefully analyzed blood samples from patients with PD (n=60) along with age/sex-matched healthy Controls (n=37) (**Table 1**). Full blood counts were performed on each sample but did not reveal any differences in the number of platelets, leukocytes, monocytes, granulocytes except for erythrocytes, where a small significant difference ($p$=0.049) was seen between PD patients and Controls (**Figure 1A**). We then labeled each cell type as well as each EV population present in plasma to generate accurate counts of EV by FACS. A series of specific labelings highlighted a notable increase in the mean number of EEV in PD patients with respect to their age- and sex-matched healthy Controls ($p$=0.04; **Figure 1B-C**). None of the EV derived from the other blood cell populations showed differences between PD and Controls.

Based on this observation, we evaluated the diagnostic value of EV for PD by taking a closer look at the data distribution. However, this uncovered that only 5 patients were responsible for this significant difference (**Figure 1C**, red inset). Further investigation, using a diagnostic accuracy test, revealed that the relevant proportion of the area under the Receiver Operating Characteristic (ROC) curve was 0.508 (data not shown), implying that the number of EEV could not be used as a discriminant between PD patients and healthy Controls. This was also confirmed by performing a Bayesian analysis of the data demonstrating that the proposed predictor of the onset of PD would be correct in less than 1% of the cases (data not shown). We obtained a similar result when we separated the patients into mild and moderate states according to their UPDRS scores or by cohort (data not shown).

**EV counts and clinical features**

Despite the absence of a diagnostic difference in EEV counts, we explored whether there could be a relationship between the number of EEV and clinical measures such as H&Y stage, BDI, MMSE and ACE, but we found no significant correlations (data shown for H&Y, **Figure 2A**). However, preliminary analyses revealed a correlation of $R^2$=0.37 with a $p$ value of 0.0056 when plotting EEV counts/erythrocytes according to the UPDRS clinical rating scales (**Figure 2B**). In depth statistical analyses further revealed intriguing, but striking correlations between the number of vesicles derived from the red blood cells of PD patients and their total UPDRS (**Figure 2C**). Statistical linear regression analysis was performed for each group and the $R^2$ values obtained demonstrated that in both cases, at least 87% of the variation in the total number of EEV/erythrocytes was due to the variation of the UPDRS (**Figure 2C**). Moreover, the

results were significant with respect to the *p* values obtained for each fit as they fell below the 5% confidence level. This could not be accounted for by medication, as there was no correlation with the patients LEDD (**Figure 2D-E**). Importantly, these results were then corroborated in an independent cohort of 42 PD patients where the correlations yielded an $R^2$=0.05 and a *p* value of 0.15 when plotting EEV counts/erythrocytes against scores obtained with the UPDRS clinical rating scale (**Figure S4A**).

In contrast to PD, correlation analyses failed to reveal an association between the number of EEV and HD stage using the UHDRS score (**Figure S5**).

**Proteomic signature of EEV in PD**

Given that these correlations are based on a small number of patients (cohort 1; n=19 and cohort 2; n=42), we sought to corroborate these results by examining the specific protein signature of EEV from mild and moderate PD patients (with respect to their UPDRS scores) and age-matched Controls. Given the significant amounts of hemoglobin within erythrocytes that could mask the true nature of the protein signature in EEV, we performed a label free quantitative proteomic analysis by nanoLC/MSMS (Wither et al., 2016) using two distinct approaches: with and without hemoglobin (**Figure 3A-B**). By removing hemoglobin, we identified a total of 818 proteins in comparison with 356 when we did not undertake this methodological step (refer to **Table S3** for complete list of proteins) – a modification which is clearly needed to give a much more accurate evaluation of the protein content of EEV. Additionally, a Gene Ontology enrichment analysis on the 'Cellular Component' ontology on the two sets of identified proteins in comparison with the whole human proteome, revealed that our samples are enriched with elements associated with 'vesicles' and 'hemoglobin complex' (**Figure S6**).

Out of the 818 proteins identified in the proteome of EEV, 8 had expressions that were significantly different in patients with various stages of PD (**Figure 3C**). Hierarchical clustering, coupled to a heatmap, allowed us to group individuals according to stages of disease (Control, mild PD and moderate PD) and provided compelling evidence that the 8 proteins identified could also be grouped into three categories. Proteins of group I were highly and predominantly expressed in Controls, proteins of group II were highly and predominantly expressed in mild PD patients and proteins belonging to group III were highly and predominantly expressed in moderate PD patients (**Figure 3D**). This data set was further confirmed by volcano plots (**Figure 3E**).

Finally, we assessed whether α-Syn – which is not only the main component of Lewy bodies but is highly expressed in most blood cells – was differentially expressed in normal vs. diseased conditions. For this, we opted to use scanning electron microscopy, but this did not reveal any morphological changes between resting and activated erythrocytes in either condition (**Figure 4A**). We further used transmission electron microscopy to quantify the number of EEV containing α-Syn and phosphorylated (serine 129) forms of the protein, but again there were no significant differences between PD patients and age- and sex-matched healthy Controls (**Figure 4B-C**). Quantified α-Syn levels in EEV from PD patients and Controls using commercial ELISA kits corroborated these results (**Figure 4D**).

**DISCUSSION**

The primary goal of our study was to provide an accurate description of EV in PD patients. In order to do this, we took into account all relevant technical parameters and refined a number of approaches that may have been contentious in previous publications. These technical improvements included: 1) better methods to clearly identify EV when using FACS; 2) specific labeling to determine, with precision, the cell origin of the EV; 3) the demonstration of minimal test-retest variability intra-patient; 4) the deletion of hemoglobin from the samples for proteomic analyses which, as suspected, revealed numerous proteins which currently remain unidentified and finally, 5) the development of a user-friendly test which has the potential to be easily performed by western blots in any laboratory contexts using just a few microliters of blood. Once we had established the protocols for EV characterization, the second objective of this study was to explore the potential biomarker value of EVs in PD. We found that EEV counts did map to disease stage, a finding that was corroborated by a unique protein signature in control subjects, mild and moderate PD patients. Our observations were then confirmed in a second independent cohort of PD patients, showing that our findings are robust and thus could have widespread applicability for helping stage PD patients in the future.

Blood counts were systemically performed in all patients, EV identification was replicated using the most accepted and standardized methods of repetition, stringent controls (microbeads, antibodies negative control, EDTA and Triton) (Rousseau et al., 2015) and complex combinations of antibodies which allowed for the specific labeling of vesicles. Standard techniques used to analyse EVs (e.g. ultracentrifugation followed by immunoblotting) requires several days and a considerable amount of cells to isolate EVs. However, quantification by flow cytometry takes only 1 day and requires a relatively small quantity of plasma (Konoshenko et al., 2018). We further demonstrated minimal test-retest variability. Sequential

analyses of EV during the same day from the same individual/sample (intra-assay variation) has been reported to vary between 1-12% (Vestad et al., 2017). For example, circadian rhythm has been reported to influence the activation of platelets and therefore influence EV derived from these cells (Scheer et al., 2011). In recent studies, counts of microvesicles derived from platelets across different flow cytometry platforms showed an inter-laboratory variability ranging between 28% and 37% (Vogel et al., 2016). In our hands, variability measures ranged between 1-30%, with an average at 16% ±7%, indicative of strong reproducibility.

While proteomic studies of EEV have been previously reported, their description was limited to 270 proteins (Bosman et al., 2012, 2008). We herein report on an improved method to perform this type of analyses in blood samples by removing hemoglobin; a large protein that can easily mask others within a protein signature. Indeed, the high dynamic range of protein concentrations in erythrocytes and their EEV, due to the abundance of hemoglobin, decreases the capacity of the mass spectrometer to detect signals corresponding to low abundance proteins. Analyzing the hemoglobin, separately from proteins of other molecular weights, allowed us to go deeper into the EEV proteome, identifying 129% more proteins than in the initial analysis. It is important to reiterate that our proteomic analyses were performed using very stringent parameters, which included a minimum of 2 peptides per protein and p values of less than 0.05 with an absolute z score of 1.96, corresponding to values outside of the 95% confidence range. Finally, our volcano plots and heatmap analyses revealed high specificity of the identified proteins for each group with nodes ranging between 80 and 90%. With this, reproducibility of our proteomics data is high despite the smaller sample size (analyses performed on 3 pools of 3 samples per group and subsequently on 4 individual samples per group). Reports of the role of these proteins in PD are rare. However of interest, QDPR has been reported to be essential to the bisosynthesis of norepinephrin and serotonin (Kaufman et al., 1975). ABHD14B have been shown to be dysregulated in mice following a levo-dopa treatment (Charbonnier-Beaupel et al., 2015) and that mARNs for CNRIP1 are diminished in the striatum of a primate model of PD (Zeng et al., 1999). Finally, genetic variants of USP24 are associated to PD risk factors (Li et al., 2006) while another study of blood genetic profile revealed that ATP5A1 is down regulated in idiopathic PD patients (Shamir et al., 2017).

Although staging of PD is often done using the H&Y clinical scale, we sought to use the UPDRS given its more comprehensive coverage of disease features – an approach that has recently been validated (Martínez-Martín et al., 2015). Using these scores in our initial study, we found that mild PD patients –

with a UPDRS score lower than 37 – have an increased number of EV (correlations = 0.886); and that the exact same pattern then repeats itself with patients who had UPDRS scores between 37 and 75 (correlations = 0.873) with a marked resetting of the number of EVs between these two stages. In this study, which was undertaken using patients in research clinics, patients with advanced disease (>75 UPDRS) were not recruited in large numbers because they have difficulty making it to the clinics. In order to further validate this finding, we undertook a second study in another 42 patients with PD, which also included patients with more advanced disease. In this additional independent cohort, we demonstrated that we can replicate, very closely, what we found in the first cohort. Namely, mild patients fell between the UPDRS scores of 0 – 39, moderate patients between 29 – 57 and severe patients (which we did not analyze in the first cohort), between 57 – 74 and that there EV changes paralleled that which we saw in our initial study. The overlapping zone is likely due to a number of factors including the fact that 1) this new cohort was scored by a different clinician than our first cohort. Indeed, despite the fact that neurologists are trained to score patients in a similar fashion, the UPDRS remains a subjective measure that can vary between clinicians, even when they are been validated as a rater using the MDS training videos. 2) The FACS sorting apparatus we use to quantify EEV does generate a small percentage of variability (around 8%) between runs (data not shown). 3) We opted to test patients ON medication. It is therefore possible that the patient tested in the morning, who has just recently taken his medicine, scores slightly differently on the UPDRS than the patient who has taken in meds in the morning but were assessed late afternoon.

The bi-modal distribution revealed by the correlation analysis is intriguing but it would be very difficult to establish a definite cut-off between groups. The UPDRS is based on a questionnaire of more than 70 different questions which are all based on a subjective assessment of the patient. A patient falling at the border of mild and moderate stage PD may be very difficult to categorize. We have already ruled out medication (in particular LEED) and a number of co-morbidities (depression, cancer, diabetes, hypertension, hypercholesterolemia, asthma, allergies) as contributing to this. It is important to note that, while the $R^2$ values are very impressive, the samples used for each group (cohort 1; n=19 and cohort 2; n=42) are undersized with respect to the classical Pearson's chi-squared test. Further investigation with a larger cohort should therefore achieve more confident results which we are doing now.

Overall, we have identified a novel biomarker in the blood of patients with PD that seems to correlate with disease stage and which is derived from 2 measures: the number of EEV/erythrocytes and the expression of 8 different proteins. The biological reasons as to why we find these correlations is still unresolved as is the pathological significance of the protein signature we identified. Nevertheless, our findings are robust and reproducible and further support recent findings that plasma EV derived from the CNS and containing α-syn correlate with the UPDRS scores in PD patients (Shi et al., 2014). Our results unveil a useful new biomarker, and while the EEV counts used a particular type of flow cytometer that is not necessarily accessible to all laboratories, the identification of specific proteins that match clinical stages of PD implies that these could be more easily tested/detected in samples using simple western blots. If replicated in other studies, we would then have a biomarker that could be easily tested in any laboratories or clinical context.

**Acknowledgements**

The authors would like to thank all the students and staff who helped with the blood collections in Cambridge UK, Quebec City and Montreal, Mr. Richard Janvier for his very skilful electron microscopy preparation and analyses, Mr. Gilles Chabot for art work and the Bioimaging platform of the Infectious Disease Research Centre, funded by an equipment and infrastructure grant from the Canadian Foundation for Innovation, for the coordination of the project, we thank Mrs. Lynn Jean from the CHU de Montréal, and importantly, all patients and their families for being so generous with their time in participating in this study.

**Author Contributions**

J.L.P. participated in the design of the experiments and all aspects of the study including blood drive, experiments, data analysis and interpretation and preparations of figures. He also helped write some sections of the manuscript.

I.S.-A. participated in the design of the experiments and blood drives, took part in some data analysis and interpretation.

R.L. elaborated the statistical analysis strategy, performed statistical analyses related to Figure 2 and wrote part of the texts relating to the correlation results.

J.P. performed statistical analyses related to Figure 2.

H.L.D. participated in the analysis of data, preparation of figures and experiments in Figure S2.G and Figure S4.

N.C. was involved in the original design of the flow cytometry experiments and participated in the blood drive in Cambridge.

F.R.-D. contributed to the design and analyses of the proteomic experiments, performed the nanoLC-MS/MS and the Free Label quantification and helped with the figure design and writing of methodological aspects of the manuscript.

A.T.V. helped with the proteomic analyses, generated Figure 3 and wrote related methodological aspects of the manuscript.

S.L.M. helped with patient recruitment in Cambridge and participated in the preparation of blood drive in Cambridge.

A-C.D. was involved in the design of electron microscopy experiments and performed related analyses.

A.D. contributed to the proteomic analyses and data interpretation

S.L. had the initial idea to study EEV in HD, set up the collaboration and was involved in discussions pertaining to the study.

N.D. recruited patients – Quebec PD cohort.

M.L. recruited patients – Quebec PD cohort.

S.C. recruited patients – Montreal HD cohort.

R.A.B. helped in the recruiting of patients, participated in data interpretation and revised the manuscript.

E.B. initiated the study and was involved in the experimental design. He also revised the manuscript.

F.C. initiated the study and was involved in the experimental design. She supervised the project and wrote the manuscript.

**References**

Abd-Elhadi, S., Honig, A., Simhi-Haham, D., Schechter, M., Linetsky, E., Ben-Hur, T., Sharon, R., 2015. Total and Proteinase K-Resistant α-Synuclein Levels in Erythrocytes, Determined by their Ability to Bind Phospholipids, Associate with Parkinson's Disease. Sci. Rep. 5, 11120. https://doi.org/10.1038/srep11120

Alvarez-Erviti, L., Seow, Y., Schapira, A.H., Gardiner, C., Sargent, I.L., Wood, M.J.A., Cooper, J.M., 2011. Lysosomal dysfunction increases exosome-mediated alpha-synuclein release and transmission. Neurobiol. Dis. 42, 360–367. https://doi.org/10.1016/j.nbd.2011.01.029

Araki, K., Yagi, N., Nakatani, R., Sekiguchi, H., So, M., Yagi, H., Ohta, N., Nagai, Y., Goto, Y., Mochizuki, H., 2016. A small-angle X-ray scattering study of alpha-synuclein from human red blood cells. Sci. Rep. 6, 30473. https://doi.org/10.1038/srep30473

Barbour, R., Kling, K., Anderson, J.P., Banducci, K., Cole, T., Diep, L., Fox, M., Goldstein, J.M., Soriano, F., Seubert, P., Chilcote, T.J., 2008. Red blood cells are the major source of alpha-synuclein in blood. Neurodegener. Dis. 5, 55–59. https://doi.org/10.1159/000112832

Bartels, T., Choi, J.G., Selkoe, D.J., 2011. α-Synuclein occurs physiologically as a helically folded tetramer that resists aggregation. Nature 477, 107–110. https://doi.org/10.1038/nature10324

Berg, D., Postuma, R.B., Bloem, B., Chan, P., Dubois, B., Gasser, T., Goetz, C.G., Halliday, G.M., Hardy, J., Lang, A.E., Litvan, I., Marek, K., Obeso, J., Oertel, W., Olanow, C.W., Poewe, W., Stern, M., Deuschl, G., 2014. Time to redefine PD? Introductory statement of the MDS Task Force on the definition of Parkinson's disease. Mov. Disord. Off. J. Mov. Disord. Soc. 29, 454–462. https://doi.org/10.1002/mds.25844

Bosman, G.J.C.G.M., Lasonder, E., Groenen-Döpp, Y.A.M., Willekens, F.L.A., Werre, J.M., 2012. The proteome of erythrocyte-derived microparticles from plasma: new clues for erythrocyte aging and vesiculation. J. Proteomics 76 Spec No., 203–210. https://doi.org/10.1016/j.jprot.2012.05.031

Bosman, G.J.C.G.M., Lasonder, E., Luten, M., Roerdinkholder-Stoelwinder, B., Novotný, V.M.J., Bos, H., De Grip, W.J., 2008. The proteome of red cell membranes and vesicles during storage in blood bank conditions. Transfusion (Paris) 48, 827–835. https://doi.org/10.1111/j.1537-2995.2007.01630.x

Charbonnier-Beaupel, F., Malerbi, M., Alcacer, C., Tahiri, K., Carpentier, W., Wang, C., During, M., Xu, D., Worley, P.F., Girault, J.-A., Hervé, D., Corvol, J.-C., 2015. Gene expression analyses identify Narp contribution in the development of L-DOPA-induced dyskinesia. J. Neurosci. Off. J. Soc. Neurosci. 35, 96–111. https://doi.org/10.1523/JNEUROSCI.5231-13.2015

Cox, J., Mann, M., 2008. MaxQuant enables high peptide identification rates, individualized p.p.b.-range mass accuracies and proteome-wide protein quantification. Nat. Biotechnol. 26, 1367–1372. https://doi.org/10.1038/nbt.1511

Danzer, K.M., Kranich, L.R., Ruf, W.P., Cagsal-Getkin, O., Winslow, A.R., Zhu, L., Vanderburg, C.R., McLean, P.J., 2012. Exosomal cell-to-cell transmission of alpha synuclein oligomers. Mol. Neurodegener. 7, 42. https://doi.org/10.1186/1750-1326-7-42

Duchez, A.-C., Boudreau, L.H., Naika, G.S., Bollinger, J., Belleannée, C., Cloutier, N., Laffont, B., Mendoza-Villarroel, R.E., Lévesque, T., Rollet-Labelle, E., Rousseau, M., Allaeys, I., Tremblay, J.J., Poubelle, P.E., Lambeau, G., Pouliot, M., Provost, P., Soulet, D., Gelb, M.H., Boilard, E., 2015. Platelet microparticles are internalized in neutrophils via the concerted activity of 12-lipoxygenase and

secreted phospholipase A2-IIA. Proc. Natl. Acad. Sci. U. S. A. 112, E3564-3573. https://doi.org/10.1073/pnas.1507905112

El-Agnaf, O.M.A., Salem, S.A., Paleologou, K.E., Curran, M.D., Gibson, M.J., Court, J.A., Schlossmacher, M.G., Allsop, D., 2006. Detection of oligomeric forms of alpha-synuclein protein in human plasma as a potential biomarker for Parkinson's disease. FASEB J. Off. Publ. Fed. Am. Soc. Exp. Biol. 20, 419–425. https://doi.org/10.1096/fj.03-1449com

Emmanouilidou, E., Melachroinou, K., Roumeliotis, T., Garbis, S.D., Ntzouni, M., Margaritis, L.H., Stefanis, L., Vekrellis, K., 2010. Cell-produced alpha-synuclein is secreted in a calcium-dependent manner by exosomes and impacts neuronal survival. J. Neurosci. Off. J. Soc. Neurosci. 30, 6838–6851. https://doi.org/10.1523/JNEUROSCI.5699-09.2010

Fauvet, B., Mbefo, M.K., Fares, M.-B., Desobry, C., Michael, S., Ardah, M.T., Tsika, E., Coune, P., Prudent, M., Lion, N., Eliezer, D., Moore, D.J., Schneider, B., Aebischer, P., El-Agnaf, O.M., Masliah, E., Lashuel, H.A., 2012. α-Synuclein in central nervous system and from erythrocytes, mammalian cells, and Escherichia coli exists predominantly as disordered monomer. J. Biol. Chem. 287, 15345–15364. https://doi.org/10.1074/jbc.M111.318949

Fraser, K.B., Moehle, M.S., Daher, J.P.L., Webber, P.J., Williams, J.Y., Stewart, C.A., Yacoubian, T.A., Cowell, R.M., Dokland, T., Ye, T., Chen, D., Siegal, G.P., Galemmo, R.A., Tsika, E., Moore, D.J., Standaert, D.G., Kojima, K., Mobley, J.A., West, A.B., 2013. LRRK2 secretion in exosomes is regulated by 14-3-3. Hum. Mol. Genet. 22, 4988–5000. https://doi.org/10.1093/hmg/ddt346

Grey, M., Dunning, C.J., Gaspar, R., Grey, C., Brundin, P., Sparr, E., Linse, S., 2015. Acceleration of α-synuclein aggregation by exosomes. J. Biol. Chem. 290, 2969–2982. https://doi.org/10.1074/jbc.M114.585703

György, B., Módos, K., Pállinger, E., Pálóczi, K., Pásztói, M., Misják, P., Deli, M.A., Sipos, A., Szalai, A., Voszka, I., Polgár, A., Tóth, K., Csete, M., Nagy, G., Gay, S., Falus, A., Kittel, A., Buzás, E.I., 2011. Detection and isolation of cell-derived microparticles are compromised by protein complexes resulting from shared biophysical parameters. Blood 117, e39-48. https://doi.org/10.1182/blood-2010-09-307595

Havlis, J., Thomas, H., Sebela, M., Shevchenko, A., 2003. Fast-response proteomics by accelerated in-gel digestion of proteins. Anal. Chem. 75, 1300–1306.

Helferich, A.M., Ruf, W.P., Grozdanov, V., Freischmidt, A., Feiler, M.S., Zondler, L., Ludolph, A.C., McLean, P.J., Weishaupt, J.H., Danzer, K.M., 2015. α-synuclein interacts with SOD1 and promotes its oligomerization. Mol. Neurodegener. 10, 66. https://doi.org/10.1186/s13024-015-0062-3

Ho, D.H., Yi, S., Seo, H., Son, I., Seol, W., 2014. Increased DJ-1 in urine exosome of Korean males with Parkinson's disease. BioMed Res. Int. 2014, 704678. https://doi.org/10.1155/2014/704678

Hughes, A.J., Daniel, S.E., Ben-Shlomo, Y., Lees, A.J., 2002. The accuracy of diagnosis of parkinsonian syndromes in a specialist movement disorder service. Brain J. Neurol. 125, 861–870.

Kaufman, S., Holtzman, N.A., Milstien, S., Butler, L.J., Krumholz, A., 1975. Phenylketonuria due to a deficiency of dihydropteridine reductase. N. Engl. J. Med. 293, 785–790. https://doi.org/10.1056/NEJM197510162931601

Kong, S.M.Y., Chan, B.K.K., Park, J.-S., Hill, K.J., Aitken, J.B., Cottle, L., Farghaian, H., Cole, A.R., Lay, P.A., Sue, C.M., Cooper, A.A., 2014. Parkinson's disease-linked human PARK9/ATP13A2 maintains zinc homeostasis and promotes α-Synuclein externalization via exosomes. Hum. Mol. Genet. 23, 2816–2833. https://doi.org/10.1093/hmg/ddu099

Konoshenko, M.Y., Lekchnov, E.A., Vlassov, A.V., Laktionov, P.P., 2018. Isolation of Extracellular Vesicles: General Methodologies and Latest Trends. BioMed Res. Int. 2018, 8545347. https://doi.org/10.1155/2018/8545347

Kunadt, M., Eckermann, K., Stuendl, A., Gong, J., Russo, B., Strauss, K., Rai, S., Kügler, S., Falomir Lockhart, L., Schwalbe, M., Krumova, P., Oliveira, L.M.A., Bähr, M., Möbius, W., Levin, J., Giese, A., Kruse, N., Mollenhauer, B., Geiss-Friedlander, R., Ludolph, A.C., Freischmidt, A., Feiler, M.S., Danzer, K.M., Zweckstetter, M., Jovin, T.M., Simons, M., Weishaupt, J.H., Schneider, A., 2015. Extracellular vesicle sorting of α-Synuclein is regulated by sumoylation. Acta Neuropathol. (Berl.) 129, 695–713. https://doi.org/10.1007/s00401-015-1408-1

Lacroix, R., Judicone, C., Poncelet, P., Robert, S., Arnaud, L., Sampol, J., Dignat-George, F., 2012. Impact of pre-analytical parameters on the measurement of circulating microparticles: towards standardization of protocol. J. Thromb. Haemost. JTH 10, 437–446. https://doi.org/10.1111/j.1538-7836.2011.04610.x

Li, Y., Schrodi, S., Rowland, C., Tacey, K., Catanese, J., Grupe, A., 2006. Genetic evidence for ubiquitin-specific proteases USP24 and USP40 as candidate genes for late-onset Parkinson disease. Hum. Mutat. 27, 1017–1023. https://doi.org/10.1002/humu.20382

Linares, R., Tan, S., Gounou, C., Arraud, N., Brisson, A.R., 2015. High-speed centrifugation induces aggregation of extracellular vesicles. J. Extracell. Vesicles 4, 29509.

Maere, S., Heymans, K., Kuiper, M., 2005. BiNGO: a Cytoscape plugin to assess overrepresentation of gene ontology categories in biological networks. Bioinforma. Oxf. Engl. 21, 3448–3449. https://doi.org/10.1093/bioinformatics/bti551

Martínez-Martín, P., Rodríguez-Blázquez, C., Mario Alvarez, null, Arakaki, T., Arillo, V.C., Chaná, P., Fernández, W., Garretto, N., Martínez-Castrillo, J.C., Rodríguez-Violante, M., Serrano-Dueñas, M., Ballesteros, D., Rojo-Abuin, J.M., Chaudhuri, K.R., Merello, M., 2015. Parkinson's disease severity levels and MDS-Unified Parkinson's Disease Rating Scale. Parkinsonism Relat. Disord. 21, 50–54. https://doi.org/10.1016/j.parkreldis.2014.10.026

Massano, J., Bhatia, K.P., 2012. Clinical approach to Parkinson's disease: features, diagnosis, and principles of management. Cold Spring Harb. Perspect. Med. 2, a008870. https://doi.org/10.1101/cshperspect.a008870

Melachroinou, K., Xilouri, M., Emmanouilidou, E., Masgrau, R., Papazafiri, P., Stefanis, L., Vekrellis, K., 2013. Deregulation of calcium homeostasis mediates secreted α-synuclein-induced neurotoxicity. Neurobiol. Aging 34, 2853–2865. https://doi.org/10.1016/j.neurobiolaging.2013.06.006

Minetti, G., Ciana, A., Balduini, C., 2004. Differential sorting of tyrosine kinases and phosphotyrosine phosphatases acting on band 3 during vesiculation of human erythrocytes. Biochem. J. 377, 489–497. https://doi.org/10.1042/BJ20031401

Nakai, M., Fujita, M., Waragai, M., Sugama, S., Wei, J., Akatsu, H., Ohtaka-Maruyama, C., Okado, H., Hashimoto, M., 2007. Expression of alpha-synuclein, a presynaptic protein implicated in Parkinson's disease, in erythropoietic lineage. Biochem. Biophys. Res. Commun. 358, 104–110. https://doi.org/10.1016/j.bbrc.2007.04.108

Nguyen, D.B., Ly, T.B.T., Wesseling, M.C., Hittinger, M., Torge, A., Devitt, A., Perrie, Y., Bernhardt, I., 2016. Characterization of Microvesicles Released from Human Red Blood Cells. Cell. Physiol. Biochem. Int. J. Exp. Cell. Physiol. Biochem. Pharmacol. 38, 1085–1099.

https://doi.org/10.1159/000443059

Nikam, S., Nikam, P., Ahaley, S.K., Sontakke, A.V., 2009. Oxidative stress in Parkinson's disease. Indian J. Clin. Biochem. IJCB 24, 98–101. https://doi.org/10.1007/s12291-009-0017-y

Porro, C., Trotta, T., Panaro, M.A., 2015. Microvesicles in the brain: Biomarker, messenger or mediator? J. Neuroimmunol. 288, 70–78. https://doi.org/10.1016/j.jneuroim.2015.09.006

Pretorius, E., Swanepoel, A.C., Buys, A.V., Vermeulen, N., Duim, W., Kell, D.B., 2014. Eryptosis as a marker of Parkinson's disease. Aging 6, 788–819. https://doi.org/10.18632/aging.100695

Quek, C., Hill, A.F., 2017. The role of extracellular vesicles in neurodegenerative diseases. Biochem. Biophys. Res. Commun. 483, 1178–1186. https://doi.org/10.1016/j.bbrc.2016.09.090

R Core Team, 2016. R: A language and environment for statistical computing. R Found. Stat. Comput.

Renella, R., Schlehe, J.S., Selkoe, D.J., Williams, D.A., LaVoie, M.J., 2014. Genetic deletion of the GATA1-regulated protein α-synuclein reduces oxidative stress and nitric oxide synthase levels in mature erythrocytes. Am. J. Hematol. 89, 974–977. https://doi.org/10.1002/ajh.23796

Rousseau, M., Belleannee, C., Duchez, A.-C., Cloutier, N., Levesque, T., Jacques, F., Perron, J., Nigrovic, P.A., Dieude, M., Hebert, M.-J., Gelb, M.H., Boilard, E., 2015. Detection and quantification of microparticles from different cellular lineages using flow cytometry. Evaluation of the impact of secreted phospholipase A2 on microparticle assessment. PloS One 10, e0116812. https://doi.org/10.1371/journal.pone.0116812

Scheer, F.A.J.L., Michelson, A.D., Frelinger, A.L., Evoniuk, H., Kelly, E.E., McCarthy, M., Doamekpor, L.A., Barnard, M.R., Shea, S.A., 2011. The human endogenous circadian system causes greatest platelet activation during the biological morning independent of behaviors. PloS One 6, e24549. https://doi.org/10.1371/journal.pone.0024549

Shamir, R., Klein, C., Amar, D., Vollstedt, E.-J., Bonin, M., Usenovic, M., Wong, Y.C., Maver, A., Poths, S., Safer, H., Corvol, J.-C., Lesage, S., Lavi, O., Deuschl, G., Kuhlenbaeumer, G., Pawlack, H., Ulitsky, I., Kasten, M., Riess, O., Brice, A., Peterlin, B., Krainc, D., 2017. Analysis of blood-based gene expression in idiopathic Parkinson disease. Neurology 89, 1676–1683. https://doi.org/10.1212/WNL.0000000000004516

Shevchenko, A., Wilm, M., Vorm, O., Mann, M., 1996. Mass spectrometric sequencing of proteins silver-stained polyacrylamide gels. Anal. Chem. 68, 850–858.

Shi, M., Liu, C., Cook, T.J., Bullock, K.M., Zhao, Y., Ginghina, C., Li, Y., Aro, P., Dator, R., He, C., Hipp, M.J., Zabetian, C.P., Peskind, E.R., Hu, S.-C., Quinn, J.F., Galasko, D.R., Banks, W.A., Zhang, J., 2014. Plasma exosomal α-synuclein is likely CNS-derived and increased in Parkinson's disease. Acta Neuropathol. (Berl.) 128, 639–650. https://doi.org/10.1007/s00401-014-1314-y

Stuendl, A., Kunadt, M., Kruse, N., Bartels, C., Moebius, W., Danzer, K.M., Mollenhauer, B., Schneider, A., 2016. Induction of α-synuclein aggregate formation by CSF exosomes from patients with Parkinson's disease and dementia with Lewy bodies. Brain J. Neurol. 139, 481–494. https://doi.org/10.1093/brain/awv346

Sudha, K., Rao, A.V., Rao, S., Rao, A., 2003. Free radical toxicity and antioxidants in Parkinson's disease. Neurol. India 51, 60–62.

Suzuki, R., Shimodaira, H., 2006. Pvclust: an R package for assessing the uncertainty in hierarchical clustering. Bioinforma. Oxf. Engl. 22, 1540–1542. https://doi.org/10.1093/bioinformatics/btl117

Tomlinson, P.R., Zheng, Y., Fischer, R., Heidasch, R., Gardiner, C., Evetts, S., Hu, M., Wade-Martins, R., Turner, M.R., Morris, J., Talbot, K., Kessler, B.M., Tofaris, G.K., 2015. Identification of distinct circulating exosomes in Parkinson's disease. Ann. Clin. Transl. Neurol. 2, 353–361. https://doi.org/10.1002/acn3.175

Tsunemi, T., Hamada, K., Krainc, D., 2014. ATP13A2/PARK9 regulates secretion of exosomes and α-synuclein. J. Neurosci. Off. J. Soc. Neurosci. 34, 15281–15287. https://doi.org/10.1523/JNEUROSCI.1629-14.2014

Vestad, B., Llorente, A., Neurauter, A., Phuyal, S., Kierulf, B., Kierulf, P., Skotland, T., Sandvig, K., Haug, K.B.F., Øvstebø, R., 2017. Size and concentration analyses of extracellular vesicles by nanoparticle tracking analysis: a variation study. J. Extracell. Vesicles 6, 1344087. https://doi.org/10.1080/20013078.2017.1344087

Vogel, R., Coumans, F.A.W., Maltesen, R.G., Böing, A.N., Bonnington, K.E., Broekman, M.L., Broom, M.F., Buzás, E.I., Christiansen, G., Hajji, N., Kristensen, S.R., Kuehn, M.J., Lund, S.M., Maas, S.L.N., Nieuwland, R., Osteikoetxea, X., Schnoor, R., Scicluna, B.J., Shambrook, M., de Vrij, J., Mann, S.I., Hill, A.F., Pedersen, S., 2016. A standardized method to determine the concentration of extracellular vesicles using tunable resistive pulse sensing. J. Extracell. Vesicles 5, 31242.

Wang, X., Yu, S., Li, F., Feng, T., 2015. Detection of α-synuclein oligomers in red blood cells as a potential biomarker of Parkinson's disease. Neurosci. Lett. 599, 115–119. https://doi.org/10.1016/j.neulet.2015.05.030

Willis, G.R., Kourembanas, S., Mitsialis, S.A., 2017. Toward Exosome-Based Therapeutics: Isolation, Heterogeneity, and Fit-for-Purpose Potency. Front. Cardiovasc. Med. 4, 63. https://doi.org/10.3389/fcvm.2017.00063

Wither, M.J., Hansen, K.C., Reisz, J.A., 2016. Mass Spectrometry-Based Bottom-Up Proteomics: Sample Preparation, LC-MS/MS Analysis, and Database Query Strategies. Curr. Protoc. Protein Sci. 86, 16.4.1-16.4.20. https://doi.org/10.1002/cpps.18

Zeng, B.Y., Dass, B., Owen, A., Rose, S., Cannizzaro, C., Tel, B.C., Jenner, P., 1999. Chronic L-DOPA treatment increases striatal cannabinoid CB1 receptor mRNA expression in 6-hydroxydopamine-lesioned rats. Neurosci. Lett. 276, 71–74.

**Figures legends**

**Table 1. Participant clinical information – PD cohort**. Disease severity as measured using the H&Y scale (score): Mild (1-1.5); Moderate (2-2.5); Severe (3-3.5). **p* < 0.05 vs. CTRL. Statistical analyses were performed using a Kruskal Wallis test followed by Dunn's multiple comparison test.

**Figure 1. A**. **Blood cell quantification**. Full blood counts performed in PD patients (*n*=57) revealed no significant differences in the total number of any cell type between patients and their respective healthy sex- and age-matched CTRL (*n*=37), except for erythrocytes. Statistical analyses were performed using unpaired t-tests when data followed normal distributions according to the Shapiro-Wilk test or Mann-Witney in cases of non-normality. **B**. **Cell-derived EV quantification**. The quantification of EV in platelet-free plasma of PD patients and controls was performed by high-sensitivity flow cytometry. Phosphatidylserine was evaluated with Annexin V binding. The complete blood count was obtained at the time of blood sampling for 35|37 Controls and 57|59 PD and was used to calculate the EV per cell ratio. Statistical analyses were performed using a Two-Way ANOVA. * For erythrocyte-derived EV quantification, 1 outlier (determined using Grubbs' method with alpha=0.0001) was removed. **C. Diagnostic Value.** Distribution plots of CD235a+ EV/total number of erythrocytes between PD and healthy sex- and age-matched CTRL (PD, n=42; CTRL, n=24). **Abbreviation:** CD235a-45-41-31-15-14, cluster of differentiation; CTRL, Control; EV, extracellular vesicle; EEV, erythrocyte-derived extracellular vesicle; PD, Parkinson's disease; PS, phosphatidylserine; UPDRS, Unified Parkinson's Disease Rating Scale.

**Figure 2. Relationship between EEV and clinical measures of PD. A**. Absence of correlations between EEV/Erythrocyte counts and H&Y stage. **B**. Correlations between EEV/Erythrocyte counts with total UPDRS scores. **C**. Robust correlations between the number of EEV/total number of erythrocytes and UPDRS scores (PD, *n*=20, from the UK cohort exclusively since the Quebec cohort did not have recent UPDRS scores available). **D**. EV/erythrocytes ratios, UPDRS scores and LEDD values for all PD patients used in the correlation analyses. **E**. Absence of correlation between the number of EEV and LEDD. Correlations reported were determined using Pearson's goodness-of-fit test. **Abbreviation:** CD235a, glycophorin A; CTRL, Control; EEV, erythrocyte-derived extracellular vesicle; H&Y, Hoehn and Yahr; LEDD, Levodopa equivalent daily dose; PD, Parkinson's disease; UPDRS, Unified Parkinson's Disease Rating Scale.

**Figure 3. A-B. Proteomic analyses with and without hemoglobin**. To ensure the specificity of the protein signature detected in EEV, we performed proteomic analyses using two distinct methodologies. **A**. The first set of analyses by nanoLC-MS/MS and Label Free Quantification was performed on the complete proteome of the EEV, yielding 356 proteins. **B**. The second set of analyses was also performed on the entire EEV proteome but this time, isolating hemoglobin and quantifying the proteins present in both fractions. This approach uncovered 708 proteins in the EEV proteome with an additional 110 proteins in the hemoglobin fraction for a total of 818 proteins, indicating that removing hemoglobin provides a much more accurate evaluation of the protein content of EEV. **C-D. Specific protein signature of EEV in PD patients**. **B**. NanoLC-MS/MS Label-free analysis of EEV in PD patients and healthy age-matched CTRL revealed a total of 818 proteins, of which 8 had an expression that was significantly different as a function of PD stage (**C**). The proteins/genes have been further separated into 3 groups in relation to their variations in comparison to CTRL (Group I), mild PD (Group II) or moderate PD (Group III). **D**. Heatmap establishing correlations between disease stages and the abundance of the variable proteins. Cold and hot colours represent low and high correlation levels, respectively. The AU *p* value is indicated for each node. Protein level changes were determined by Welch's test *p* value < 0.05 and absolute value of z-score > 1.96, **p*<0.05, ***p*<0.01. **Abbreviations**: AU, Approximately Unbiased; CTRL Control; PD,

Parkinson's disease. **E**. The protein ratios (log2(ratio)) of the three comparisons (mild PD/CTRL, moderate PD/CTRL and moderate PD/mild PD) were plotted over the corresponding Welch's test *p* value (-log10(p-value)). The graphs display a V shape, as expected, and only the proteins falling outside the limits of a *p* value < 0.05 and absolute value of z-score > 1.96 (identified by black lines) were considered as variant proteins (red dots). Two variant proteins were excluded given that they were quantified using only one peptide. **Abbreviations**: ABHD14B, alpha/beta hydrolase domain-containing protein 14B; AIDA, axin interactor dorsalization-associated protein; AKR1A1, alcohol dehydrogenase NADP+; ATP5A1, ATP synthase subunit alpha mitochondrial; CNRIP1, cannabinoid receptor-interacting protein 1; CTRL: Control; NADSYN1, glutamine-dependent NAD(+) synthetase; USP24, ubiquitin carboxyl-terminal hydrolase 24; PD, Parkinson's disease; QDPR, Quinoid Dihydropteridine Reductase.

**Figure 4. Detection of normal and phosphorylated α-Syn in EEV**. **A**. Representative scanning electron micrographs of resting and activated erythrocytes in both PD patients and healthy sex- and age-matched CTRL. Scale bar: 2µm. **B**. Representative transmission electron microscopy images of immunogold labeling for α-Syn and α-Syn pS129 in activated erythrocytes and EEV (some examples delineated by dotted lines). Arrowheads point to positive immunolabeling for either α-Syn or α-Syn pS129. Scale bar: 100nm. **C**. Quantification of α-Syn in EEV as detected by transmission electron microscopy and expressed as the percentage of EEVs positive for α-Syn/total number of EEV in healthy sex- and age-matched CTRL and PD patients (*n*=100 erythrocytes sampled in *n*=3 CTRL and *n*=3 PD). **D**. Quantification of α-Syn in EEV by ELISA assays in healthy sex- and age-matched CTRL, mild and moderate stage patients (*n*=4 erythrocytes per group; *n*=13 EEV per group) showed no measurable changes in α-Syn levels between PD and healthy sex- and age-matched CTRL. Statistical analyses were performed using a Mann-Whitney *U* test (**C**) or a Kruskal-Wallis test (**D**). **Abbreviations**: α-Syn, α-synuclein; α-Syn pS129, α-synuclein phosphorylated Serine 129; CTRL, Control; EEV, erythrocyte-derived extracellular vesicle; PD, Parkinson's disease.

**Supplementary figures**

**Figure S1. Erythrocyte and EV implication in PD**: **summary of the literature.** The search for a reliable biomarker in PD has included investigations on neuronal cells in specific *in vitro* systems, on cellular elements within the circulatory system, the CSF and urine with a targeted interest on the expression of α-Syn. However, none of these studies have convincingly identified a robust marker of PD. **Abbreviations**: αSyn, α-synuclein; CAT, Catalase; GPx, glutathione peroxidase; L1CAM, L1 cell adhesion molecule; LRRK2, Leucine-rich repeat kinase 2; RBC, red blood cells; SOD, superoxide dismutase; ✓ presence; ↑ increase; ↓ decrease.

**Figure S2. Optimization of EV detection: controls for flow cytometry**. *Controls for EV identification*. **A**. To properly set the EV gate, fluorescent silica beads of 100nm (*Red*), 500nm (*Blue*) and 1000nm (*Yellow*) were acquired on a flow cytometer Canto II modified with a FSC-PMT small particle option. **B**. Serial dilutions of EEV (1, 2, 4 and 10) were used to confirm the linearity of the quantification. **C**. FSC-PMT/SSC gates of PFP stained with annexin V and respective fluorochrome-conjugated antibodies directed against erythrocyte (CD235a+), endothelial (CD31+/CD41-), platelet (CD41+) and leukocyte (CD14+CD45+, monocytes; CD15+CD45+, granulocytes)-derived EVs. *Controls for EV labeling*. **D**. Treatment with the ion chelator EDTA inhibited the binding of annexin V to phosphatidylserine. **E**. Minimal background was observed using antibodies in the absence of PFP and was subtracted from all subsequent EV quantifications. **F**. EV sensitivity to 0.5% triton was further assessed **G**. *Reproducibility of EEV counts over time*. EEV/Erythrocytes counts and CV% obtained for the 25 additional participants. Each subject provided 2 samples at two distinct time points (C#-1: Patient#-Time 1, C#-2: Patient#-Time 2) yielding 2 measurements per patient. **Abbreviations**: AnnV, annexinV; EV, extracellular vesicle; EEV, erythrocyte-derived extracellular vesicle; FSC PMT-H, forward scatter photomultiplier tube; PBS, phosphate buffered saline; PFP, platelet free plasma; SSC-H, side scatter.

**Figure S3. Blood counts and exclusion criteria**. **A**. Evaluated hematocrit, mean corpuscular hemoglobin and mean corpuscular volumes were similar between groups (PD, *n*=43; CTRL, *n*=24). **B**. CRP (indicative of an inflammatory response) and free hemoglobin (indicative of hemolysis) (**C**) were further quantified in the PFP (PD, *n*=59; CTRL, *n*=37). Individuals presenting with levels exceeding 45 000ng/ml were excluded from the study to remove the possibility that these factors contributed to increased EEV concentrations. Statistical analyses were performed using Kruskal-Wallis test (**A-B**) and Mann-Whitney *U* tests (**C-E**). **Abbreviations**: CTRL, controls; CRP, C-reactive protein; PD, Parkinson's disease; PFP, platelet-free plasma.

**Figure S4. Relation between EEV and clinical measures of PD in additional cohort. A**. Correlations between EEV/Erythrocyte counts with total UPDRS scores for mild (**B**), moderate (**C**) and severe patients (**D**) **E**. EV/erythrocytes ratios, UPDRS scores and LEDD values for all PD patients used in the correlation analyses. **F**. Absence of correlation between the number of EEV and LEDD. Correlations reported were determined using Pearson's goodness-of-fit test.

**Figure S5**. **A**. **Cell-derived EV quantification of – HD cohort**. The quantification of EV in platelet-free plasma of HD patients and controls was performed by high-sensitivity flow cytometry. Phosphatidylserine was evaluated with Annexin V binding. The complete blood count was obtained at the time of blood sampling for 53|54 CTRL, 10 pre-manifest and 48|50|51 HD patients and was used to calculate the EV per cell ratio. Statistical analyses were performed using Two-Way ANOVA. **B.** Distribution plots of CD235a+/total number of erythrocytes revealed no differences between HD and healthy sex- and age-matched CTRL (HD, *n*=50; Pre-HD, *n*=10; CTRL, *n*=52) and **C.** no statistically

significant correlations were found between the number of EEV/total number of erythrocytes and UHDRS scores (HD, $n$=42). Correlations were determined using Pearson's goodness-of-fit test, $^{*}p<0.05$. **Abbreviations**: ACE, Addenbrooke's Cognitive Examination; BDI, Beck Depression Inventory; BDS, Burden of Disease Score; CD235a, glycophorin A; CTRL, Controls; EEV, erythrocyte-derived extracellular vesicle; EV, extracellular vesicle; HD, Huntington's disease; H&Y, Hoehn and Yahr; MMSE, Mini-Mental State Examination; Pre-HD, Pre-manifest; PS, phosphatidylserine; TFC, Total Functional Capacity; UHDRS, Unified Huntington's Disease Rating Scale.

**Figure S6.** A Gene Ontology enrichment analysis was performed on the Cellular Component ontology using BinGO software. The list of 356 identified proteins in the entire EEV (**A**) and the list of the 818 identified proteins when hemoglobin was analyzed separately (**B**) were compared to the whole human proteome (reference list). Circle size is proportional to the number of proteins matching the corresponding GO term and the color scale corresponds to the $p$ value of enrichment (darker orange corresponds to greater statistical enrichments).

**Table S1. Participant clinical information – HD cohort**. Disease severity levels in relation to the TFC scale: Stage 1 (11-13); Stage 2 (7-10); Stage 3 (3-6); Stage 4 (1-2); Stage 5 (0). Disease severity was evaluated within 6 months of blood sampling. Comorbidities were determined from medical information reported by the participant or caregiver. **Blood cell quantification**. Full blood counts performed in HD patients at different stages of the disease (Pre-HD, n=10; Stage 1, n=15; Stage 2, n=12; Stage 3, n=11; Stage 4, n=10; Stage 5, n=2) revealed no significant differences in the total number of any cell type between patients and their respective healthy sex- and age-matched CTRL ($n$=54), except for erythrocytes. Statistical analyses were performed using a Kruskal Wallis test followed by Dunn's multiple comparison test.

**Table S2**. **Participant clinical information – PD cohort no.2**. Disease severity as measured using the UPDRS scale (score): Mild (0,39); Moderate (29,73); Severe (57,74). $^{*}p < 0.05$ vs. CTRL. Statistical analyses were performed using a Kruskal Wallis test followed by Dunn's multiple comparison test.

**Table S3. Complete list of proteins identified in the EEV proteome**. Lists of the protein groups identified by LC-MS/MS analysis using Andromeda/MaxQuant search engine in the Uniprot Complete Proteome *Homo sapiens* database for the non-depleted sample (356 proteins) (**A**) or when hemoglobin was analyzed separately (818 proteins) (**B**). The lists were filtered at 1% False Discovery Rate using a target/decoy database search.

# Figure 1.

**A**

## Blood cell quantification

| Cell type | Units | CTRL n | CTRL Mean | CTRL SD | PD n | PD Mean | PD SD | *p* value |
|---|---|---|---|---|---|---|---|---|
| Erythrocytes | $10^9$/ml | 35 | 4.75 | 0.61 | 56 | 4.56 | 0.47 | **0.049** |
| Platelets | $10^6$/ml | 35 | 235 | 44 | 56 | 217 | 50 | 0.083 |
| Leukocytes | $10^6$/ml | 35 | 6.91 | 1.62 | 56 | 6.53 | 1.97 | 0.347 |
| Monocytes | $10^6$/ml | 35 | 0.56 | 0.14 | 56 | 0.53 | 0.18 | 0.308 |
| Granulocytes | $10^6$/ml | 35 | 4.34 | 1.38 | 56 | 4.32 | 1.62 | 0.979 |

**B**

## Cell-derived EV quantification

| Cell type | Markers | Units | CTRL n | CTRL Mean | CTRL SEM | PD n | PD Mean | PD SEM | *p* value |
|---|---|---|---|---|---|---|---|---|---|
| Erythrocytes | **CD235a+PS-** | **$10^3$/µl** | **36** | **18.2** | **46.5** | **59** | **32.0** | **36.3** | **0.04** |
| | CD235a+PS+ | $10^3$/µl | 36 | 0.22 | 0.07 | 59 | 0.29 | 0.05 | 0.70 |
| | **CD235a+ total** | **$10^3$/µl** | **36** | **18.4** | **47.0** | **59** | **32.3** | **36.7** | **0.04** |
| | **EV CD235a+/erythrocyte** | | **34** | **0.0039** | **0.011** | **57** | **0.0069** | **0.008** | **0.03** |
| Platelets | CD41+PS- | $10^3$/µl | 37 | 7.88 | 1.68 | 59 | 10.3 | 1.33 | 0.27 |
| | CD41+PS+ | $10^3$/µl | 37 | 15.2 | 3.20 | 59 | 17.9 | 2.53 | 0.51 |
| | CD41+ total | $10^3$/µl | 37 | 23.1 | 4.62 | 59 | 28.2 | 3.66 | 0.38 |
| | EV CD41+/platelet | | 35 | 0.106 | 0.021 | 57 | 0.125 | 0.016 | 0.49 |
| Endothelial cells | CD31+CD41-PS- | $10^3$/µl | 37 | 15.8 | 8.04 | 59 | 11.7 | 6.37 | 0.75 |
| | CD31+CD41-PS+ | $10^3$/µl | 37 | 0.91 | 0.13 | 59 | 0.92 | 0.10 | 0.96 |
| | CD31+CD41- total | $10^3$/µl | 37 | 16.7 | 8.03 | 59 | 12.6 | 6.36 | 0.75 |
| Leukocytes | CD45+ total | $10^3$/µl | 37 | 10.4 | 2.21 | 59 | 13.8 | 1.75 | 0.26 |
| Monocytes | CD45-CD14+ PS- | $10^3$/µl | 37 | 1.70 | 0.30 | 59 | 1.62 | 0.24 | 0.85 |
| | CD45-CD14+ PS+ | $10^3$/µl | 37 | 1.20 | 4.00 | 59 | 5.84 | 3.17 | 0.50 |
| | CD45+CD14+ PS- | $10^3$/µl | 37 | 0.16 | 0.04 | 59 | 0.14 | 0.03 | 0.74 |
| | CD45+CD14+PS+ | $10^3$/µl | 37 | 0.60 | 0.79 | 59 | 1.47 | 0.63 | 0.59 |
| | CD14+ total | $10^3$/µl | 37 | 3.66 | 4.88 | 59 | 9.06 | 3.87 | 0.60 |
| | EV CD14+ /monocyte | | 35 | 7.08 | 1.99 | 57 | 9.16 | 1.56 | 0.41 |
| Granulocytes | CD45-CD15+ PS- | $10^3$/µl | 37 | 12.3 | 7.96 | 59 | 16.7 | 6.30 | 0.92 |
| | CD45-CD15+ PS+ | $10^3$/µl | 37 | 2.21 | 0.77 | 59 | 1.39 | 0.61 | 0.47 |
| | CD45+CD15+ PS- | $10^3$/µl | 37 | 0.55 | 0.36 | 59 | 1.15 | 0.29 | 0.20 |
| | CD45+CD15+PS+ | $10^3$/µl | 37 | 1.01 | 0.30 | 59 | 1.25 | 0.24 | 0.56 |
| | CD15+ total | $10^3$/µl | 37 | 16.0 | 8.83 | 59 | 20.6 | 6.99 | 0.91 |

**C**

**Diagnostic value**

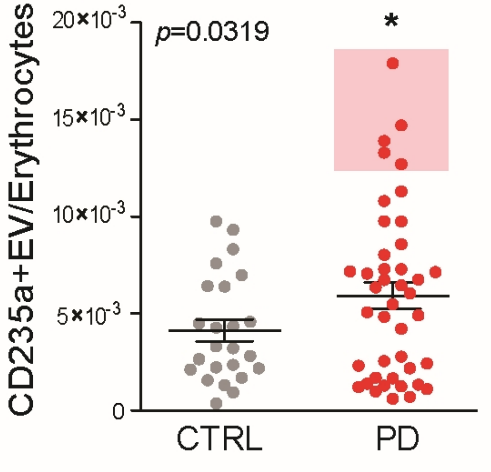

# Figure 2.

## EEV in relation to clinical measures

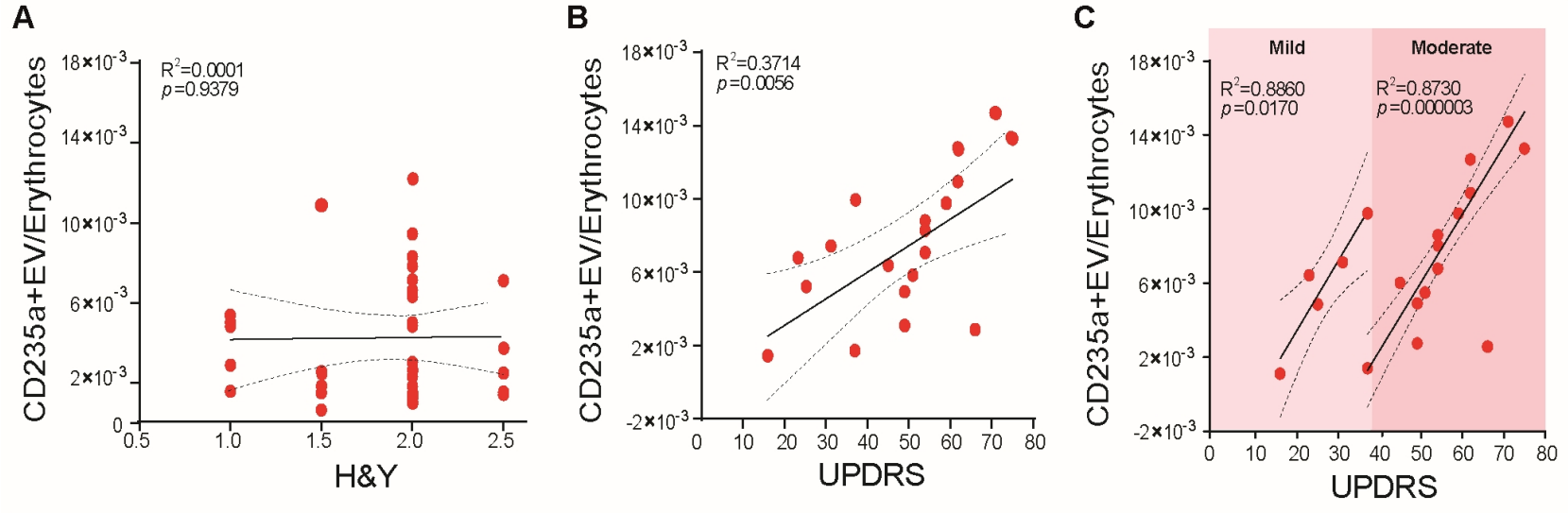


## LEDD and EV

D

| Patients | EV/erythrocyte | UPDRS | LEDD |
|---|---|---|---|
| PD1 | $1.10x10^{-3}$ | 16 | 100mg |
| PD2 | $6.45x10^{-3}$ | 23 | 386mg |
| PD3 | $4.83x10^{-3}$ | 25 | 220mg |
| PD4 | $7.14x10^{-3}$ | 31 | 705mg |
| PD5 | $9.75x10^{-3}$ | 37 | 100mg |
| PD6 | $1.38x10^{-3}$ | 37 | 300mg |
| PD7 | $6.04x10^{-3}$ | 45 | 820mg |
| PD8 | $2.78x10^{-3}$ | 49 | 740mg |
| PD9 | $4.91x10^{-3}$ | 49 | 950mg |
| PD10 | $5.47x10^{-3}$ | 51 | 250mg |
| PD11 | $6.75x10^{-3}$ | 54 | 740mg |
| PD12 | $8.57x10^{-3}$ | 54 | 475mg |
| PD13 | $8.03x10^{-3}$ | 54 | 550mg |
| PD14 | $9.77x10^{-3}$ | 59 | 850mg |
| PD15 | $10.8x10^{-3}$ | 62 | 450mg |
| PD16 | $12.7x10^{-3}$ | 62 | 500mg |
| PD17 | $25.5x10^{-3}$ | 66 | nil |
| PD18 | $14.7x10^{-3}$ | 71 | 254mg |
| PD19 | $13.3x10^{-3}$ | 75 | 700mg |

E

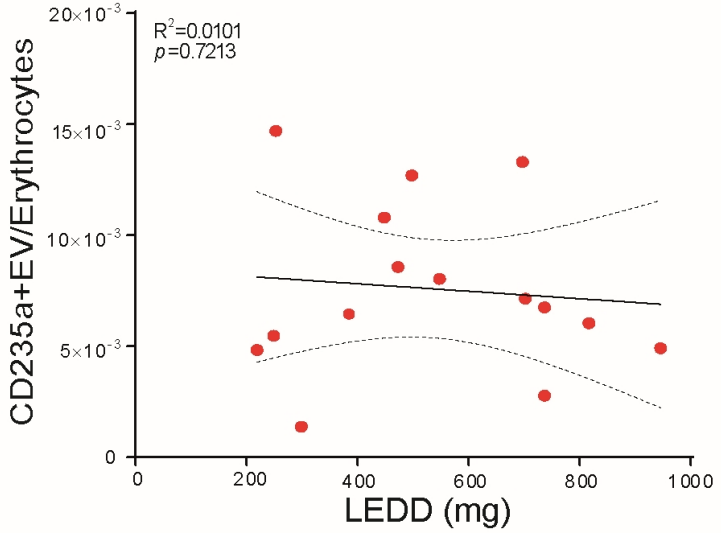

# Figure 3.

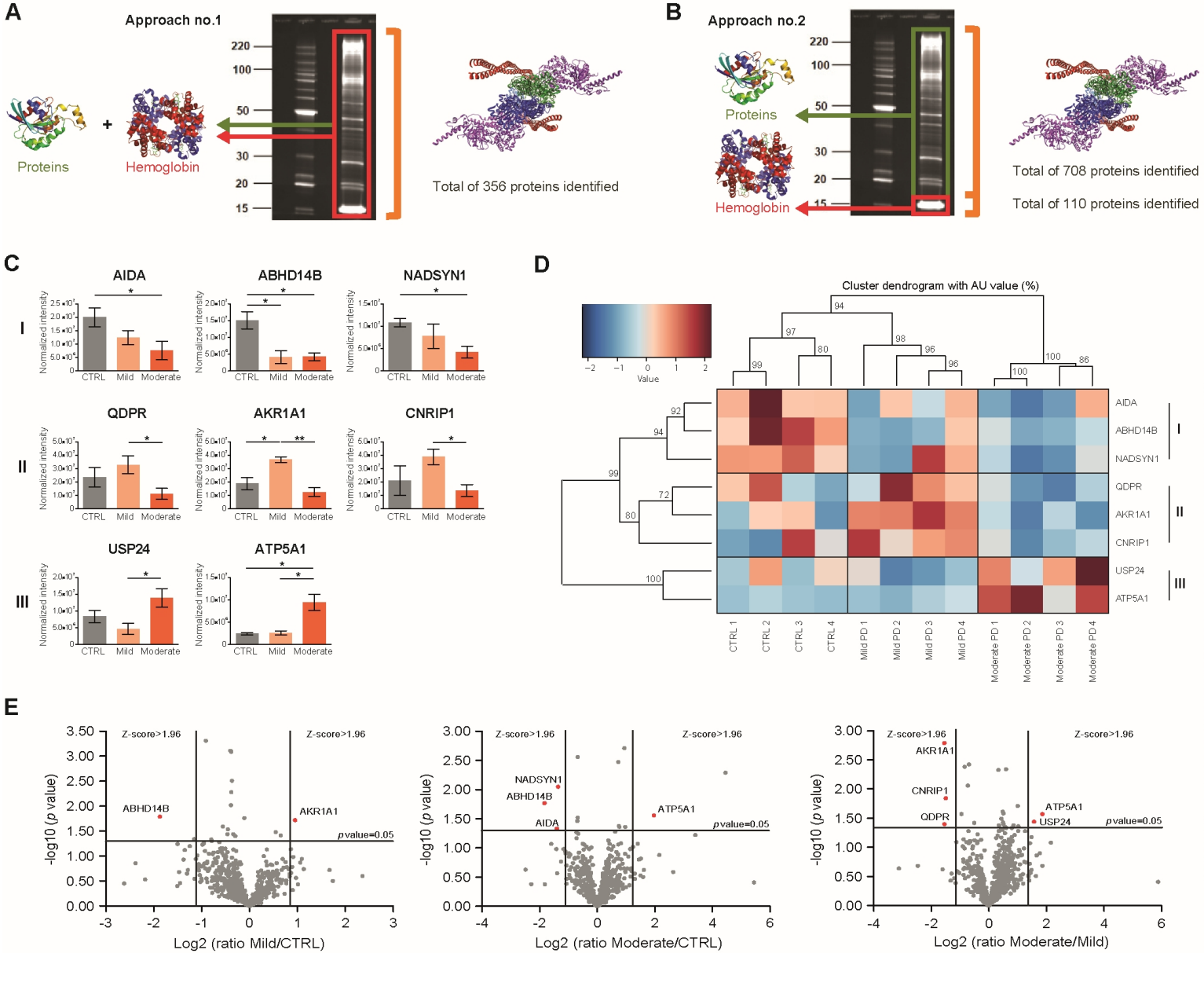
A
Approach no.1
Proteins
Hemoglobin
220
100
50
30
20
15
Total of 356 proteins identified
B
Approach no.2
Proteins
Hemoglobin
Total of 708 proteins identified
Total of 110 proteins identified
C
AIDA
ABHD14B
NADSYN1
QDPR
AKR1A1
CNRIP1
USP24
ATP5A1
Normalized intensity
CTRL
Mild
Moderate
I
II
III
D
Cluster dendrogram with AU value (%)
Value
AIDA
ABHD14B
NADSYN1
QDPR
AKR1A1
CNRIP1
USP24
ATP5A1
CTRL 1
CTRL 2
CTRL 3
CTRL 4
Mild PD 1
Mild PD 2
Mild PD 3
Mild PD 4
Moderate PD 1
Moderate PD 2
Moderate PD 3
Moderate PD 4
E
Z-score>1.96
ABHD14B
AKR1A1
NADSYN1
AIDA
ATP5A1
CNRIP1
QDPR
USP24
pvalue=0.05
-log10 (p value)
Log2 (ratio Mild/CTRL)
Log2 (ratio Moderate/CTRL)
Log2 (ratio Moderate/Mild)

# Figure 4.

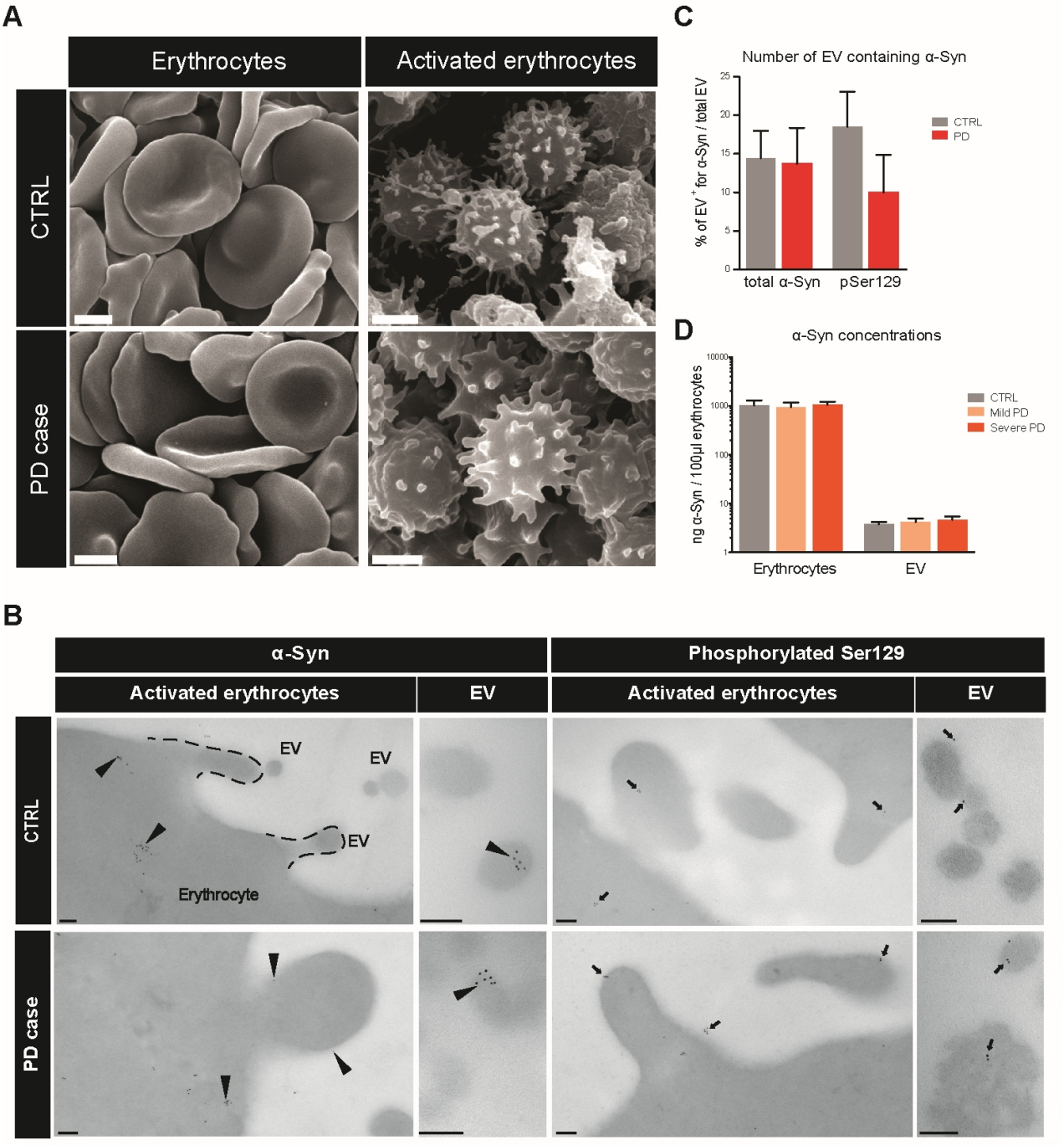
A
Erythrocytes
Activated erythrocytes
CTRL
PD case
C
Number of EV containing α-Syn
% of EV+ for α-Syn / total EV
25
20
15
10
5
0
CTRL
PD
total α-Syn
pSer129
D
α-Syn concentrations
ng α-Syn / 100µl erythrocytes
10000
1000
100
10
1
CTRL
Mild PD
Severe PD
Erythrocytes
EV
B
α-Syn
Phosphorylated Ser129
Activated erythrocytes
EV
Activated erythrocytes
EV
CTRL
PD case
EV
EV
EV
Erythrocyte

## SI Materials and methods

### Preparation of platelet-free plasma and EV labeling

For all experiments, diluted annexin-V buffer (BD Pharmingen, Mississauga, ON, Canada) and phosphate buffered saline (PBS) were filtered on 0.22µm pore size membranes (PALL, Mississauga, ON, Canada). To quantify EV according to their cell of origin, the following surface markers were used: CD235a+ (erythrocytes) (5µl), CD31+/CD41- (endothelial cells) (1µl), CD41+ (platelets) (5µl), CD45+ (leukocytes) (3µl), CD45+CD14+ (monocytes) (10µl), and CD45+CD15+ (granulocytes) (2µl), with or without annexin-V staining (5µl). PFP (5µl) was incubated with Phenylalanyl-prolyl-arginyl Chloromethyl Ketone (PPACK) 10mM (Calbiochem, Etobicoke, ON, Canada) for 5 minutes followed by a 30-minute incubation with antibodies and annexin-V in a final PBS volume of 100µl, all at room temperature. Finally, samples were diluted to a final volume of 2ml prior to FACS analysis. The following antibodies were purchased from BD Pharmingen and used for all analyses: FITC-conjugated mouse anti-human CD235a (clone GA-R2 (HIR2), 1/20), PE-conjugated mouse anti-human CD31 (clone WM59, 1/100), V450-conjugated mouse anti-human CD41a (clone HIP8, 1/20), V450-conjugated mouse anti-human CD45 (clone HI30, 1/33), APC mouse anti-human CD14 (clone M5E2, 1/10), PE-conjugated mouse anti-human CD15 (clone HI98, 1/50), V450- and PerCP-Cy$^{TM}$5.5-conjugated annexin-V (1/20).

### Flow cytometry quantification

The acquisition of EV was performed at low speed at an approximated rate of 10µl/min. To determine background noise levels, antibody mixes were incubated in the absence of PFP sample and unlabeled PFP was used as a negative control. Every sample was re-identified to ensure that the experimenter was blind to clinical status.

### Production and purification of EEV

Briefly, the erythrocyte pellet was activated with 3 volumes of calcium ionophore solution (150mM NaCl; 10mM Tris-HCl; 1mM CaCl2; 5µM ionophore A23187 (Sigma, St Louis, MO)) for 30 minutes at 37°C. Calcium ionophore is key to EV biogenesis. It participates in the activation and inhibition of proteins and phospholipids at the cell membrane. Calcium ionophore A23187 induces a change in the concentration of calcium which leads to vesicle formation. In contrast to water and freezing, which are frequently used to provoke the release of EEV, calcium ionophores avoid the destruction of the erythrocyte membranes (Nguyen et al., 2016). The activation was stopped by the addition of 5mM EDTA. Remaining erythrocytes

were pelleted at 15 000g for 20 minutes. The EEV were centrifuged at 20 000g for 90 minutes and washed once in PBS. The EV pellet was re-suspended in PBS and frozen at -80°C until further analyses.

**Scanning electron microscopy**

Preparations of erythrocytes (5µl) were fixed in 2% paraformaldehyde and 2.5% glutaraldehyde in PBS buffer at least 24 hours before standard dehydration. Samples were washed 3 times for 10 minutes with sodium cacodylate buffer (0.1M, pH 7.3) and fixed with 1% osmium tetroxide in sodium cacodylate buffer for 90 minutes. Subsequently, samples were washed and processed in 50%, 70%, 90% and 100% EtOH for dehydration (10 minutes/step). Finally, samples were soaked in two subsequent baths of 100% EtOH, for 40 minutes and 10 minutes, air-dried overnight and coated with palladium. Observations were completed using a JEOL 6360LV scanning electron microscope (JEOL, Peabody, MA, USA).

**Transmission electron microscopy**

Preparations of EEV (30µl) and activated erythrocytes (5µl) were fixed in 2% paraformaldehyde at least 24 hours before being dehydrated and sealed in LR white. Slices of LR white were placed on a Formvar/carbon-coated grid and processed for immunolabeling. The tissues mounted on grids were blocked in 0.5% BSA-c (Aurion, Wageningen, The Netherlands) in HBSS and incubated for 120 minutes with rabbit anti-α-Syn antibody (Abcam, Toronto, ON, Canada) or rabbit anti-α-Syn (phospho S129) antibody (Abcam, Toronto, ON, Canada), both diluted at 1:250 in HBSS and washed several times with distilled water. Finally, the grids were incubated for 60 minutes with an anti-rabbit IgG conjugated to 6nm gold particles (EMS, Hatfield, PA, USA) diluted at 1:200, washed several times with distilled water and then fixed in 2.5% glutaraldehyde (EMS, Hatfield, PA, USA) in HBSS for 15 minutes. For this last step, the grids were treated with 3% uranyl acetate–0.075 M oxalate (pH 7.0) (EMS, Hatfield, PA, USA) for 1 minute, which was followed by several washes in distilled water. All staining experiments included negative controls where the primary antibody was omitted from the incubation media. Observations were completed with a TECNAI Spirit G2 transmission electron microscope at 80kV (FEI, Hillsboro, OR, USA).

**Mass spectrometry analysis and label free protein quantification**

The extracted peptides from the 7 slices of the same individual were pooled and analyzed by nanoLC-MS/MS. The excised hemoglobin gel slices were also analyzed in the same conditions. One µg of each individual sample was injected on a Dionex UltiMate 3000 nanoRSLC system (Thermo Scientific)

equipped with a nanoviper Acclaim Pepmap100, C18, 3µm, 75µm x 50cm column (Thermo Scientific) connected to the nanoelectrospray source of an Orbitrap Fusion mass spectrometer (Thermo Scientific). The peptides were eluted at 300nL/min using an acetonitrile gradient of 90 minutes with the mass spectrometer operating in the Data Dependent Acquisition mode. Peptide masses were measured in MS spectra detected in the orbitrap at 120K resolution. MSMS fragmentation spectra of peptides were generated by Higher energy Collisional Dissociation (HCD) and detected in the ion trap.

**Statistical analyses**

Initial statistical analyses (unpaired t-tests when data followed normal distribution according to Shapiro-Wilk test or Mann-Witney in cases of non-normality) compared the number of each type of blood cells (erythrocytes, platelets, leukocytes, neutrophils, monocytes, lymphocytes) in control groups and patients of all stages of the UK to the Canadian cohorts. Comparison between each type of EV from every cells including erythrocytes, platelets, leukocytes, neutrophils, monocytes, lymphocytes and endothelial cells were performed using Two-Way ANOVA. This revealed no statistical differences between groups, allowing us to pool cohorts for subsequent analyses. Statistical analyses pertaining EEV quantification were performed using *The Statistics and Machine Learning Toolbox* provided by MathWorks™ under MATLAB™ platform using the MATLAB®R2015a version. Results obtained include the scatter plots, classical least-square linear regressions, R-squared and *p* values, as well as Pearson's goodness-of-fit. Interval cut-off values were determined using a loop program developed in MATLAB™. Model diagnostics, including residual behaviour and homoscedastivity, were obtained using the same Toolbox. Further details on the statistical tests chosen are described directly in the result section. For α-Syn quantification, data were first tested for normality using the D'Agostino & Pearson normality test. Comparisons between groups were obtained by Mann-Whitney *U* test or Kruskal-Wallis ANOVA and performed using Prism 6.0 (GraphPad Software, LaJolla, CA). For proteomic analyses, the 'Intensity values' contained in the output 'proteingroup.txt' file of MaxQuant were used to quantify each identified protein in each individual sample. The values were normalized by the median of each column (all intensity values of proteins for one sample). The missing values were imputed with a noise value corresponding to the 1-percentile of each sample column. For each comparison between two groups (Control, mild PD or moderate PD), proteins with too many imputed values where considered not quantifiable (a minimum of three not-imputed values in one of the 2 groups are required). A protein ratio was calculated between the two groups using the average of intensity values in each group. Finally, a statistical Welch's test was performed between the two groups. The protein ratios were transformed

into log2(ratio) then centered by calculation of a z-score (z-score = (x - μ)/σ). A protein was considered as variant if it fulfilled the following criteria: minimum of 2 peptides quantified, Welch's test *p* value < 0.05 and absolute value of z-score > 1.96 (corresponding to values outside of the 95% confidence interval). The Gene Ontology enrichment analysis on the identified proteins was performed on the Cytoscape platform (v. 3.4.0) using the BinGO software version 3.0.3 against all human genes with GO annotation (Uniprot-GOA generated 2015-06-22) (Maere et al., 2005). Enrichment was calculated by a hypergeometric test and Bonferroni Family-Wise Error Rate (FWER) was used to correct for multiple testing. The data for the resulting 8 proteins was standardized, hierarchically clustered and visualized as a heatmap by using the statistical framework R (R Core Team, 2016). The robustness of the nodes was evaluated by computing Approximately Unbiased (AU) *p* values using the R package pvclust (10000 bootstraps, average method and correlation-based dissimilarity matrix) (Suzuki and Shimodaira, 2006).

**Figure S1.**

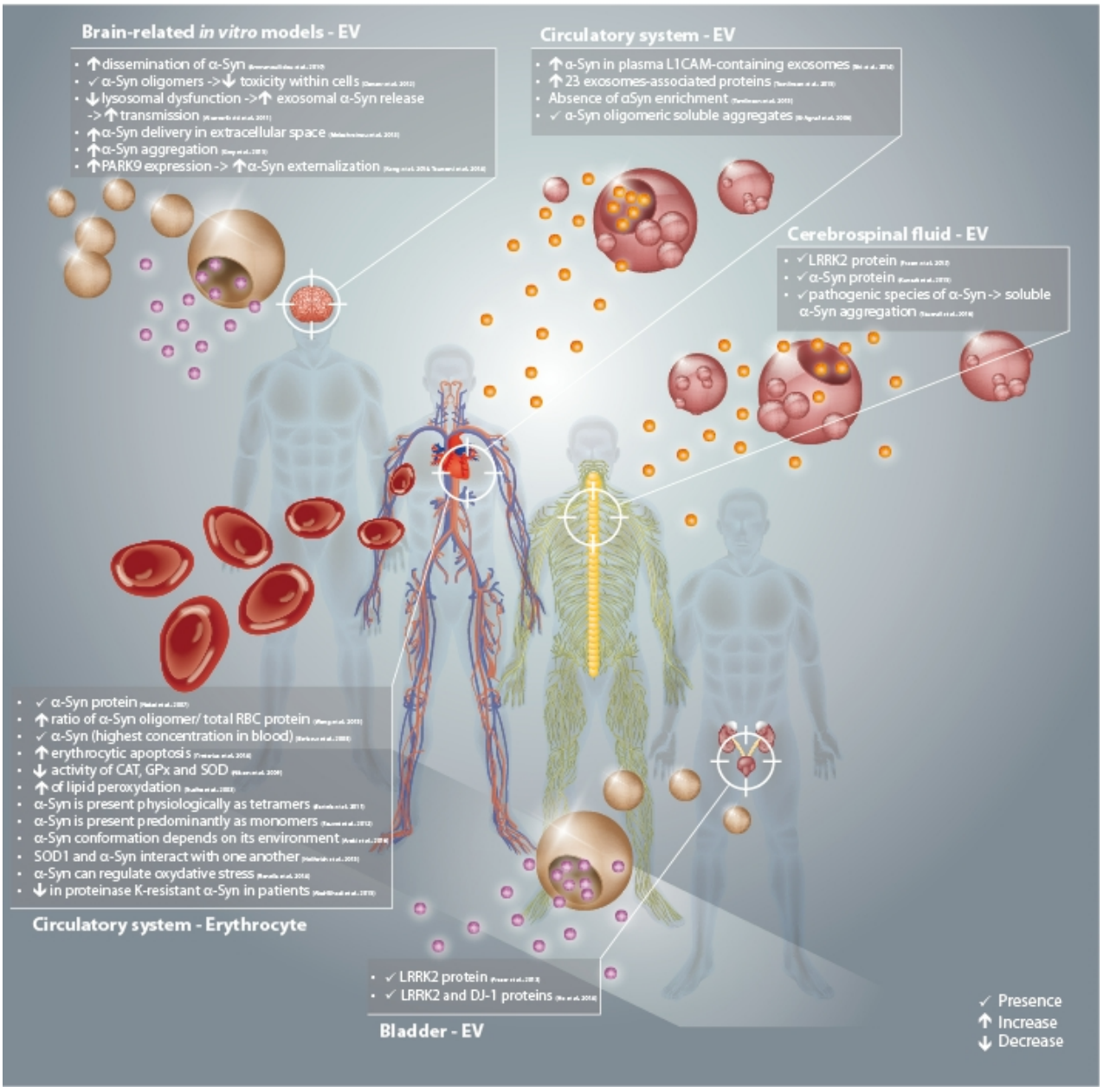
Brain-related *in vitro* models - EV
↑dissemination of α-Syn
✓ α-Syn oligomers -> ↓ toxicity within cells
↓lysosomal dysfunction -> ↑ exosomal α-Syn release -> ↑ transmission
↑α-Syn delivery in extracellular space
↑α-Syn aggregation
↑PARK9 expression -> ↑α-Syn externalization
Circulatory system - EV
↑α-Syn in plasma L1CAM-containing exosomes
↑23 exosomes-associated proteins
Absence of αSyn enrichment
✓ α-Syn oligomeric soluble aggregates
Cerebrospinal fluid - EV
✓ LRRK2 protein
✓ α-Syn protein
✓ pathogenic species of α-Syn -> soluble α-Syn aggregation
✓ α-Syn protein
↑ratio of α-Syn oligomer/ total RBC protein
✓ α-Syn (highest concentration in blood)
↑erythrocytic apoptosis
↓ activity of CAT, GPx and SOD
↑of lipid peroxydation
α-Syn is present physiologically as tetramers
α-Syn is present predominantly as monomers
α-Syn conformation depends on its environment
SOD1 and α-Syn interact with one another
α-Syn can regulate oxydative stress
↓in proteinase K-resistant α-Syn in patients
Circulatory system - Erythrocyte
✓ LRRK2 protein
✓ LRRK2 and DJ-1 proteins
Bladder - EV
✓ Presence
↑ Increase
↓ Decrease

# Figure S2.

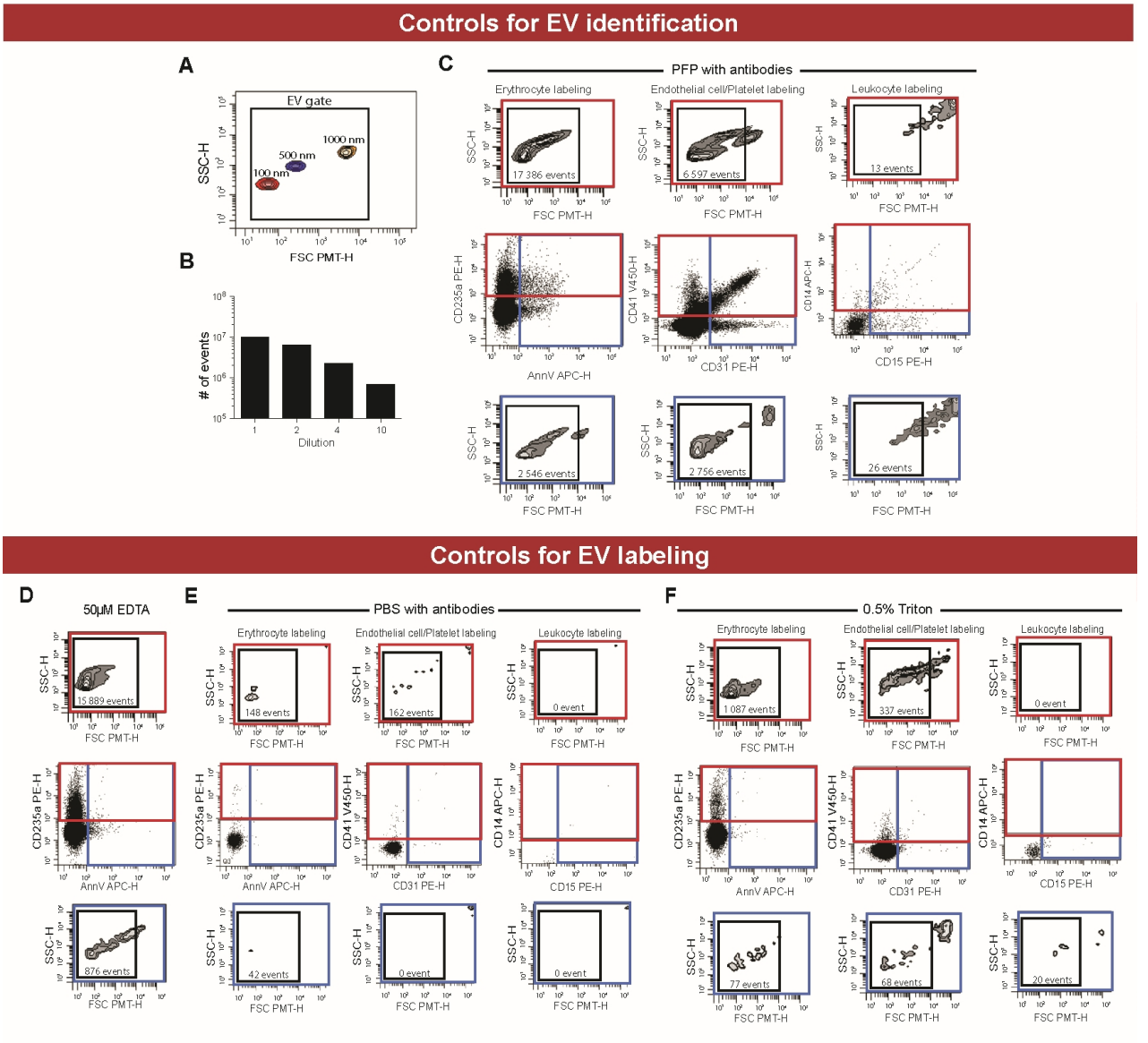
Controls for EV identification
A
EV gate
1000 nm
500 nm
100 nm
SSC-H
FSC PMT-H
B
# of events
Dilution
C
PFP with antibodies
Erythrocyte labeling
Endothelial cell/Platelet labeling
Leukocyte labeling
17 386 events
6 597 events
13 events
2 546 events
2 756 events
26 events
CD235a PE-H
AnnV APC-H
CD41 V450-H
CD31 PE-H
CD14 APC-H
CD15 PE-H
Controls for EV labeling
D
50µM EDTA
15 889 events
876 events
E
PBS with antibodies
148 events
162 events
0 event
42 events
0 event
0 event
F
0.5% Triton
1 087 events
337 events
0 event
77 events
68 events
20 events
EEV/Erythrocytes intra-patient variability
G
CD235a+EV/Erythrocytes
Patients
C1 C2 C3 C4 C5 C6 C7 C8 C9 C10 C11 C12 C13 C14 C15 C16 C17 C18 C19 C20 C21 C22 C23 C24 C25
15% 20% 12% 28% 15% 31% 9% 18% 15% 2% 12% 21% 1% 7% 13% 13% 30% 23% 11% 8% 30% 3% 18% 24% 21%

# Figure S3.

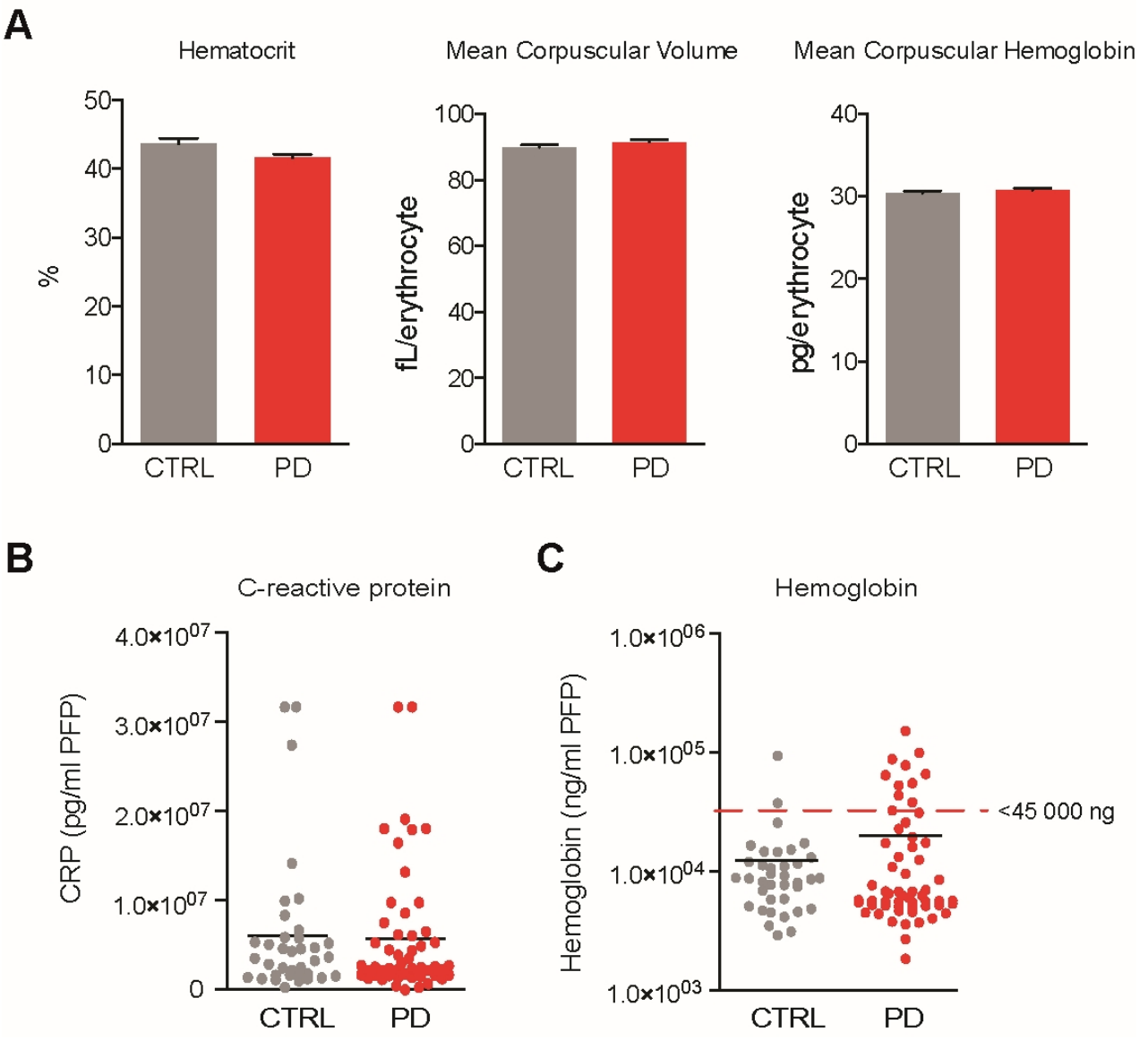
A
Hematocrit
%
50
40
30
20
10
0
CTRL
PD
Mean Corpuscular Volume
fL/erythrocyte
100
80
60
40
20
0
CTRL
PD
Mean Corpuscular Hemoglobin
pg/erythrocyte
40
30
20
10
0
CTRL
PD
B
C-reactive protein
CRP (pg/ml PFP)
4.0×10^07
3.0×10^07
2.0×10^07
1.0×10^07
0
CTRL
PD
C
Hemoglobin
Hemoglobin (ng/ml PFP)
1.0×10^06
1.0×10^05
1.0×10^04
1.0×10^03
<45 000 ng
CTRL
PD

# Figure S4.

## EEV in relation to UPDRS - cohort 2

PD patients - entire group

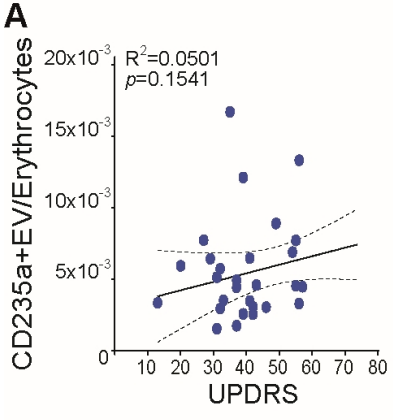


Mild PD patients

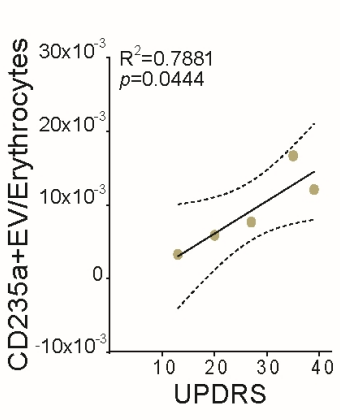


Moderate PD patients

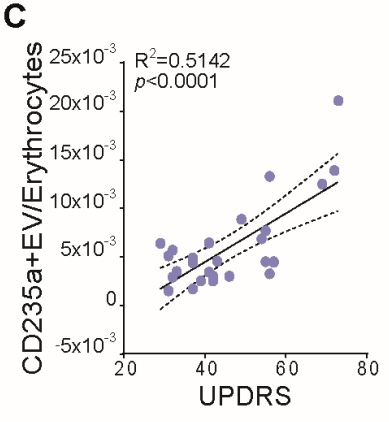


Severe PD patients

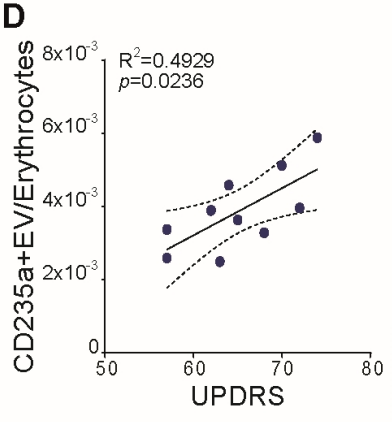


## LEDD and EV

E

| Patient | EV/erythrocytes | UPDRS | LEDD |
|---|---|---|---|
| P1 | 3,31E-03 | 13 | 125mg |
| P2 | 5,88E-03 | 20 | 499mg |
| P3 | 7,74E-03 | 27 | 900mg |
| P4 | 1,67E-02 | 35 | 281mg |
| P5 | 2,53E-03 | 39 | 316mg |
| P6 | 6,42E-03 | 29 | 281mg |
| P7 | 1,49E-03 | 31 | 280mg |
| P8 | 5,15E-03 | 31 | 375mg |
| P9 | 5,74E-03 | 32 | 441mg |
| P10 | 2,94E-03 | 32 | 188mg |
| P11 | 3,47E-03 | 33 | 3808mg |
| P12 | 4,93E-03 | 37 | 698,5mg |
| P13 | 1,74E-03 | 37 | 375mg |
| P14 | 4,41E-03 | 37 | 550mg |
| P15 | 1,21E-02 | 39 | 660mg |
| P16 | 6,44E-03 | 41 | 300mg |
| P17 | 3,43E-03 | 41 | 1364mg |
| P18 | 3,03E-03 | 42 | 1000mg |
| P19 | 2,51E-03 | 42 | 3059mg |
| P20 | 4,56E-03 | 43 | 1238mg |
| P21 | 3,00E-03 | 46 | 675mg |

| Patient | EV/erythrocytes | UPDRS | LEDD |
|---|---|---|---|
| P22 | 8,87E-03 | 49 | nil |
| P23 | 6,86E-03 | 54 | 500mg |
| P24 | 7,68E-03 | 55 | 3126mg |
| P25 | 4,51E-03 | 55 | 769mg |
| P26 | 1,33E-02 | 56 | 450mg |
| P27 | 3,26E-03 | 56 | nil |
| P28 | 4,50E-03 | 57 | 757mg |
| P29 | 3,38E-03 | 57 | 5288mg |
| P30 | 1,25E-02 | 69 | 1100mg |
| P31 | 3,97E-03 | 72 | 540mg |
| P32 | 2,11E-02 | 73 | 2328mg |
| P33 | 4,44E-03 | 57 | 281mg |
| P34 | 2,60E-03 | 57 | 244mg |
| P35 | 3,90E-03 | 62 | 400mg |
| P36 | 2,50E-03 | 63 | 1019mg |
| P37 | 4,59E-03 | 64 | 600mg |
| P38 | 3,64E-03 | 65 | 1397mg |
| P39 | 3,29E-03 | 68 | 1550mg |
| P40 | 5,13E-03 | 70 | 1313mg |
| P41 | 1,39E-02 | 72 | 2694mg |
| P42 | 5,89E-03 | 74 | 600mg |

F

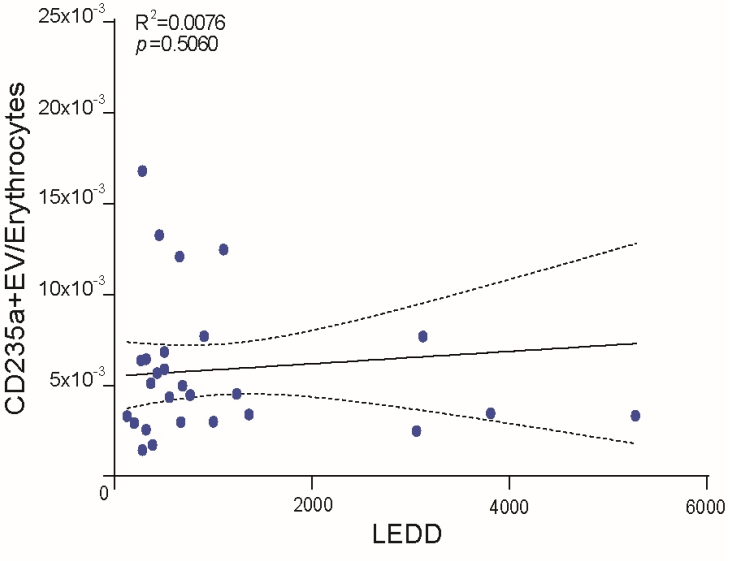

# Figure S5.

**A**

**Cell-derived EV quantification – HD cohort**

| Cell types | Markers | Units | CTRL | | | HD pre-manifest | | | HD | | | *p* value |
|---|---|---|---|---|---|---|---|---|---|---|---|---|
| | | | *n* | Mean | SEM | *n* | Mean | SEM | *n* | Mean | SEM | |
| Erythrocytes | CD235a+PS- | $10^3$/µl | 54 | 15.2 | 2.0 | 10 | 10.3 | 3.5 | 51 | 14.1 | 1.4 | 0.16 |
| | **CD235a+PS+** | **$10^3$/µl** | 54 | 1.1 | 0.2 | **10** | **0.4** | **0.2** | **51** | **1.1** | **0.1** | **0.04** |
| | CD235a+ total | $10^3$/µl | 54 | 16.4 | 2.0 | 10 | 10.7 | 3.5 | 51 | 15.3 | 1.5 | 0.09 |
| | EV CD235a+/erythrocyte | | 54 | 0.0035 | 0.0005 | 10 | 0.0023 | 0.0008 | 50 | 0.0033 | 0.0003 | 0.11 |
| Platelets | CD41+PS- | $10^3$/µl | 54 | 9.2 | 2.2 | 10 | 4.3 | 1.3 | 50 | 6.1 | 1.0 | 0.78 |
| | CD41+PS+ | $10^3$/µl | 54 | 19.3 | 4.8 | 10 | 7.1 | 2.0 | 50 | 12.4 | 2.4 | 0.74 |
| | CD41+ total | $10^3$/µl | 54 | 28.4 | 6.9 | 10 | 11.4 | 3.2 | 50 | 18.6 | 3.4 | 0.70 |
| | EV CD41+/platelet | | 53 | 0.12 | 0.03 | 10 | 0.05 | 0.02 | 48 | 0.08 | 0.01 | 0.34 |
| Endothelial cells | CD31+CD41-PS- | $10^3$/µl | 54 | 1.4 | 0.3 | 10 | 0.6 | 0.2 | 50 | 1.2 | 0.2 | 0.31 |
| | CD31+CD41-PS+ | $10^3$/µl | 54 | 0.68 | 0.16 | 10 | 0.25 | 0.06 | 50 | 0.46 | 0.09 | 0.59 |
| | CD31+CD41- total | $10^3$/µl | 54 | 2.1 | 0.4 | 10 | 0.8 | 0.2 | 50 | 1.7 | 0.3 | 0.26 |
| Leukocytes | CD45+ total | $10^3$/µl | 54 | 33.4 | 2.7 | 10 | 31.6 | 5.3 | 51 | 31.7 | 2.4 | 0.88 |
| Monocytes | CD45-CD14+ PS- | $10^3$/µl | 54 | 3.4 | 1.1 | 10 | 1.6 | 0.2 | 51 | 1.6 | 0.1 | 0.91 |
| | CD45-CD14+ PS+ | $10^3$/µl | 54 | 1.8 | 0.3 | 10 | 0.8 | 0.3 | 51 | 1.5 | 0.2 | 0.14 |
| | CD45+CD14+ PS- | $10^3$/µl | 54 | 0.18 | 0.07 | 10 | 0.069 | 0.016 | 51 | 0.056 | 0.008 | 0.34 |
| | CD45+CD14+PS+ | $10^3$/µl | 54 | 0.62 | 0.12 | 10 | 0.24 | 0.06 | 51 | 0.55 | 0.14 | 0.12 |
| | CD14+ total | $10^3$/µl | 54 | 6.0 | 1.3 | 10 | 2.6 | 0.4 | 51 | 3.7 | 0.4 | 0.08 |
| | EV CD14+ /monocyte | | 53 | 12.3 | 2.5 | 10 | 5.7 | 0.6 | 48 | 8.0 | 1.0 | 0.13 |
| Granulocytes | CD45-CD15+ PS- | $10^3$/µl | 54 | 1.2 | 0.1 | 10 | 1.2 | 0.3 | 51 | 1.5 | 0.2 | 0.33 |
| | CD45-CD15+ PS+ | $10^3$/µl | 54 | 0.12 | 0.04 | 10 | 0.18 | 0.08 | 51 | 0.22 | 0.11 | 0.33 |
| | CD45+CD15+ PS- | $10^3$/µl | 54 | 0.20 | 0.05 | 10 | 0.07 | 0.02 | 51 | 0.15 | 0.04 | 0.64 |
| | CD45+CD15+PS+ | $10^3$/µl | 54 | 0.25 | 0.05 | 10 | 0.13 | 0.06 | 51 | 0.20 | 0.04 | 0.39 |
| | CD15+ total | $10^3$/µl | 54 | 1.7 | 0.2 | 10 | 1.6 | 0.4 | 51 | 0.20 | 0.3 | 0.67 |
| | EV CD15+ /granulocyte | | 53 | 0.41 | 0.04 | 10 | 0.42 | 0.13 | 48 | 0.50 | 0.08 | 0.75 |

**Diagnostic value**

**B**

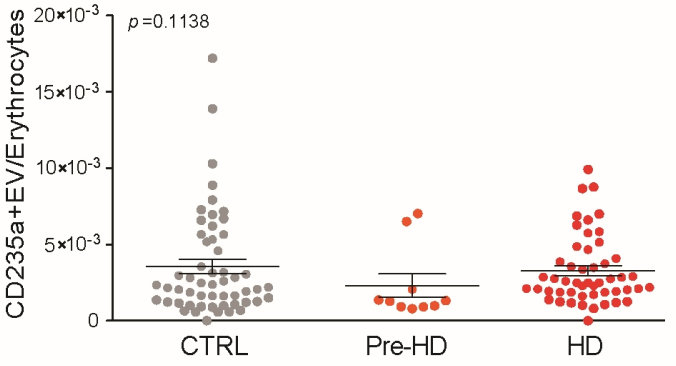


**EEV in relation to clinical measures**

**C**

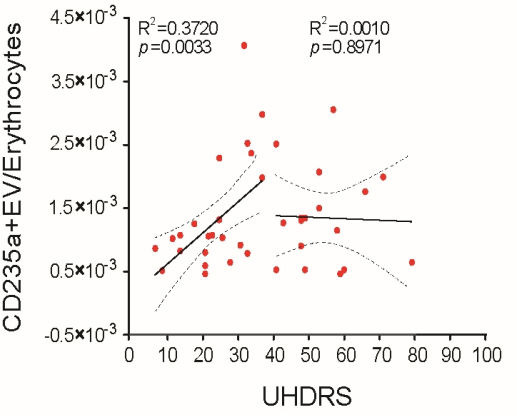

# Figure S6.

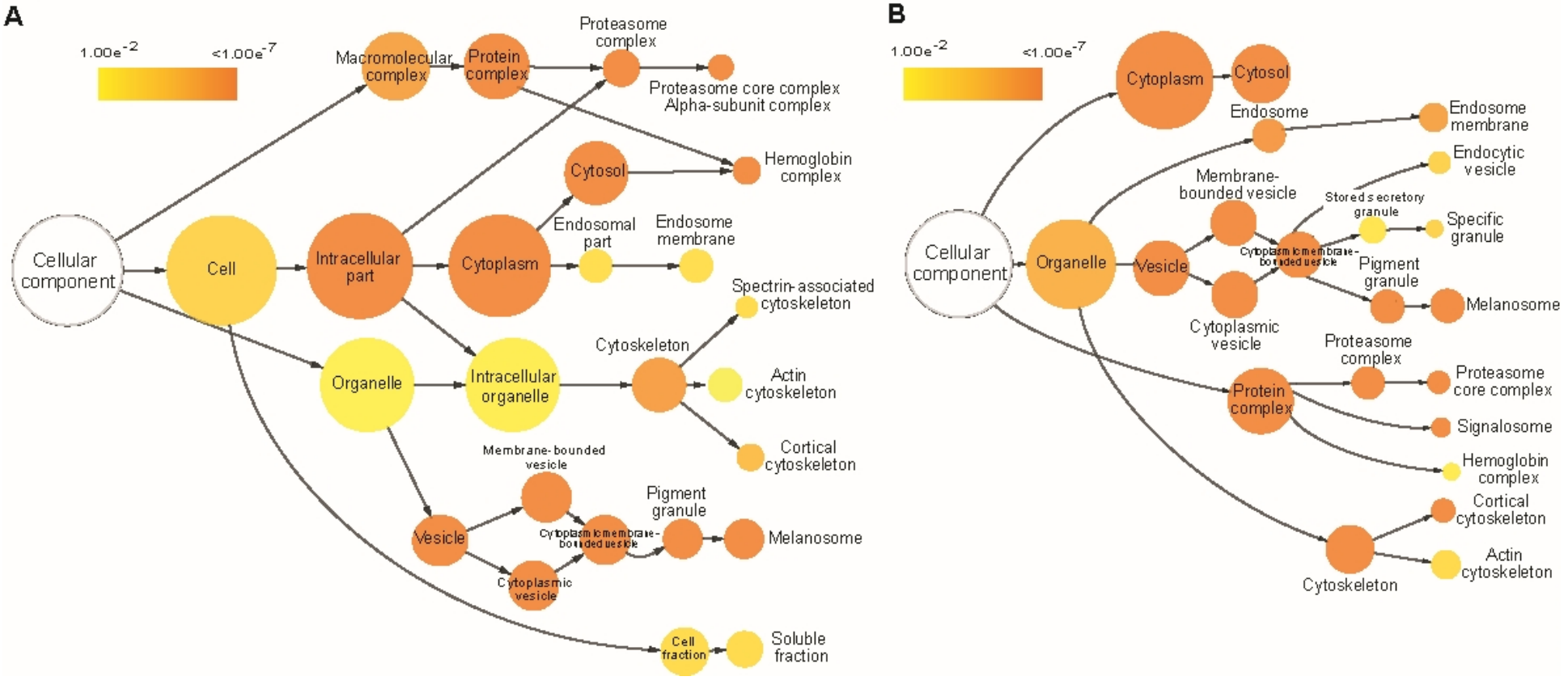
A
1.00e-2
<1.00e-7
Cellular component
Cell
Organelle
Macromolecular complex
Protein complex
Proteasome complex
Proteasome core complex
Alpha-subunit complex
Hemoglobin complex
Intracellular part
Intracellular organelle
Cytosol
Cytoplasm
Endosomal part
Endosome membrane
Spectrin-associated cytoskeleton
Cytoskeleton
Actin cytoskeleton
Cortical cytoskeleton
Membrane-bounded vesicle
Vesicle
Cytoplasmic membrane-bounded vesicle
Cytoplasmic vesicle
Pigment granule
Melanosome
Cell fraction
Soluble fraction
B
1.00e-2
<1.00e-7
Cellular component
Organelle
Cytoplasm
Cytosol
Endosome
Endosome membrane
Endocytic vesicle
Membrane-bounded vesicle
Stored secretory granule
Specific granule
Vesicle
Cytoplasmic membrane-bounded vesicle
Pigment granule
Melanosome
Cytoplasmic vesicle
Protein complex
Proteasome complex
Proteasome core complex
Signalosome
Hemoglobin complex
Cortical cytoskeleton
Actin cytoskeleton
Cytoskeleton

## Table 1. Participant clinical information

| PD cohort | | | | | | |
|---|---|---|---|---|---|---|
| | CTRL | PD Patients – Stages of disease | | | | |
| | | Unknown | Mild | Moderate | Severe | *p* value |
| ***n*** | 37 | 7 | 12 | 33 | 8 | |
| **Age** | 66.8 | 69.8 | 66.7 | 71.1 | 75.0* | **0.04** |
| **Gender F (M)** | 18 (19) | 1 (6) | 6 (6) | 16 (17) | 0 (8) | **0.05** |
| **Disease severity** | | | | | | |
| **Hoehn & Yahr (*n*)** | | | 1 ± 0.3 (12) | 2 ± 0.2 (33) | 3 ± 0.5 (8) | **<0.0001** |
| **UPDRS (*n*)** | | | 38 ± 11 (6) | 52 ± 19 (17) | 73 ± 20 (6) | **0.02** |
| **MMSE (*n*)** | | | 29 ± 2 (7) | 29 ± 1 (19) | 26 ± 3 (6) | **0.01** |
| **BDI (*n*)** | | | 3 ± 2 (6) | 4 ± 2 (17) | 13 ± 7 (4) | **0.03** |
| **ACE (*n*)** | | | 96 ± 4 (6) | 92 ± 7 (17) | 84 ± 14 (6) | 0.13 |
| **Comorbidities** | | | | | | |
| **Depression** | 3 | 1 | 2 | 1 | 2 | 0.29 |
| **Cancer** | 5 | 0 | 3 | 4 | 1 | 0.64 |
| **Diabetes** | 2 | 0 | 0 | 1 | 2 | 0.10 |
| **Hypertension** | 10 | 1 | 2 | 10 | 3 | 0.76 |
| **Hypercholesterolemia** | 5 | 0 | 1 | 6 | 1 | 0.73 |
| **Asthma** | 3 | 1 | 1 | 5 | 0 | 0.71 |
| **Allergies** | 2 | 0 | 2 | 6 | 2 | 0.28 |

**Table 1. Participant clinical information – PD cohort**. Disease severity as measured using the H&Y scale (score): Mild (1-1.5); Moderate (2-2.5); Severe (3-3.5). *$p < 0.05$ vs. CTRL. Statistical analyses were performed using a Kruskal Wallis test followed by Dunn's multiple comparison test.

## Table S1. Participant clinical information

### HD cohort

| | CTRL | HD Patients – Stages of disease | | | | | | |
|---|---|---|---|---|---|---|---|---|
| | | Pre-HD | Stage 1 | Stage 2 | Stage 3 | Stage 4 | Stage 5 | *p* value |
| ***n*** | 55 | 11 | 15 | 13 | 12 | 10 | 2 | |
| **Age** | 55.0 | 37.5 | 53.1 | 54.2 | 58.3 | 58.1 | 55.5 | **0.02** |
| **Gender F (M)** | 31 (22) | 6 (5) | 5 (10) | 4 (9) | 8 (4) | 7 (3) | 1 (1) | 0.26 |
| **Disease severity** | | | | | | | | |
| **CAG (*n*)** | 28.3 (3) | 41.1 (10) | 42.3 (13) | 42.6 (12) | 43.7 (7) | 44.3 (7) | | **<0.001** |
| **UHDRS (*n*)** | | 2.7 (11) | 15.7 (14) | 34.5 (11) | 42.9 (12) | 55.9 (10) | 67.5 (2) | **<0.001** |
| **TFC (*n*)** | 13 (16) | 13 (11) | 12.5 (15) | 7.8 (13) | 4.3 (12) | 1.6 (10) | 0 (2) | **<0.001** |
| **BDS (*n*)** | | 206 (10) | 337 (13) | 356 (12) | 442 (7) | 465 (7) | | **<0.001** |
| **Comorbidities** | | | | | | | | |
| **Depression** | 8 | 1 | 1 | 3 | 6 | 4 | 1 | **0.0497** |
| **Cancer** | 0 | 0 | 0 | 0 | 0 | 0 | 0 | |
| **Diabetes** | 3 | 1 | 1 | 1 | 1 | 1 | 0 | 0.99 |
| **Hypertension** | 4 | 1 | 2 | 1 | 1 | 2 | 0 | 0.92 |
| **Hypercholesterolemia** | 8 | 1 | 1 | 0 | 0 | 1 | 0 | 0.32 |
| **Asthma** | 0 | 0 | 1 | 0 | 0 | 0 | 0 | 0.65 |
| **Allergies** | 3 | 0 | 2 | 2 | 0 | 0 | 0 | 0.33 |

### Blood cell quantification

| Cell type | Units | CTRL | | | Pre-HD | | | Stage 1 | | | Stage 2 | | | Stage 3 | | | Stage 4 | | | Stage 5 | | | *p* value |
|---|---|---|---|---|---|---|---|---|---|---|---|---|---|---|---|---|---|---|---|---|---|---|---|
| | | n | Mean | SD | n | Mean | SD | n | Mean | SD | n | Mean | SD | n | Mean | SD | n | Mean | SD | n | Mean | SD | |
| **Erythrocytes** | $10^9$/ml | 54 | 4.58 | 0.36 | 10 | 4.59 | 0.36 | 15 | 4.75 | 0.37 | 12 | 4.56 | 0.29 | 11 | 4.69 | 0.44 | 10 | 4.76 | 0.39 | 2 | 4.35 | 0.26 | 0.44 |
| **Platelets** | $10^6$/ml | 54 | 229 | 51 | 10 | 259 | 85 | 15 | 232 | 68 | 12 | 218 | 54 | 11 | 268 | 63 | 10 | 212 | 46 | 2 | 305 | 55 | 0.09 |
| **Leukocytes** | $10^6$/ml | 54 | 6.61 | 1.60 | 10 | 6.97 | 1.64 | 15 | 6.30 | 1.13 | 12 | 7.67 | 2.97 | 11 | 6.97 | 2.00 | 10 | 6.84 | 2.07 | 2 | 5.30 | 1.56 | 0.47 |
| **Monocytes** | $10^6$/ml | 54 | 0.51 | 0.16 | 10 | 0.48 | 0.57 | 15 | 0.49 | 0.50 | 12 | 0.55 | 0.18 | 11 | 0.58 | 0.24 | | 0.51 | 0.16 | 2 | 0.61 | 0.42 | 0.79 |

**Table S1. Participant clinical information – HD cohort**. Disease severity levels in relation to the TFC scale: Stage 1 (11-13); Stage 2 (7-10); Stage 3 (3-6); Stage 4 (1-2); Stage 5 (0). Disease severity was evaluated within 6 months of blood sampling. Comorbidities were determined from medical information reported by the participant or caregiver. **Blood cell quantification**. Full blood counts performed in HD patients at different stages of the disease (Pre-HD, n=10; Stage 1, n=15; Stage 2, n=12; Stage 3, n=11; Stage 4, n=10; Stage 5, n=2) revealed no significant differences in the total number of any cell type between patients and their respective healthy sex- and age-matched CTRL (*n*=54), except for erythrocytes. Statistical analyses were performed using a Kruskal Wallis test followed by Dunn's multiple comparison test.

**Table S2. Participant clinical information**

| PD cohort – cohort 2 | | | | |
|---|---|---|---|---|
| | PD Patients – Stages of disease | | | |
| | Mild | Moderate | Severe | *p* value |
| ***n*** | 5 | 27 | 10 | |
| **Age** | 63.4 | 68.5 | 71.3 | 0.26 |
| **Gender F (M)** | 2 (3) | 11 (16) | 4 (6) | 0.99 |
| **Disease severity** | | | | |
| **UPDRS (*n*)** | 27 ± 8 (5) | 46 ± 11 (27) | 71 (10) | **<0.0001** |
| **Comorbidities** | | | | |
| **Depression** | 0 | 5 | 1 | 0.51 |
| **Cancer** | 0 | 0 | 0 | NA |
| **Diabetes** | 0 | 0 | 0 | NA |
| **Hypertension** | 0 | 3 | 0 | 0.42 |
| **Hypercholesterolemia** | 0 | 3 | 0 | 0.42 |
| **Asthma** | 0 | 2 | 0 | 0.56 |
| **Allergies** | 0 | 1 | 0 | 0.75 |

**Table S2. Participant clinical information – PD cohort no.2.** Disease severity as measured using the UPDRS scale (score): Mild (0,39); Moderate (29,73); Severe (57,74). *$p < 0.05$ vs. CTRL. Statistical analyses were performed using a Kruskal Wallis test followed by Dunn's multiple comparison test.

## Table S3. Complete list of proteins identified in the EVV proteome

**A.** Uniprot Complete Proteome *Homo sapiens* database for the non-depleted sample

| Protein ID | Protein names | Gene names | Razor + unique peptides |
|---|---|---|---|
| P02549 | Spectrin alpha chain, erythrocytic 1 | SPTA1 | 136 |
| P11277 | Spectrin beta chain, erythrocytic | SPTB | 123 |
| P16157 | Ankyrin-1 | ANK1 | 70 |
| P02730 | Band 3 anion transport protein | SLC4A1 | 38 |
| P55072 | Transitional endoplasmic reticulum ATPase | VCP | 33 |
| P16452 | Erythrocyte membrane protein band 4.2 | EPB42 | 33 |
| P11171 | Protein 4.1 | EPB41 | 33 |
| P04040 | Catalase | CAT | 32 |
| Q13228 | Selenium-binding protein 1 | SELENBP1 | 29 |
| B4DT77 | Annexin;Annexin A7 | ANXA7 | 27 |
| Q8WUM4 | Programmed cell death 6-interacting protein | PDCD6IP | 27 |
| P35612 | Beta-adducin | ADD2 | 26 |
| P68871 | Hemoglobin subunit beta;LVV-hemorphin-7;Spinorphin | HBB | 25 |
| Q00610 | Clathrin heavy chain 1 | CLTC | 25 |
| P69905 | Hemoglobin subunit alpha | HBA1 | 22 |
| B4DVE7 | Annexin A11 | ANXA11 | 20 |
| J3QLD9 | Flotillin-2 | FLOT2 | 20 |
| P08758 | Annexin A5;Annexin | ANXA5 | 19 |
| P09525 | Annexin A4;Annexin | ANXA4 | 18 |
| O75955; | Flotillin-1 | FLOT1 | 18 |
| P11142 | Heat shock cognate 71 kDa protein | HSPA8 | 18 |
| P32119 | Peroxiredoxin-2 | PRDX2 | 17 |
| P00491 | Purine nucleoside phosphorylase | PNP | 17 |
| P27105 | Erythrocyte band 7 integral membrane protein | STOM | 17 |
| P00918 | Carbonic anhydrase 2 | CA2 | 17 |
| P23634 | Plasma membrane calcium-transporting ATPase 4 | ATP2B4 | 17 |
| C9JIF9 | Acylamino-acid-releasing enzyme | APEH | 17 |
| P00915 | Carbonic anhydrase 1 | CA1 | 16 |
| P63261 | Actin, cytoplasmic 2 | ACTG1 | 16 |
| Q5VU58 | Tropomyosin alpha-3 chain | TPM3 | 16 |
| P30041 | Peroxiredoxin-6 | PRDX6 | 16 |
| E7EU23 | Rab GDP dissociation inhibitor beta | GDI2 | 16 |
| Q00013 | 55 kDa erythrocyte membrane protein | MPP1 | 16 |
| E7EV01 | Calpain-5 | CAPN5 | 16 |
| J3KPS3 | Fructose-bisphosphate aldolase A | ALDOA | 15 |
| Q08495 | Dematin | DMTN | 15 |
| P23276 | Kell blood group glycoprotein | KEL | 15 |
| P69892 | Hemoglobin subunit gamma-2 | HBG2 | 14 |

| | | | |
|---|---|---|---|
| P60174 | Triosephosphate isomerase | TPI1 | 14 |
| P62258 | 14-3-3 protein epsilon | YWHAE | 14 |
| O75326 | Semaphorin-7A | SEMA7A | 14 |
| O75340 | Programmed cell death protein 6 | PDCD6 | 13 |
| E7EV99 | Alpha-adducin | ADD1 | 13 |
| Q5VZU9 | Tripeptidyl-peptidase 2 | TPP2 | 13 |
| P53396 | ATP-citrate synthase | ACLY | 13 |
| C9J0K6 | Sorcin | SRI | 12 |
| P04406 | Glyceraldehyde-3-phosphate dehydrogenase | GAPDH | 12 |
| P07738 | Bisphosphoglycerate mutase | BPGM | 12 |
| B7Z3I9 | Delta-aminolevulinic acid dehydratase | ALAD | 12 |
| Q86X55 | Histone-arginine methyltransferase CARM1 | CARM1 | 12 |
| P07195 | L-lactate dehydrogenase B chain;L-lactate dehydrogenase | LDHB | 12 |
| P23526 | Adenosylhomocysteinase | AHCY | 12 |
| Q32Q12 | Nucleoside diphosphate kinase | NME1-NME2 | 12 |
| B7Z7A9 | Phosphoglycerate kinase 1 | PGK1 | 11 |
| P11166 | Solute carrier family 2, facilitated glucose transporter member 1 | SLC2A1 | 11 |
| P22303 | Acetylcholinesterase | ACHE | 11 |
| Q9NP58 | ATP-binding cassette sub-family B member 6, mitochondrial | ABCB6 | 11 |
| P40925 | Malate dehydrogenase, cytoplasmic;Malate dehydrogenase | MDH1 | 11 |
| P00352 | Retinal dehydrogenase 1 | ALDH1A1 | 11 |
| F2Z2V0 | Copine-1 | CPNE1 | 11 |
| K7EMC9 | WW domain-binding protein 2 | WBP2 | 10 |
| F5H7S3 | Tropomyosin alpha-1 chain | TPM1 | 10 |
| A6NN80 | Annexin A6;Annexin | ANXA6 | 10 |
| P30043 | Flavin reductase (NADPH) | BLVRB | 9 |
| H7BXD5 | Grancalcin | GCA | 9 |
| P04083 | Annexin A1;Annexin | ANXA1 | 9 |
| P62937 | Peptidyl-prolyl cis-trans isomerase | PPIA | 9 |
| P37837 | Transaldolase | TALDO1 | 9 |
| Q06830 | Peroxiredoxin-1 | PRDX1 | 9 |
| O75131 | Copine-3 | CPNE3 | 9 |
| P00390 | Glutathione reductase, mitochondrial | GSR | 9 |
| E7EQB2 | Lactotransferrin | LTF | 9 |
| P07384 | Calpain-1 catalytic subunit | CAPN1 | 9 |
| P02042 | Hemoglobin subunit delta | HBD | 8 |
| P30086 | Phosphatidylethanolamine-binding protein 1;Hippocampal cholinergic neurostimulating peptide | PEBP1 | 8 |
| P35613 | Basigin | BSG | 8 |
| Q9H0U4 | Ras-related protein Rab-1B;Putative Ras-related protein Rab-1C | RAB1B;RAB1C | 8 |
| P63092 | Guanine nucleotide-binding protein G(s) subunit alpha isoforms | GNAS | 8 |
| P48506 | Glutamate--cysteine ligase catalytic subunit | GCLC | 8 |
| P06702 | Protein S100-A9 | S100A9 | 7 |
| Q9UBV8 | Peflin | PEF1 | 7 |
| P17931 | Galectin-3;Galectin | LGALS3 | 7 |

| | | | |
|---|---|---|---|
| P28066 | Proteasome subunit alpha type-5 | PSMA5 | 7 |
| P07451 | Carbonic anhydrase 3 | CA3 | 7 |
| E7EQ12 | Calpastatin | CAST | 7 |
| P50895 | Basal cell adhesion molecule | BCAM | 7 |
| P28074 | Proteasome subunit beta type-5 | PSMB5 | 7 |
| G3V5Z7 | Proteasome subunit alpha type;Proteasome subunit alpha type-6 | PSMA6 | 7 |
| P25786 | Proteasome subunit alpha type-1 | PSMA1 | 7 |
| G3V1D3 | Dipeptidyl peptidase 3 | DPP3 | 7 |
| P49247 | Ribose-5-phosphate isomerase | RPIA | 7 |
| Q5T9B7 | Adenylate kinase isoenzyme 1 | AK1 | 7 |
| P25789 | Proteasome subunit alpha type-4; Proteasome subunit beta type | PSMA4 | 7 |
| B4E022 | Transketolase | TKT | 7 |
| J3QS39 | Ubiquitin-60S ribosomal protein L40;Ubiquitin;60S ribosomal protein L40;Ubiquitin-40S ribosomal protein S27a;Ubiquitin;40S ribosomal protein S27a;Polyubiquitin-B;Ubiquitin;Polyubiquitin-C;Ubiquitin | UBB;RPS27A;UBC;UBA52;UBBP4 | 6 |
| H0Y7A7 | Calmodulin | CALM2 | 6 |
| P28070 | Proteasome subunit beta type-4 | PSMB4 | 6 |
| Q9H4G4 | Golgi-associated plant pathogenesis-related protein 1 | GLIPR2 | 6 |
| Q9BY43 | Charged multivesicular body protein 4a | CHMP4A | 6 |
| P48426 | Phosphatidylinositol 5-phosphate 4-kinase type-2 alpha | PIP4K2A | 6 |
| P28289 | Tropomodulin-1 | TMOD1 | 6 |
| P07911 | Uromodulin;Uromodulin, secreted form | UMOD | 6 |
| Q9GZP4 | PITH domain-containing protein 1 | PITHD1 | 6 |
| P78417 | Glutathione S-transferase omega-1 | GSTO1 | 6 |
| P25788 | Proteasome subunit alpha type-3 | PSMA3 | 6 |
| O14818 | Proteasome subunit alpha type-7;Proteasome subunit alpha type-7-like | PSMA7;PSMA8 | 6 |
| P08107 | Heat shock 70 kDa protein 1A/1B | HSPA1A | 6 |
| H0YD13 | CD44 antigen | CD44 | 6 |
| P61225 | Ras-related protein Rap-2b;Ras-related protein Rap-2c;Ras-related protein Rap-2a | RAP2B;RAP2A;RAP2C | 6 |
| P05109 | Protein S100-A8;Protein S100-A8, N-terminally processed | S100A8 | 6 |
| P23528 | Cofilin-1 | CFL1 | 6 |
| Q99808 | Equilibrative nucleoside transporter 1 | SLC29A1 | 6 |
| P84077 | ADP-ribosylation factor 1;ADP-ribosylation factor 3;ADP-ribosylation factor 5;ADP-ribosylation factor 4 | ARF1;ARF3;ARF5;ARF4 | 6 |
| P31946 | 14-3-3 protein beta/alpha;14-3-3 protein beta/alpha, N-terminally processed | YWHAB | 6 |
| C9JIS1 | Guanine nucleotide-binding protein G(I)/G(S)/G(T) subunit beta-2;Guanine nucleotide-binding protein subunit beta-4 | GNB2;GNB4 | 6 |
| P53990 | IST1 homolog | IST1 | 6 |
| Q99497 | Protein DJ-1 | PARK7 | 6 |
| F5H7U0 | 6-phosphogluconate dehydrogenase, decarboxylating | PGD | 6 |
| B7Z7E9 | Aspartate aminotransferase, cytoplasmic | GOT1 | 6 |
| P62834 | Ras-related protein Rap-1A;Ras-related protein Rap-1b;Ras-related protein Rap-1b-like protein | RAP1A;RAP1B | 6 |
| P04899 | Guanine nucleotide-binding protein G(i) subunit alpha-2 | GNAI2 | 6 |
| P25325 | 3-mercaptopyruvate sulfurtransferase;Sulfurtransferase | MPST | 6 |
| Q9NP79 | Vacuolar protein sorting-associated protein VTA1 homolog | VTA1 | 6 |
| P00492 | Hypoxanthine-guanine phosphoribosyltransferase | HPRT1 | 6 |

| | | | |
|---|---|---|---|
| Q16531 | DNA damage-binding protein 1 | DDB1 | 6 |
| P22314 | Ubiquitin-like modifier-activating enzyme 1 | UBA1 | 6 |
| P00441 | Superoxide dismutase [Cu-Zn] | SOD1 | 5 |
| H7BY58 | Protein-L-isoaspartate O-methyltransferase;Protein-L-isoaspartate(D-aspartate) O-methyltransferase | PCMT1 | 5 |
| P10768 | S-formylglutathione hydrolase | ESD | 5 |
| P09543 | 2,3-cyclic-nucleotide 3-phosphodiesterase | CNP | 5 |
| P06733 | Alpha-enolase;Enolase | ENO1 | 5 |
| P26038 | Moesin | MSN | 5 |
| O75368 | SH3 domain-binding glutamic acid-rich-like protein | SH3BGRL | 5 |
| K7EQ48 | Glucose-6-phosphate isomerase | GPI | 5 |
| P25787 | Proteasome subunit alpha type-2 | PSMA2 | 5 |
| P49721 | Proteasome subunit beta type-2 | PSMB2 | 5 |
| F5H8J2 | Protein disulfide-isomerase | P4HB | 5 |
| C9J9P4 | Phospholipid scramblase 1 | PLSCR1 | 5 |
| P09211 | Glutathione S-transferase P | GSTP1 | 5 |
| B5MDF5 | GTP-binding nuclear protein Ran | RAN | 5 |
| P07900 | Heat shock protein HSP 90-alpha | HSP90AA1 | 5 |
| K7EQ02 | DAZ-associated protein 1 | DAZAP1 | 5 |
| Q13630 | GDP-L-fucose synthase | TSTA3 | 5 |
| F5H0T1 | Stress-induced-phosphoprotein 1 | STIP1 | 5 |
| P50502 | Hsc70-interacting protein;Putative protein FAM10A5;Putative protein FAM10A4 | ST13;ST13P5;ST13P4 | 5 |
| P20618 | Proteasome subunit beta type-1 | PSMB1 | 5 |
| P62805 | Histone H4 | HIST1H4A | 5 |
| P51148 | Ras-related protein Rab-5C | RAB5C | 5 |
| H7C2G2 | Ecto-ADP-ribosyltransferase 4 | ART4 | 5 |
| J3KQ18 | D-dopachrome decarboxylase;D-dopachrome decarboxylase-like protein | DDT;DDTL | 5 |
| H3BPK3 | Hydroxyacylglutathione hydrolase, mitochondrial | HAGH | 5 |
| B4DIT7 | Protein-glutamine gamma-glutamyltransferase 2 | TGM2 | 5 |
| O43633 | Charged multivesicular body protein 2a | CHMP2A | 5 |
| B4DQH4 | T-complex protein 1 subunit theta | CCT8 | 5 |
| Q9UN37 | Vacuolar protein sorting-associated protein 4A | VPS4A | 5 |
| I3L397 | Eukaryotic translation initiation factor 5A-1;Eukaryotic translation initiation factor 5A-1-like | EIF5A;EIF5AL1 | 5 |
| Q9Y5Z4 | Heme-binding protein 2 | HEBP2 | 5 |
| Q9UKV8 | Protein argonaute-2 | AGO2 | 5 |
| F5H442 | Tumor susceptibility gene 101 protein | TSG101 | 5 |
| H3BLV0 | Complement decay-accelerating factor | CD55 | 5 |
| P02008 | Hemoglobin subunit zeta | HBZ | 5 |
| E7EPV7 | Alpha-synuclein | SNCA | 4 |
| P63104 | 14-3-3 protein zeta/delta | YWHAZ | 4 |
| P02724 | Glycophorin-A | GYPA;GPErik | 4 |
| U3KQE2 | Calpain small subunit 1 | CAPNS1 | 4 |
| Q9NP59 | Solute carrier family 40 member 1 | SLC40A1 | 4 |
| Q5QPM9 | Proteasome inhibitor PI31 subunit | PSMF1 | 4 |
| C9J8U2 | Nicotinate phosphoribosyltransferase | NAPRT | 4 |

| | | | |
|---|---|---|---|
| P61981 | 14-3-3 protein gamma;14-3-3 protein gamma, N-terminally processed | YWHAG | 4 |
| Q9UQ80 | Proliferation-associated protein 2G4 | PA2G4 | 4 |
| E5RJR5 | S-phase kinase-associated protein 1 | SKP1 | 4 |
| Q9NRV9 | Heme-binding protein 1 | HEBP1 | 4 |
| Q9H444 | Charged multivesicular body protein 4b | CHMP4B | 4 |
| P10599 | Thioredoxin | TXN | 4 |
| Q5VSJ9 | Blood group Rh(CE) polypeptide;Blood group Rh(D) polypeptide | RHCE;RHD | 4 |
| Q9UK41 | Vacuolar protein sorting-associated protein 28 homolog | VPS28 | 4 |
| Q9Y3I1 | F-box only protein 7 | FBXO7 | 4 |
| P61026 | Ras-related protein Rab-10 | RAB10 | 4 |
| Q14974 | Importin subunit beta-1 | KPNB1 | 4 |
| P27797 | Calreticulin | CALR | 4 |
| P18669 | Phosphoglycerate mutase 1;Probable phosphoglycerate mutase 4 | PGAM1;PGAM4 | 4 |
| P54725 | UV excision repair protein RAD23 homolog A | RAD23A | 4 |
| P30613 | Pyruvate kinase PKLR | PKLR | 4 |
| P63000 | Ras-related C3 botulinum toxin substrate 1;Ras-related C3 botulinum toxin substrate 3;Ras-related C3 botulinum toxin substrate 2 | RAC1;RAC3;RAC2 | 4 |
| P05164 | Myeloperoxidase | MPO | 4 |
| F5GWY2 | Bifunctional purine biosynthesis protein PURH;Phosphoribosylaminoimidazolecarboxamide formyltransferase;IMP cyclohydrolase | ATIC | 4 |
| P48637 | Glutathione synthetase | GSS | 4 |
| F5H5V4 | 26S proteasome non-ATPase regulatory subunit 9 | PSMD9 | 4 |
| G5E9R5 | Low molecular weight phosphotyrosine protein phosphatase | ACP1 | 3 |
| P46976 | Glycogenin-1 | GYG1 | 3 |
| P28072 | Proteasome subunit beta type-6 | PSMB6 | 3 |
| P26447 | Protein S100-A4 | S100A4 | 3 |
| F5GXQ0 | BRO1 domain-containing protein BROX | BROX | 3 |
| P08754 | Guanine nucleotide-binding protein G(k) subunit alpha | GNAI3 | 3 |
| Q99436 | Proteasome subunit beta type-7 | PSMB7 | 3 |
| P62942 | Peptidyl-prolyl cis-trans isomerase | FKBP1A | 3 |
| U3KQK0 | Histone H2B | HIST1H2B | 3 |
| J3QKR3 | Proteasome subunit beta type-3 | PSMB3 | 3 |
| P01116 | GTPase KRas;GTPase KRas, N-terminally processed;GTPase HRas;GTPase HRas, N-terminally processed;GTPase NRas | KRAS;HRAS;NRAS | 3 |
| P13489 | Ribonuclease inhibitor | RNH1 | 3 |
| Q08722 | Leukocyte surface antigen CD47 | CD47 | 3 |
| Q5T123 | SH3 domain-binding glutamic acid-rich-like protein 3 | SH3BGRL3 | 3 |
| Q8WYQ7 | Galectin;Galectin-9 | LGALS9 | 3 |
| O75695 | Protein XRP2 | RP2 | 3 |
| P00167 | Cytochrome b5 | CYB5A | 3 |
| Q9Y4D1 | Disheveled-associated activator of morphogenesis 1 | DAAM1 | 3 |
| P11021 | 78 kDa glucose-regulated protein | HSPA5 | 3 |
| H7C1D4 | Translin | TSN | 3 |
| P07737 | Profilin-1 | PFN1 | 3 |
| M0R389 | Platelet-activating factor acetylhydrolase IB subunit gamma | PAFAH1B3 | 3 |
| A6NJA2 | Ubiquitin carboxyl-terminal hydrolase 14 | USP14 | 3 |
| P10644 | cAMP-dependent protein kinase type I-alpha regulatory subunit | PRKAR1A | 3 |

| | | | |
|---|---|---|---|
| Q9BS40 | Latexin | LXN | 3 |
| G5EA52 | Protein disulfide-isomerase A3 | PDIA3 | 3 |
| P53004 | Biliverdin reductase A | BLVRA | 3 |
| Q04656 | Copper-transporting ATPase 1 | ATP7A | 3 |
| H9KV70 | Neutrophil gelatinase-associated lipocalin | LCN2 | 3 |
| O00299 | Chloride intracellular channel protein 1 | CLIC1 | 3 |
| F8WF69 | Clathrin light chain A | CLTA | 3 |
| G3V2F7 | Ubiquitin-conjugating enzyme E2 variant 1;Ubiquitin-conjugating enzyme E2 variant 2 | UBE2V1;UBE2V2 | 3 |
| F8WDS9 | LanC-like protein 1 | LANCL1 | 3 |
| P60891 | Ribose-phosphate pyrophosphokinase 1 | PRPS1 | 3 |
| K7ESE8 | Bleomycin hydrolase | BLMH | 3 |
| H0YNE3 | Proteasome activator complex subunit 1 | PSME1 | 3 |
| P16930 | Fumarylacetoacetase | FAH | 3 |
| F8VSD4 | Ubiquitin-conjugating enzyme E2 N | UBE2N | 3 |
| P07203 | Glutathione peroxidase 1 | GPX1 | 3 |
| P62328 | Thymosin beta-4;Hematopoietic system regulatory peptide | TMSB4X;TMSB4XP4 | 3 |
| E5RIW3 | Tubulin-specific chaperone A | TBCA | 3 |
| M0R0Y2 | Alpha-soluble NSF attachment protein | NAPA | 3 |
| P15374 | Ubiquitin carboxyl-terminal hydrolase isozyme L3 | UCHL3 | 3 |
| P04921 | Glycophorin-C | GYPC | 2 |
| H0YDI1 | Lymphocyte function-associated antigen 3 | CD58 | 2 |
| B4E220 | Aquaporin-1 | AQP1 | 2 |
| C9JEN3 | Protein lifeguard 3 | TMBIM1 | 2 |
| F5H2R5 | Rho GDP-dissociation inhibitor 2 | ARHGDIB | 2 |
| Q53TN4 | Cytochrome b reductase 1 | CYBRD1 | 2 |
| Q9NZD4 | Alpha-hemoglobin-stabilizing protein | AHSP | 2 |
| Q8NHG7 | Small VCP/p97-interacting protein | SVIP | 2 |
| Q5JYX0 | Cell division control protein 42 homolog | CDC42 | 2 |
| Q71RC9 | Small integral membrane protein 5 | SMIM5 | 2 |
| E9PNW4 | CD59 glycoprotein | CD59 | 2 |
| P09105 | Hemoglobin subunit theta-1 | HBQ1 | 2 |
| R4GN98 | Protein S100;Protein S100-A6 | S100A6 | 2 |
| O75531 | Barrier-to-autointegration factor;Barrier-to-autointegration factor, N-terminally processed | BANF1 | 2 |
| Q5T6W5 | Heterogeneous nuclear ribonucleoprotein K | HNRNPK | 2 |
| F5H4Q5 | Vacuolar protein sorting-associated protein 37C | VPS37C | 2 |
| J3QK90 | NSFL1 cofactor p47 | NSFL1C | 2 |
| H3BV85 | BolA-like protein 2 | BOLA2B;BOLA2 | 2 |
| Q9NRX4 | 14 kDa phosphohistidine phosphatase | PHPT1 | 2 |
| H3BS66 | Small integral membrane protein 1 | SMIM1 | 2 |
| E7ESC6 | Exportin-7 | XPO7 | 2 |
| P68402 | Platelet-activating factor acetylhydrolase IB subunit beta | PAFAH1B2 | 2 |
| Q9BRF8 | Serine/threonine-protein phosphatase CPPED1 | CPPED1 | 2 |
| P08246 | Neutrophil elastase | ELANE | 2 |
| E9PN50 | 26S protease regulatory subunit 6A | PSMC3 | 2 |

| | | | |
|---|---|---|---|
| E7EUC7 | UTP--glucose-1-phosphate uridylyltransferase | UGP2 | 2 |
| B8ZZB8 | CB1 cannabinoid receptor-interacting protein 1 | CNRIP1 | 2 |
| E9PCS3 | 26S proteasome non-ATPase regulatory subunit 2 | PSMD2 | 2 |
| P59666 | Neutrophil defensin 3;HP 3-56;Neutrophil defensin 2;Neutrophil defensin 1;HP 1-56;Neutrophil defensin 2 | DEFA3;DEFA 1 | 2 |
| O15400 | Syntaxin-7 | STX7 | 2 |
| P00338 | L-lactate dehydrogenase A chain | LDHA | 2 |
| P61970 | Nuclear transport factor 2 | NUTF2 | 2 |
| E7EMV0 | Protein diaphanous homolog 1 | DIAPH1 | 2 |
| F5GY90 | Porphobilinogen deaminase | HMBS | 2 |
| P61020 | Ras-related protein Rab-5B | RAB5B | 2 |
| Q99828 | Calcium and integrin-binding protein 1 | CIB1 | 2 |
| B4DUA0 | Plastin-2 | LCP1 | 2 |
| C9JTY3 | Protein TFG | TFG | 2 |
| P27348 | 14-3-3 protein theta | YWHAQ | 2 |
| H0YKZ7 | Annexin;Annexin A2;Putative annexin A2-like protein | ANXA2;ANXA 2P2 | 2 |
| P08238 | Heat shock protein HSP 90-beta | HSP90AB1 | 2 |
| J3KQP6 | Ras-related protein Rab-11B;Ras-related protein Rab-11A | RAB11A;RAB 11B | 2 |
| A6NMU3 | Signal transducing adapter molecule 1 | STAM | 2 |
| P53985 | Monocarboxylate transporter 1 | SLC16A1 | 2 |
| F6USW4 | F-actin-capping protein subunit beta | CAPZB | 2 |
| O14964 | Hepatocyte growth factor-regulated tyrosine kinase substrate | HGS | 2 |
| P20020 | Plasma membrane calcium-transporting ATPase 1;Calcium-transporting ATPase | ATP2B1 | 2 |
| P36959 | GMP reductase 1 | GMPR | 2 |
| Q9Y376 | Calcium-binding protein 39 | CAB39 | 2 |
| Q9Y6M5 | Zinc transporter 1 | SLC30A1 | 2 |
| Q8IZ83 | Aldehyde dehydrogenase family 16 member A1 | ALDH16A1 | 2 |
| Q99459 | Cell division cycle 5-like protein | CDC5L | 2 |
| P06132 | Uroporphyrinogen decarboxylase | UROD | 2 |
| J3KNT0 | Fascin | FSCN1 | 2 |
| P49189 | 4-trimethylaminobutyraldehyde dehydrogenase | ALDH9A1 | 2 |
| H3BNT7 | 26S proteasome non-ATPase regulatory subunit 7 | PSMD7 | 2 |
| P05023 | Sodium/potassium-transporting ATPase subunit alpha-1;Sodium/potassium-transporting ATPase subunit alpha-3;Sodium/potassium-transporting ATPase subunit alpha-2;Sodium/potassium-transporting ATPase subunit alpha-4;Potassium-transporting ATPase alpha chain 1;Potassium-transporting ATPase alpha chain 2 | ATP1A1;ATP 1A2;ATP1A3; ATP1A4;ATP 4A;ATP12A | 2 |
| P34932 | Heat shock 70 kDa protein 4 | HSPA4 | 2 |
| K7EMV3 | Histone H3 | H3F3B | 2 |
| Q8IU68 | Transmembrane channel-like protein 8 | TMC8 | 2 |
| E7ENZ3 | T-complex protein 1 subunit epsilon | CCT5 | 2 |
| Q5TZA2 | Rootletin | CROCC | 2 |
| Q9P203 | BTB/POZ domain-containing protein 7 | BTBD7 | 2 |
| Q7LBR1 | Charged multivesicular body protein 1b | CHMP1B | 2 |
| U3KQ56 | Glyoxylate reductase/hydroxypyruvate reductase | GRHPR | 2 |
| H0YJ11 | Alpha-actinin-1;Alpha-actinin-2;Alpha-actinin-4 | ACTN1;ACTN 4;ACTN2 | 2 |
| Q9UDT6 | CAP-Gly domain-containing linker protein 2 | CLIP2 | 2 |

| | | | |
|---|---|---|---|
| P09960 | Leukotriene A-4 hydrolase | LTA4H | 2 |
| Q5HY54 | Filamin-A | FLNA | 2 |
| E9PJL5 | Uncharacterized protein C12orf55;Putative uncharacterized protein C12orf63 | C12orf55;C12orf63 | 2 |
| G3V2U7 | Acylphosphatase;Acylphosphatase-1 | FBN3;ACYP1 | 2 |
| E9PQN4 | Complement receptor type 1 | CR1 | 2 |
| Q9BSL1 | Ubiquitin-associated domain-containing protein 1 | UBAC1 | 2 |
| Q04917 | 14-3-3 protein eta | YWHAH | 2 |
| B7ZBP9 | Serine/threonine-protein phosphatase 2A activator | PPP2R4;DKFZp781M17165 | 2 |
| Q8NDC0 | MAPK-interacting and spindle-stabilizing protein-like | MAPK1IP1L | 1 |
| P68133 | Actin, alpha skeletal muscle;Actin, alpha cardiac muscle 1;Actin, gamma-enteric smooth muscle;Actin, aortic smooth muscle | ACTA1;ACTC1;ACTG2;ACTA2 | 1 |
| P69891 | Hemoglobin subunit gamma-1 | HBG1 | 1 |
| S4R3Y4 | Protein AMBP;Alpha-1-microglobulin;Inter-alpha-trypsin inhibitor light chain;Trypstatin | AMBP | 1 |
| I3L3E4 | Charged multivesicular body protein 6 | CHMP6 | 1 |
| Q16570 | Atypical chemokine receptor 1 | ACKR1 | 1 |
| Q5VY30 | Retinol-binding protein 4;Plasma retinol-binding protein(1-182);Plasma retinol-binding protein(1-181);Plasma retinol-binding protein(1-179);Plasma retinol-binding protein(1-176) | RBP4 | 1 |
| E7END7 | Ras-related protein Rab-1A | RAB1A | 1 |
| Q5VU59 | | TPM3 | 1 |
| P17066 | Heat shock 70 kDa protein 6;Putative heat shock 70 kDa protein 7 | HSPA6;HSPA7 | 1 |
| Q04760 | Lactoylglutathione lyase | GLO1 | 1 |
| D6RD66 | WD repeat-containing protein 1 | WDR1 | 1 |
| K7EM02 | Katanin p60 ATPase-containing subunit A-like 2 | KATNAL2 | 1 |
| P14209 | CD99 antigen | CD99 | 1 |
| E9PIR7 | Thioredoxin reductase 1, cytoplasmic | GML;TXNRD1 | 1 |
| K7EMQ9 | | EIF3K | 1 |
| P15531 | Nucleoside diphosphate kinase A | NME1 | 1 |
| H7BZT4 | Small ubiquitin-related modifier 4;Small ubiquitin-related modifier 2;Small ubiquitin-related modifier 3 | SUMO2;SUMO3;SUMO4 | 1 |
| O00560 | Syntenin-1 | SDCBP | 1 |
| Q9BVM4 | Gamma-glutamylaminecyclotransferase | GGACT | 1 |
| K7EKH5 | Fructose-bisphosphate aldolase C | ALDOC | 1 |
| P49773 | Histidine triad nucleotide-binding protein 1 | HINT1 | 1 |
| H0YBY6 | Disks large-associated protein 2 | DLGAP2 | 1 |
| Q9Y624 | Junctional adhesion molecule A | F11R | 1 |
| B1AKQ8 | Guanine nucleotide-binding protein G(I)/G(S)/G(T) subunit beta-1;Guanine nucleotide-binding protein G(I)/G(S)/G(T) subunit beta-3 | GNB1;GNB3 | 1 |
| K7EKN6 | Urea transporter 1 | SLC14A1 | 1 |
| I3L0K2 | Thioredoxin domain-containing protein 17 | TXNDC17 | 1 |
| A8MXY0 | Syntaxin-4 | STX4 | 1 |
| O14773 | Tripeptidyl-peptidase 1 | TPP1 | 1 |
| E9PNW0 | Nucleosome assembly protein 1-like 1;Nucleosome assembly protein 1-like 4 | NAP1L4;NAP1L1 | 1 |
| Q5TDH0 | Protein DDI1 homolog 2 | DDI2 | 1 |
| Q96JM4 | Leucine-rich repeat and IQ domain-containing protein 1 | LRRIQ1 | 1 |
| F5GWT9 | Phosphoribosylformylglycinamidine synthase | PFAS | 1 |

| | | | |
|---|---|---|---|
| F2Z3J2 | 26S proteasome non-ATPase regulatory subunit 5 | PSMD5 | 1 |
| J3QL74 | Zinc finger and BTB domain-containing protein 14 | ZBTB14 | 1 |
| E9PJC7 | CD82 antigen | CD82 | 1 |
| Q9H936 | Mitochondrial glutamate carrier 1 | SLC25A22 | 1 |
| D6RD63 | COP9 signalosome complex subunit 4 | COPS4 | 1 |
| Q6B0K9 | Hemoglobin subunit mu | HBM | 1 |
| Q31611 | HLA class I histocompatibility antigen, alpha chain G | HLA-G | 1 |
| H7BY04 | Laminin subunit gamma-3 | LAMC3 | 1 |
| Q9UL25 | Ras-related protein Rab-21 | RAB21 | 1 |
| H7C3P7 | Ras-related protein Ral-A | RALA | 1 |
| P08311 | Cathepsin G | CTSG | 1 |
| E9PE37 | Ras-related protein Rab-2A;Ras-related protein Rab-2B | RAB2B;RAB2A | 1 |
| G3V1N2 | | HBA2 | 1 |
| P00387 | NADH-cytochrome b5 reductase 3;NADH-cytochrome b5 reductase 3 membrane-bound form;NADH-cytochrome b5 reductase 3 soluble form | CYB5R3 | 1 |
| O75339 | Cartilage intermediate layer protein 1;Cartilage intermediate layer protein 1 C1;Cartilage intermediate layer protein 1 C2 | CILP | 1 |
| P14324 | Farnesyl pyrophosphate synthase | FDPS | 1 |
| K7EKG2 | Thioredoxin-like protein 1 | TXNL1 | 1 |

**B.** Uniprot Complete Proteome *Homo sapiens* database when the heamoglobin was analyzed separately

| Protein ID | Protein names | Gene names | Razor + unique peptides |
|---|---|---|---|
| P02549 | Spectrin alpha chain, erythrocytic 1 | SPTA1 | 197 |
| P11277 | Spectrin beta chain, erythrocytic | SPTB | 177 |
| P16157 | Ankyrin-1 | ANK1 | 94 |
| P55072 | Transitional endoplasmic reticulum ATPase | VCP | 53 |
| P111714 | Protein 4.1 | EPB41 | 52 |
| P35579 | Myosin-9 | MYH9 | 44 |
| Q8WUM4 | Programmed cell death 6-interacting protein | PDCD6IP | 43 |
| P02730 | Band 3 anion transport protein | SLC4A1 | 43 |
| P16452 | Erythrocyte membrane protein band 4.2 | EPB42 | 42 |
| P04040 | Catalase | CAT | 40 |
| A0A087WVQ6 | Clathrin heavy chain;Clathrin heavy chain 1 | CLTC | 38 |
| P35612 | Beta-adducin | ADD2 | 37 |
| P16157 | Ankyrin-1 | ANK1 | 36 |
| Q14254 | Flotillin-2 | FLOT2 | 33 |
| P20073 | Annexin A7 | ANXA7 | 31 |
| O75955 | Flotillin-1 | FLOT1 | 30 |
| P53396 | ATP-citrate synthase | ACLY | 30 |
| P06753 | | TPM3 | 29 |
| P49368 | T-complex protein 1 subunit gamma | CCT3 | 29 |
| P236344 | Plasma membrane calcium-transporting ATPase 4 | ATP2B4 | 28 |

| | | | |
|---|---|---|---|
| P11142 | Heat shock cognate 71 kDa protein | HSPA8 | 28 |
| P60709 | Actin, cytoplasmic 1;Actin, cytoplasmic 1, N-terminally processed | ACTB | 28 |
| Q5T4S7 | E3 ubiquitin-protein ligase UBR4 | UBR4 | 27 |
| P78371 | T-complex protein 1 subunit beta | CCT2 | 26 |
| P28289 | Tropomodulin-1 | TMOD1 | 26 |
| P50395 | Rab GDP dissociation inhibitor beta | GDI2 | 25 |
| P27105 | Erythrocyte band 7 integral membrane protein | STOM | 25 |
| P68871 | Hemoglobin subunit beta;LVV-hemorphin-7;Spinorphin | HBB | 25 |
| P02730 | Band 3 anion transport protein | SLC4A1 | 25 |
| Q00013 | 55 kDa erythrocyte membrane protein | MPP1 | 24 |
| J3KPS3 | Fructose-bisphosphate aldolase;Fructose-bisphosphate aldolase A | ALDOA | 24 |
| P00352 | Retinal dehydrogenase 1 | ALDH1A1 | 24 |
| Q86VP6 | Cullin-associated NEDD8-dissociated protein 1 | CAND1 | 24 |
| P49327 | Fatty acid synthase | FASN | 24 |
| Q13228 | Selenium-binding protein 1 | SELENBP1 | 22 |
| P00915 | Carbonic anhydrase 1 | CA1 | 22 |
| P50991 | T-complex protein 1 subunit delta | CCT4 | 22 |
| P50990 | T-complex protein 1 subunit theta | CCT8 | 22 |
| P32119 | Peroxiredoxin-2 | PRDX2 | 21 |
| P50995 | Annexin A11 | ANXA11 | 21 |
| P69905 | Hemoglobin subunit alpha | HBA1 | 21 |
| P00558 | Phosphoglycerate kinase 1 | PGK1 | 20 |
| H7BXK9 | ATP-binding cassette sub-family B member 6, mitochondrial | ABCB6 | 20 |
| P08758 | Annexin A5;Annexin | ANXA5 | 20 |
| P09525 | Annexin A4;Annexin | ANXA4 | 20 |
| P07900 | Heat shock protein HSP 90-alpha | HSP90AA1 | 20 |
| P48643 | T-complex protein 1 subunit epsilon | CCT5 | 20 |
| P07384 | Calpain-1 catalytic subunit | CAPN1 | 20 |
| P22314 | Ubiquitin-like modifier-activating enzyme 1 | UBA1 | 19 |
| P04406 | Glyceraldehyde-3-phosphate dehydrogenase | GAPDH | 19 |
| Q08495 | Dematin | DMTN | 19 |
| Q99832 | T-complex protein 1 subunit eta | CCT7 | 19 |
| P29144 | Tripeptidyl-peptidase 2 | TPP2 | 19 |
| P30041 | Peroxiredoxin-6 | PRDX6 | 18 |
| E9PM69 | 26S protease regulatory subunit 6A | PSMC3 | 18 |
| P40227 | T-complex protein 1 subunit zeta | CCT6A | 18 |
| P50570 | Dynamin-2 | DNM2 | 18 |
| E7EQB2 | Lactotransferrin;Lactoferricin-H;Kaliocin-1;Lactoferroxin-A;Lactoferroxin-B;Lactoferroxin-C | LTF | 18 |
| P31948 | Stress-induced-phosphoprotein 1 | STIP1 | 18 |
| E7ESC6 | Exportin-7 | XPO7 | 18 |
| E7EV99 | Alpha-adducin | ADD1 | 17 |
| P62258 | 14-3-3 protein epsilon | YWHAE | 17 |
| P30613 | Pyruvate kinase PKLR | PKLR | 17 |
| A0A0G2JIW1 | Heat shock 70 kDa protein 1B;Heat shock 70 kDa protein 1A | HSPA1B;HSPA1A | 17 |

| | | | |
|---|---|---|---|
| Q16531 | DNA damage-binding protein 1 | DDB1 | 17 |
| P11021 | 78 kDa glucose-regulated protein | HSPA5 | 17 |
| F5H2F4 | C-1-tetrahydrofolate synthase, cytoplasmic;Methylenetetrahydrofolate dehydrogenase | MTHFD1 | 17 |
| P07195 | L-lactate dehydrogenase B chain;L-lactate dehydrogenase | LDHB | 16 |
| P45974 | Ubiquitin carboxyl-terminal hydrolase 5 | USP5 | 16 |
| O43242 | 26S proteasome non-ATPase regulatory subunit 3 | PSMD3 | 16 |
| C9J0K6 | Sorcin | SRI | 16 |
| P08133 | Annexin A6;Annexin | ANXA6 | 16 |
| Q13200 | 26S proteasome non-ATPase regulatory subunit 2 | PSMD2 | 16 |
| P23276 | Kell blood group glycoprotein | KEL | 16 |
| P34932 | Heat shock 70 kDa protein 4 | HSPA4 | 16 |
| A0A0A0MSI0 | Peroxiredoxin-1 | PRDX1 | 16 |
| Q9Y230 | RuvB-like 2 | RUVBL2 | 16 |
| Q5XPI4 | E3 ubiquitin-protein ligase RNF123 | RNF123 | 16 |
| P68871 | Hemoglobin subunit beta;LVV-hemorphin-7;Spinorphin | HBB | 15 |
| P60174 | Triosephosphate isomerase | TPI1 | 15 |
| P00491 | Purine nucleoside phosphorylase | PNP | 15 |
| C9JIF9 | Acylamino-acid-releasing enzyme | APEH | 15 |
| H7BYY1 | Tropomyosin alpha-1 chain | TPM1 | 15 |
| P35998 | 26S protease regulatory subunit 7 | PSMC2 | 15 |
| P17987 | T-complex protein 1 subunit alpha | TCP1 | 15 |
| P09543 | 2,3-cyclic-nucleotide 3-phosphodiesterase | CNP | 15 |
| Q99460 | 26S proteasome non-ATPase regulatory subunit 1 | PSMD1 | 15 |
| Q9Y4E8 | Ubiquitin carboxyl-terminal hydrolase 15 | USP15 | 15 |
| Q9C0C9 | E2/E3 hybrid ubiquitin-protein ligase UBE2O | UBE2O | 15 |
| P26038 | Moesin | MSN | 15 |
| P04083 | Annexin A1;Annexin | ANXA1 | 14 |
| P30043 | Flavin reductase (NADPH) | BLVRB | 14 |
| P11166 | Solute carrier family 2, facilitated glucose transporter member 1 | SLC2A1 | 14 |
| P00918 | Carbonic anhydrase 2 | CA2 | 14 |
| P06733 | Alpha-enolase | ENO1 | 14 |
| Q5TDH0 | Protein DDI1 homolog 2 | DDI2 | 14 |
| B0QZ18 | Copine-1 | CPNE1 | 14 |
| O75326 | Semaphorin-7A | SEMA7A | 14 |
| P05164 | Myeloperoxidase | MPO | 14 |
| Q9Y265 | RuvB-like 1 | RUVBL1 | 14 |
| P29401 | Transketolase | TKT | 14 |
| I3L0N3 | Vesicle-fusing ATPase | NSF | 14 |
| Q4VB86 | Protein 4.1 | EPB41 | 14 |
| P11277 | Spectrin beta chain, erythrocytic | SPTB | 14 |
| P13716 | Delta-aminolevulinic acid dehydratase | ALAD | 13 |
| P07738 | Bisphosphoglycerate mutase | BPGM | 13 |
| P48506 | Glutamate--cysteine ligase catalytic subunit | GCLC | 13 |
| Q99816 | Tumor susceptibility gene 101 protein | TSG101 | 13 |
| O14818 | Proteasome subunit alpha type-7 | PSMA7 | 13 |

| | | | |
|---|---|---|---|
| P23526 | Adenosylhomocysteinase | AHCY | 13 |
| P61225 | Ras-related protein Rap-2b | RAP2B | 13 |
| O00231 | 26S proteasome non-ATPase regulatory subunit 11 | PSMD11 | 13 |
| P11413 | Glucose-6-phosphate 1-dehydrogenase | G6PD | 13 |
| P00338 | L-lactate dehydrogenase A chain | LDHA | 12 |
| Q99808 | Equilibrative nucleoside transporter 1 | SLC29A1 | 12 |
| A6NJA2 | Ubiquitin carboxyl-terminal hydrolase;Ubiquitin carboxyl-terminal hydrolase 14 | USP14 | 12 |
| Q06323 | Proteasome activator complex subunit 1 | PSME1 | 12 |
| P28074 | Proteasome subunit beta type-5 | PSMB5 | 12 |
| B3KQV6 | Serine/threonine-protein phosphatase 2A 65 kDa regulatory subunit A alpha isoform | PPP2R1A | 12 |
| Q14974 | Importin subunit beta-1 | KPNB1 | 12 |
| P25786 | Proteasome subunit alpha type-1;Proteasome subunit alpha type | PSMA1 | 12 |
| Q86X55 | Histone-arginine methyltransferase CARM1 | CARM1 | 12 |
| A6NG10 | WW domain-binding protein 2 | WBP2 | 12 |
| P63092 | Guanine nucleotide-binding protein G(s) subunit alpha | GNAS | 12 |
| P31939 | Bifunctional purine biosynthesis protein PURH;Phosphoribosylaminoimidazolecarboxamide formyltransferase;IMP cyclohydrolase | ATIC | 12 |
| P52209 | 6-phosphogluconate dehydrogenase, decarboxylating | PGD | 12 |
| A0A087X0C8 | Calpain-5 | CAPN5 | 12 |
| F8W9S7 | GTPase-activating protein and VPS9 domain-containing protein 1 | GAPVD1 | 12 |
| P60842 | Eukaryotic initiation factor 4A-I | EIF4A1 | 12 |
| P69905 | Hemoglobin subunit alpha | HBA1 | 11 |
| Q6XQN6 | Nicotinate phosphoribosyltransferase | NAPRT | 11 |
| P48637 | Glutathione synthetase | GSS | 11 |
| H7BZ94 | Protein disulfide-isomerase | P4HB | 11 |
| P21980 | Protein-glutamine gamma-glutamyltransferase 2 | TGM2 | 11 |
| P50895 | Basal cell adhesion molecule | BCAM | 11 |
| A0A087X2I1 | 26S protease regulatory subunit 10B | PSMC6 | 11 |
| G3V1D3 | Dipeptidyl peptidase 3 | DPP3 | 11 |
| P05023 | Sodium/potassium-transporting ATPase subunit alpha-1;Sodium/potassium-transporting ATPase subunit alpha-3 | ATP1A1;ATP1A3 | 11 |
| P40925 | Malate dehydrogenase, cytoplasmic;Malate dehydrogenase | MDH1 | 11 |
| Q9UKV8 | Protein argonaute-2 | AGO2 | 11 |
| P30566 | Adenylosuccinate lyase | ADSL | 11 |
| P20618 | Proteasome subunit beta type-1 | PSMB1 | 11 |
| P17858 | ATP-dependent 6-phosphofructokinase, liver type | PFKL | 11 |
| A0A087X253 | AP-2 complex subunit beta | AP2B1 | 11 |
| O95782 | AP-2 complex subunit alpha-1 | AP2A1 | 11 |
| O00232 | 26S proteasome non-ATPase regulatory subunit 12 | PSMD12 | 11 |
| Q9BSL1 | Ubiquitin-associated domain-containing protein 1 | UBAC1 | 11 |
| A0A087WUL0 | Bifunctional ATP-dependent dihydroxyacetone kinase/FAD-AMP lyase (cyclizing);ATP-dependent dihydroxyacetone kinase;FAD-AMP lyase (cyclizing) | TKFC;DAK | 11 |
| P69891 | Hemoglobin subunit gamma-1 | HBG1 | 11 |
| A0A087WZE4 | Spectrin alpha chain, erythrocytic 1 | SPTA1 | 11 |
| P48426 | Phosphatidylinositol 5-phosphate 4-kinase type-2 alpha | PIP4K2A | 10 |
| P10644 | cAMP-dependent protein kinase type I-alpha regulatory subunit | PRKAR1A | 10 |
| Q9BWD1 | Acetyl-CoA acetyltransferase, cytosolic | ACAT2 | 10 |

| | | | |
|---|---|---|---|
| P62191 | 26S protease regulatory subunit 4 | PSMC1 | 10 |
| E9PBS1 | Multifunctional protein ADE2;Phosphoribosylaminoimidazole-succinocarboxamide synthase;Phosphoribosylaminoimidazole carboxylase | PAICS | 10 |
| M0R0Y2 | Alpha-soluble NSF attachment protein | NAPA | 10 |
| P78417 | Glutathione S-transferase omega-1 | GSTO1 | 10 |
| P25789 | Proteasome subunit alpha type-4;Proteasome subunit alpha type;Proteasome subunit beta type | PSMA4 | 10 |
| Q9H0U4 | Ras-related protein Rab-1B;Putative Ras-related protein Rab-1C | RAB1B;RAB1C | 10 |
| Q16401 | 26S proteasome non-ATPase regulatory subunit 5 | PSMD5 | 10 |
| P30101 | Protein disulfide-isomerase A3 | PDIA3 | 10 |
| D6RAX7 | COP9 signalosome complex subunit 4 | COPS4 | 10 |
| O75340 | Programmed cell death protein 6 | PDCD6 | 10 |
| Q96P70 | Importin-9 | IPO9 | 10 |
| P38606 | V-type proton ATPase catalytic subunit A | ATP6V1A | 10 |
| A0A0G2JH68 | Protein diaphanous homolog 1 | DIAPH1 | 10 |
| Q5T9B7 | Adenylate kinase isoenzyme 1 | AK1 | 10 |
| O14980 | Exportin-1 | XPO1 | 10 |
| P43686 | 26S protease regulatory subunit 6B | PSMC4 | 10 |
| H0YH81 | ATP synthase subunit beta;ATP synthase subunit beta, mitochondrial | ATP5B | 10 |
| Q04656 | Copper-transporting ATPase 1 | ATP7A | 10 |
| P16452 | Erythrocyte membrane protein band 4.2 | EPB42 | 10 |
| Q9BY43 | Charged multivesicular body protein 4a | CHMP4A | 9 |
| P51148 | Ras-related protein Rab-5C | RAB5C | 9 |
| Q9NRV9 | Heme-binding protein 1 | HEBP1 | 9 |
| Q9UNZ2 | NSFL1 cofactor p47 | NSFL1C | 9 |
| Q16851 | UTP--glucose-1-phosphate uridylyltransferase | UGP2 | 9 |
| P28066 | Proteasome subunit alpha type-5 | PSMA5 | 9 |
| A0A0C4DGQ5 | Calpain small subunit 1 | CAPNS1 | 9 |
| A0A087X1Z3 | Proteasome activator complex subunit 2 | PSME2 | 9 |
| Q01518 | Adenylyl cyclase-associated protein 1 | CAP1 | 9 |
| B1AKQ8 | Guanine nucleotide-binding protein G(I)/G(S)/G(T) subunit beta-1 | GNB1 | 9 |
| O75131 | Copine-3 | CPNE3 | 9 |
| P54725 | UV excision repair protein RAD23 homolog A | RAD23A | 9 |
| P11215 | Integrin alpha-M | ITGAM | 9 |
| Q93008 | Probable ubiquitin carboxyl-terminal hydrolase FAF-X | USP9X | 9 |
| Q96G03 | Phosphoglucomutase-2 | PGM2 | 9 |
| P49721 | Proteasome subunit beta type-2 | PSMB2 | 9 |
| Q15008 | 26S proteasome non-ATPase regulatory subunit 6 | PSMD6 | 9 |
| Q9UNQ0 | ATP-binding cassette sub-family G member 2 | ABCG2 | 9 |
| P22303 | Acetylcholinesterase;Carboxylic ester hydrolase | ACHE | 9 |
| G3V5Z7 | Proteasome subunit alpha type;Proteasome subunit alpha type-6 | PSMA6 | 9 |
| O15439 | Multidrug resistance-associated protein 4 | ABCC4 | 9 |
| P37837 | Transaldolase | TALDO1 | 9 |
| O14744 | Protein arginine N-methyltransferase 5 | PRMT5 | 9 |
| P02042 | Hemoglobin subunit delta | HBD | 9 |
| P25788 | Proteasome subunit alpha type-3 | PSMA3 | 8 |

| | | | |
|---|---|---|---|
| J3QS39 | Ubiquitin-60S ribosomal protein L40;Ubiquitin;60S ribosomal protein L40;Ubiquitin-40S ribosomal protein S27a;Ubiquitin;40S ribosomal protein S27a;Polyubiquitin-B;Ubiquitin;Polyubiquitin-C;Ubiquitin | UBB;RPS27A;UBC;UBA52;UBBP4 | 8 |
| O94919 | Endonuclease domain-containing 1 protein | ENDOD1 | 8 |
| P31946 | 14-3-3 protein beta/alpha | YWHAB | 8 |
| P60891 | Ribose-phosphate pyrophosphokinase 1;Ribose-phosphate pyrophosphokinase 2;Ribose-phosphate pyrophosphokinase 3 | PRPS1;PRPS2;PRPS1L1 | 8 |
| P62195 | 26S protease regulatory subunit 8 | PSMC5 | 8 |
| A0A024RA52 | Proteasome subunit alpha type;Proteasome subunit alpha type-2 | PSMA2 | 8 |
| P04899 | Guanine nucleotide-binding protein G(i) subunit alpha-2 | GNAI2 | 8 |
| Q13561 | Dynactin subunit 2 | DCTN2 | 8 |
| P53004 | Biliverdin reductase A | BLVRA | 8 |
| P00387 | NADH-cytochrome b5 reductase 3 | CYB5R3 | 8 |
| P16152 | Carbonyl reductase [NADPH] 1 | CBR1 | 8 |
| P06744 | Glucose-6-phosphate isomerase | GPI | 8 |
| Q99733 | Nucleosome assembly protein 1-like 4 | NAP1L4 | 8 |
| P04792 | Heat shock protein beta-1 | HSPB1 | 8 |
| P17612 | cAMP-dependent protein kinase catalytic subunit alpha;cAMP-dependent protein kinase catalytic subunit beta | PRKACA;KIN27;PRKACB | 8 |
| P20340 | Ras-related protein Rab-6A | RAB6A | 8 |
| P13796 | Plastin-2 | LCP1 | 8 |
| P52907 | F-actin-capping protein subunit alpha-1 | CAPZA1 | 8 |
| Q14697 | Neutral alpha-glucosidase AB | GANAB | 8 |
| P08514 | Integrin alpha-IIb;Integrin alpha-IIb heavy chain;Integrin alpha-IIb light chain, form 1;Integrin alpha-IIb light chain, form 2 | ITGA2B | 8 |
| P26641 | Elongation factor 1-gamma | EEF1G | 8 |
| Q9UQ80 | Proliferation-associated protein 2G4 | PA2G4 | 8 |
| Q9Y4D1 | Disheveled-associated activator of morphogenesis 1 | DAAM1 | 8 |
| P11166 | Solute carrier family 2, facilitated glucose transporter member 1 | SLC2A1 | 8 |
| P63261 | Actin, cytoplasmic 2;Actin, cytoplasmic 2, N-terminally processed;Actin, cytoplasmic 1;Actin, cytoplasmic 1, N-terminally processed;Actin, gamma-enteric smooth muscle;Actin, alpha skeletal muscle;Actin, alpha cardiac muscle 1;Actin, aortic smooth muscle | ACTG1;ACTB;ACTG2;ACTA1;ACTC1;ACTA2 | 8 |
| P02008 | Hemoglobin subunit zeta | HBZ | 8 |
| P20073 | Annexin A7 | ANXA7 | 8 |
| P35613 | Basigin | BSG | 7 |
| P49720 | Proteasome subunit beta type-3 | PSMB3 | 7 |
| P17931 | Galectin-3;Galectin | LGALS3 | 7 |
| P63104 | 14-3-3 protein zeta/delta | YWHAZ | 7 |
| Q9H444 | Charged multivesicular body protein 4b | CHMP4B | 7 |
| O43396 | Thioredoxin-like protein 1 | TXNL1 | 7 |
| P50502 | Hsc70-interacting protein;Putative protein FAM10A4;Putative protein FAM10A5 | ST13;ST13P4;ST13P5 | 7 |
| E7EQ12 | Calpastatin | CAST | 7 |
| P49189 | 4-trimethylaminobutyraldehyde dehydrogenase | ALDH9A1 | 7 |
| Q9Y3I1 | F-box only protein 7 | FBXO7 | 7 |
| P07954 | Fumarate hydratase, mitochondrial | FH | 7 |
| F6S8N6 | Protein-L-isoaspartate O-methyltransferase;Protein-L-isoaspartate(D-aspartate) O-methyltransferase | PCMT1 | 7 |
| P49247 | Ribose-5-phosphate isomerase | RPIA | 7 |
| P62834 | Ras-related protein Rap-1A | RAP1A | 7 |

| | | | |
|---|---|---|---|
| A0A087WUQ6 | Glutathione peroxidase;Glutathione peroxidase 1 | GPX1 | 7 |
| O60256 | Phosphoribosyl pyrophosphate synthase-associated protein 2 | PRPSAP2 | 7 |
| Q00796 | Sorbitol dehydrogenase | SORD | 7 |
| O00299 | Chloride intracellular channel protein 1 | CLIC1 | 7 |
| Q99497 | Protein deglycase DJ-1 | PARK7 | 7 |
| P17174 | Aspartate aminotransferase, cytoplasmic | GOT1 | 7 |
| H7BXD5 | Grancalcin | GCA | 7 |
| E9PGT1 | Translin | TSN | 7 |
| C9J7K9 | Phospholipid scramblase 1 | PLSCR1 | 7 |
| Q13618 | Cullin-3 | CUL3 | 7 |
| O75695 | Protein XRP2 | RP2 | 7 |
| P09960 | Leukotriene A-4 hydrolase | LTA4H | 7 |
| E9PLK3 | Puromycin-sensitive aminopeptidase | NPEPPS | 7 |
| P00492 | Hypoxanthine-guanine phosphoribosyltransferase | HPRT1 | 7 |
| F5H4B6 | Aldehyde dehydrogenase family 16 member A1 | ALDH16A1 | 7 |
| D6RA82 | Annexin;Annexin A3 | ANXA3 | 7 |
| P61106 | Ras-related protein Rab-14 | RAB14 | 7 |
| Q16775 | Hydroxyacylglutathione hydrolase, mitochondrial | HAGH | 7 |
| P07355 | Annexin A2;Annexin;Putative annexin A2-like protein | ANXA2;ANXA2P2 | 7 |
| A0A087WX08 | Gamma-adducin | ADD3 | 7 |
| P08238 | Heat shock protein HSP 90-beta | HSP90AB1 | 7 |
| Q8IZY2 | ATP-binding cassette sub-family A member 7 | ABCA7 | 7 |
| P14780 | Matrix metalloproteinase-9 | MMP9 | 7 |
| P12955 | Xaa-Pro dipeptidase | PEPD | 7 |
| P68371 | Tubulin beta-4B chain;Tubulin beta-4A chain;Tubulin beta chain | TUBB4B;TUBB4A;TUBB | 7 |
| O15067 | Phosphoribosylformylglycinamidine synthase | PFAS | 7 |
| P35241 | Radixin | RDX | 7 |
| O60488 | Long-chain-fatty-acid--CoA ligase 4 | ACSL4 | 7 |
| A0A0C4DGX4 | Cullin-1 | CUL1 | 7 |
| P50148 | Guanine nucleotide-binding protein G(q) subunit alpha | GNAQ | 7 |
| Q15907 | Ras-related protein Rab-11B;Ras-related protein Rab-11A | RAB11B;RAB11A | 7 |
| P30086 | Phosphatidylethanolamine-binding protein 1;Hippocampal cholinergic neurostimulating peptide | PEBP1 | 6 |
| P55036 | 26S proteasome non-ATPase regulatory subunit 4 | PSMD4 | 6 |
| P28070 | Proteasome subunit beta type-4 | PSMB4 | 6 |
| Q9UNS2 | COP9 signalosome complex subunit 3 | COPS3 | 6 |
| P08754 | Guanine nucleotide-binding protein G(k) subunit alpha | GNAI3 | 6 |
| P61006 | Ras-related protein Rab-8A | RAB8A | 6 |
| P61019 | Ras-related protein Rab-2A | RAB2A | 6 |
| H0Y8C6 | Importin-5 | IPO5 | 6 |
| Q00577 | Transcriptional activator protein Pur-alpha | PURA | 6 |
| P52565 | Rho GDP-dissociation inhibitor 1 | ARHGDIA | 6 |
| Q9Y5Z4 | Heme-binding protein 2 | HEBP2 | 6 |
| J3KNF4 | Copper chaperone for superoxide dismutase;Superoxide dismutase [Cu-Zn] | CCS | 6 |

| | | | |
|---|---|---|---|
| A0A087WXS7 | ATPase ASNA1 | ASNA1 | 6 |
| P05089 | Arginase-1 | ARG1 | 6 |
| O95336 | 6-phosphogluconolactonase | PGLS | 6 |
| Q92508 | Piezo-type mechanosensitive ion channel component 1 | PIEZO1 | 6 |
| P84077 | ADP-ribosylation factor 1;ADP-ribosylation factor 3 | ARF1;ARF3 | 6 |
| P21281 | V-type proton ATPase subunit B, brain isoform;V-type proton ATPase subunit B, kidney isoform | ATP6V1B2;ATP6V1B1 | 6 |
| P04259 | Keratin, type II cytoskeletal 6B | KRT6B | 6 |
| Q92905 | COP9 signalosome complex subunit 5 | COPS5 | 6 |
| P61163 | Alpha-centractin | ACTR1A | 6 |
| O95373 | Importin-7 | IPO7 | 6 |
| C9JD73 | Protein phosphatase 1 regulatory subunit 7 | PPP1R7 | 6 |
| Q99536 | Synaptic vesicle membrane protein VAT-1 homolog | VAT1 | 6 |
| Q86UX7 | Fermitin family homolog 3 | FERMT3 | 6 |
| C9JFE4 | COP9 signalosome complex subunit 1 | GPS1 | 6 |
| P36959 | GMP reductase 1 | GMPR | 6 |
| B5MDF5 | GTP-binding nuclear protein Ran | RAN | 6 |
| F5GY90 | Porphobilinogen deaminase | HMBS | 6 |
| E7EX90 | Dynactin subunit 1 | DCTN1 | 6 |
| H0Y512 | Adipocyte plasma membrane-associated protein | APMAP | 6 |
| Q32Q12 | Nucleoside diphosphate kinase;Nucleoside diphosphate kinase B;Putative nucleoside diphosphate kinase | NME1-NME2;NME2;NME1;NME2P1 | 6 |
| P13807 | Glycogen [starch] synthase, muscle | GYS1 | 6 |
| K7ES02 | Bleomycin hydrolase | BLMH | 6 |
| P17213 | Bactericidal permeability-increasing protein | BPI | 6 |
| Q9UNM6 | 26S proteasome non-ATPase regulatory subunit 13 | PSMD13 | 6 |
| J3KQ32 | Obg-like ATPase 1 | OLA1 | 6 |
| Q9Y490 | Talin-1 | TLN1 | 6 |
| H0YD13 | CD44 antigen | CD44 | 6 |
| P18669 | Phosphoglycerate mutase 1;Phosphoglycerate mutase 2;Probable phosphoglycerate mutase 4 | PGAM1;PGAM2;PGAM4 | 6 |
| P23528 | Cofilin-1 | CFL1 | 6 |
| Q5SR44 | Complement receptor type 1 | CR1 | 6 |
| Q99436 | Proteasome subunit beta type-7 | PSMB7 | 6 |
| P47756 | F-actin-capping protein subunit beta | CAPZB | 6 |
| P30740 | Leukocyte elastase inhibitor | SERPINB1 | 6 |
| A0A024R571 | EH domain-containing protein 1 | EHD1 | 6 |
| P30043 | Flavin reductase (NADPH) | BLVRB | 6 |
| P32119 | Peroxiredoxin-2 | PRDX2 | 6 |
| C9J0K6 | Sorcin | SRI | 6 |
| P27105 | Erythrocyte band 7 integral membrane protein | STOM | 6 |
| P84077 | ADP-ribosylation factor 1;ADP-ribosylation factor 3;ADP-ribosylation factor 5;ADP-ribosylation factor 4 | ARF1;ARF3;ARF5;ARF4 | 6 |
| P61981 | 14-3-3 protein gamma;14-3-3 protein gamma, N-terminally processed | YWHAG | 5 |
| P09211 | Glutathione S-transferase P | GSTP1 | 5 |
| P13489 | Ribonuclease inhibitor | RNH1 | 5 |

| | | | |
|---|---|---|---|
| Q96PU5 | E3 ubiquitin-protein ligase NEDD4-like | NEDD4L | 5 |
| Q5SRN7 | HLA class I histocompatibility antigen, A; HLA class I histocompatibility antigen, B;HLA class I histocompatibility antigen, Cw | HLA-A;HLA-C;HLA-B | 5 |
| P02042 | Hemoglobin subunit delta | HBD | 5 |
| A0A087WU29 | Glycophorin-A | GYPA | 5 |
| P00390 | Glutathione reductase, mitochondrial | GSR | 5 |
| Q9UBV8 | Peflin | PEF1 | 5 |
| Q8WVM8 | Sec1 family domain-containing protein 1 | SCFD1 | 5 |
| F6TLX2 | Glyoxalase domain-containing protein 4 | GLOD4 | 5 |
| H3BQF1 | Adenine phosphoribosyltransferase | APRT | 5 |
| Q07960 | Rho GTPase-activating protein 1 | ARHGAP1 | 5 |
| F6XSS0 | Blood group Rh(CE) polypeptide;Blood group Rh(D) polypeptide | RHCE;RHD | 5 |
| A0A087WY55 | Vacuolar protein sorting-associated protein VTA1 homolog | VTA1 | 5 |
| G5E9W8 | Glycogenin-1 | GYG1 | 5 |
| P07451 | Carbonic anhydrase 3 | CA3 | 5 |
| Q08722 | Leukocyte surface antigen CD47 | CD47 | 5 |
| X6RA14 | S-formylglutathione hydrolase | ESD | 5 |
| Q8IUI8 | Cytokine receptor-like factor 3 | CRLF3 | 5 |
| Q5VW32 | BRO1 domain-containing protein BROX | BROX | 5 |
| P61026 | Ras-related protein Rab-10 | RAB10 | 5 |
| A0A087WWY3 | Filamin-A | FLNA | 5 |
| H0YGX7 | Rho GDP-dissociation inhibitor 2 | ARHGDIB | 5 |
| Q92783 | Signal transducing adapter molecule 1 | STAM | 5 |
| Q7Z6Z7 | E3 ubiquitin-protein ligase HUWE1 | HUWE1 | 5 |
| H0YHC3 | Nucleosome assembly protein 1-like 1 | NAP1L1 | 5 |
| Q5QPM7 | Proteasome inhibitor PI31 subunit | PSMF1 | 5 |
| P09104 | Gamma-enolase;Enolase | ENO2 | 5 |
| Q5T2B5 | Cullin-2 | CUL2 | 5 |
| Q8WW22 | DnaJ homolog subfamily A member 4 | DNAJA4 | 5 |
| P61201 | COP9 signalosome complex subunit 2 | COPS2 | 5 |
| X6R433 | Protein-tyrosine-phosphatase;Receptor-type tyrosine-protein phosphatase C | PTPRC | 5 |
| P63000 | Ras-related C3 botulinum toxin substrate 1 | RAC1 | 5 |
| F5GXM3 | IST1 homolog | IST1 | 5 |
| H3BLU7 | Aflatoxin B1 aldehyde reductase member 2 | AKR7A2 | 5 |
| P25325 | 3-mercaptopyruvate sulfurtransferase;Sulfurtransferase | MPST | 5 |
| A0A087X0K1 | Calcium-binding protein 39 | CAB39 | 5 |
| P23381 | Tryptophan--tRNA ligase, cytoplasmic;T1-TrpRS;T2-TrpRS | WARS | 5 |
| P01116 | GTPase KRas;GTPase KRas, N-terminally processed | KRAS | 5 |
| P30040 | Endoplasmic reticulum resident protein 29 | ERP29 | 5 |
| P05198 | Eukaryotic translation initiation factor 2 subunit 1 | EIF2S1 | 5 |
| Q6UX06 | Olfactomedin-4 | OLFM4 | 5 |
| Q96KP4 | Cytosolic non-specific dipeptidase | CNDP2 | 5 |
| Q04760 | Lactoylglutathione lyase | GLO1 | 5 |
| J3QS39 | Ubiquitin-60S ribosomal protein L40;Ubiquitin;60S ribosomal protein L40;Ubiquitin-40S ribosomal protein S27a;Ubiquitin;40S ribosomal protein S27a;Polyubiquitin-B;Ubiquitin;Polyubiquitin-C;Ubiquitin | UBB;RPS27A;UBC;UBA52;UBBP4 | 5 |

| | | | |
|---|---|---|---|
| P06702 | Protein S100-A9 | S100A9 | 5 |
| P15531 | Nucleoside diphosphate kinase A;Nucleoside diphosphate kinase;Nucleoside diphosphate kinase B | NME1;NME2; NME1-NME2 | 5 |
| E7EV99 | Alpha-adducin | ADD1 | 5 |
| P51149 | Ras-related protein Rab-7a | RAB7A | 4 |
| K7N7A8 | Aquaporin-1 | AQP1 | 4 |
| P61020 | Ras-related protein Rab-5B | RAB5B | 4 |
| X6R4N5 | Erythroid membrane-associated protein | ERMAP | 4 |
| E5RJR5 | S-phase kinase-associated protein 1 | SKP1 | 4 |
| Q9Y315 | Deoxyribose-phosphate aldolase | DERA | 4 |
| X6R8F3 | Neutrophil gelatinase-associated lipocalin | LCN2 | 4 |
| O75396 | Vesicle-trafficking protein SEC22b | SEC22B | 4 |
| Q15102 | Platelet-activating factor acetylhydrolase IB subunit gamma | PAFAH1B3 | 4 |
| P51665 | 26S proteasome non-ATPase regulatory subunit 7 | PSMD7 | 4 |
| Q96FZ7 | Charged multivesicular body protein 6 | CHMP6 | 4 |
| Q9NRQ2 | Phospholipid scramblase 4 | PLSCR4 | 4 |
| F8VWS0 | 60S acidic ribosomal protein P0;60S acidic ribosomal protein P0-like | RPLP0;RPLP 0P6 | 4 |
| O14964 | Hepatocyte growth factor-regulated tyrosine kinase substrate | HGS | 4 |
| A0A0A0MTJ9 | Neutral cholesterol ester hydrolase 1 | NCEH1 | 4 |
| A0A087WY8 2 | Junctional adhesion molecule A | F11R | 4 |
| J3QSB7 | Purine nucleoside phosphorylase;S-methyl-5-thioadenosine phosphorylase | MTAP | 4 |
| Q5VVQ6 | Ubiquitin thioesterase OTU1 | YOD1 | 4 |
| P36543 | V-type proton ATPase subunit E 1 | ATP6V1E1 | 4 |
| Q9BS40 | Latexin | LXN | 4 |
| P47755 | F-actin-capping protein subunit alpha-2 | CAPZA2 | 4 |
| Q9GZT8 | NIF3-like protein 1 | NIF3L1 | 4 |
| H6UYS7 | Alpha-synuclein | SNCA | 4 |
| P60953 | Cell division control protein 42 homolog | CDC42 | 4 |
| Q14773 | Intercellular adhesion molecule 4 | ICAM4 | 4 |
| H0Y6T7 | Nicastrin | NCSTN | 4 |
| P69891 | Hemoglobin subunit gamma-1 | HBG1 | 4 |
| P14625 | Endoplasmin | HSP90B1 | 4 |
| Q96GD0 | Pyridoxal phosphate phosphatase | PDXP | 4 |
| P08311 | Cathepsin G | CTSG | 4 |
| Q9H9Q2 | COP9 signalosome complex subunit 7b | COPS7B | 4 |
| P09417 | Dihydropteridine reductase | QDPR | 4 |
| F8WE6 | Peptidyl-prolyl cis-trans isomerase;Peptidyl-prolyl cis-trans isomerase A | PPIA | 4 |
| O15173 | Membrane-associated progesterone receptor component 2 | PGRMC2 | 4 |
| P28072 | Proteasome subunit beta type-6;Proteasome subunit beta type | PSMB6 | 4 |
| H3BSW0 | Leucine-rich repeat-containing protein 57 | LRRC57 | 4 |
| Q9UBW8 | COP9 signalosome complex subunit 7a | COPS7A | 4 |
| O00560 | Syntenin-1 | SDCBP | 4 |
| F5H157 | Ras-related protein Rab-35 | RAB35 | 4 |
| Q9H479 | Fructosamine-3-kinase | FN3K | 4 |
| Q04917 | 14-3-3 protein eta | YWHAH | 4 |

| | | | |
|---|---|---|---|
| C9JJ47 | AP-2 complex subunit mu | AP2M1 | 4 |
| C9JIG9 | Serine/threonine-protein kinase OSR1 | OXSR1 | 4 |
| Q13336 | Urea transporter 1 | SLC14A1 | 4 |
| P46926 | Glucosamine-6-phosphate isomerase 1;Glucosamine-6-phosphate isomerase;Glucosamine-6-phosphate isomerase 2 | GNPDA1;GNPDA2 | 4 |
| O43633 | Charged multivesicular body protein 2a | CHMP2A | 4 |
| F8VVB9 | Tubulin alpha-1A chain;Tubulin alpha-1C chain;Tubulin alpha-1B chain;Tubulin alpha-3C/D chain;Tubulin alpha-3E chain | TUBA1B;TUBA1C;TUBA1A;TUBA3C;TUBA3E | 4 |
| A6PVN5 | Serine/threonine-protein phosphatase 2A activator | PPP2R4 | 4 |
| B8ZZB8 | CB1 cannabinoid receptor-interacting protein 1 | CNRIP1 | 4 |
| Q9P2R3 | Rabankyrin-5 | ANKFY1 | 4 |
| Q86YS7 | C2 domain-containing protein 5 | C2CD5 | 4 |
| R4GMR5 | 26S proteasome non-ATPase regulatory subunit 8 | PSMD8 | 4 |
| E7EM64 | COP9 signalosome complex subunit 6 | COPS6 | 4 |
| J3KNI6 | Integrin beta;Integrin beta-2 | ITGB2 | 4 |
| H0Y5R6 | Uroporphyrinogen decarboxylase | UROD | 4 |
| M0R165 | Epidermal growth factor receptor substrate 15-like 1 | EPS15L1 | 4 |
| O00487 | 26S proteasome non-ATPase regulatory subunit 14 | PSMD14 | 4 |
| Q13630 | GDP-L-fucose synthase | TSTA3 | 4 |
| P55060 | Exportin-2 | CSE1L | 4 |
| P20020 | Plasma membrane calcium-transporting ATPase 1;Calcium-transporting ATPase | ATP2B1 | 4 |
| Q9NYU2 | UDP-glucose:glycoprotein glucosyltransferase 1 | UGGT1 | 4 |
| H3BND8 | Ubiquitin carboxyl-terminal hydrolase;Ubiquitin carboxyl-terminal hydrolase 7 | USP7 | 4 |
| Q9GZP4 | PITH domain-containing protein 1 | PITHD1 | 4 |
| D6RD66 | WD repeat-containing protein 1 | WDR1 | 4 |
| P48729 | Casein kinase I isoform alpha | CSNK1A1 | 4 |
| P25685 | DnaJ homolog subfamily B member 1 | DNAJB1 | 4 |
| P14550 | Alcohol dehydrogenase [NADP(+)] | AKR1A1 | 4 |
| Q6PCE3 | Glucose 1,6-bisphosphate synthase | PGM2L1 | 4 |
| Q9UPN7 | Serine/threonine-protein phosphatase 6 regulatory subunit 1 | PPP6R1 | 4 |
| P62805 | Histone H4 | HIST1H4A | 4 |
| P62937 | Peptidyl-prolyl cis-trans isomerase A | PPIA | 4 |
| P30046 | D-dopachrome decarboxylase;D-dopachrome decarboxylase-like protein | DDT;DDTL | 4 |
| Q08495 | Dematin | DMTN | 4 |
| K7EIJ0 | WW domain-binding protein 2 | WBP2 | 4 |
| E5RHP7 | Carbonic anhydrase 1 | CA1 | 4 |
| P09105 | Hemoglobin subunit theta-1 | HBQ1 | 4 |
| E7ESC6 | Exportin-7 | XPO7 | 4 |
| P61225 | Ras-related protein Rap-2b;Ras-related protein Rap-2c;Ras-related protein Rap-2a | RAP2B;RAP2A;RAP2C | 4 |
| O15400 | Syntaxin-7 | STX7 | 3 |
| Q5VZR0 | Golgi-associated plant pathogenesis-related protein 1 | GLIPR2 | 3 |
| P40199 | Carcinoembryonic antigen-related cell adhesion molecule 6 | CEACAM6 | 3 |
| P27348 | 14-3-3 protein theta | YWHAQ | 3 |
| P62820 | Ras-related protein Rab-1A | RAB1A | 3 |
| C9JEN3 | Protein lifeguard 3 | TMBIM1 | 3 |

| | | | |
|---|---|---|---|
| Q9UDX3 | SEC14-like protein 4 | SEC14L4 | 3 |
| Q9Y570 | Protein phosphatase methylesterase 1 | PPME1 | 3 |
| Q96GG9 | DCN1-like protein 1;DCN1-like protein | DCUN1D1 | 3 |
| B0YJC4 | Vimentin | VIM | 3 |
| Q86VN1 | Vacuolar protein-sorting-associated protein 36 | VPS36 | 3 |
| F8WFB9 | Endophilin-B2 | SH3GLB2 | 3 |
| A0A087WVQ9 | Elongation factor 1-alpha 1;Putative elongation factor 1-alpha-like 3 | EEF1A1;EEF1A1P5 | 3 |
| Q53TN4 | Cytochrome b reductase 1 | CYBRD1 | 3 |
| P10809 | 60 kDa heat shock protein, mitochondrial | HSPD1 | 3 |
| F5H7X1 | 26S proteasome non-ATPase regulatory subunit 9 | PSMD9 | 3 |
| E9PNW4 | CD59 glycoprotein | CD59 | 3 |
| E9PS74 | Solute carrier family 43 member 3 | SLC43A3 | 3 |
| P53985 | Monocarboxylate transporter 1 | SLC16A1 | 3 |
| Q8WWI5 | Choline transporter-like protein 1 | SLC44A1 | 3 |
| E9PIR7 | Thioredoxin reductase 1, cytoplasmic | TXNRD1 | 3 |
| Q5TD07 | Ribosyldihydronicotinamide dehydrogenase [quinone] | NQO2 | 3 |
| Q9UL25 | Ras-related protein Rab-21 | RAB21 | 3 |
| P27824 | Calnexin | CANX | 3 |
| U3KPS2 | Myeloblastin | PRTN3 | 3 |
| Q9UKU0 | Long-chain-fatty-acid--CoA ligase 6 | ACSL6 | 3 |
| P24666 | Low molecular weight phosphotyrosine protein phosphatase | ACP1 | 3 |
| H7C2G2 | NAD(P)(+)--arginine ADP-ribosyltransferase;Ecto-ADP-ribosyltransferase 4 | ART4 | 3 |
| I3L1K6 | Myosin light chain 4 | MYL4 | 3 |
| Q9UK41 | Vacuolar protein sorting-associated protein 28 homolog | VPS28 | 3 |
| Q9NUQ9 | Protein FAM49B | FAM49B | 3 |
| Q9UBQ7 | Glyoxylate reductase/hydroxypyruvate reductase | GRHPR | 3 |
| B8ZZG1 | MAGUK p55 subfamily member 6 | MPP6 | 3 |
| Q10567 | AP-1 complex subunit beta-1 | AP1B1 | 3 |
| O75387 | Large neutral amino acids transporter small subunit 3 | SLC43A1 | 3 |
| Q9BTU6 | Phosphatidylinositol 4-kinase type 2-alpha | PI4K2A | 3 |
| J3KS22 | L-xylulose reductase | DCXR | 3 |
| O15498 | Synaptobrevin homolog YKT6 | YKT6 | 3 |
| Q08211 | ATP-dependent RNA helicase A | DHX9 | 3 |
| P50416 | Carnitine O-palmitoyltransferase 1, liver isoform | CPT1A | 3 |
| P08237 | ATP-dependent 6-phosphofructokinase, muscle type | PFKM | 3 |
| P14735 | Insulin-degrading enzyme | IDE | 3 |
| Q9H0R3 | Transmembrane protein 222 | TMEM222 | 3 |
| Q14166 | Tubulin--tyrosine ligase-like protein 12 | TTLL12 | 3 |
| Q14558 | Phosphoribosyl pyrophosphate synthase-associated protein 1 | PRPSAP1 | 3 |
| A0A087WTB8 | Ubiquitin carboxyl-terminal hydrolase;Ubiquitin carboxyl-terminal hydrolase isozyme L3 | UCHL3 | 3 |
| Q9NPQ8 | Synembryn-A | RIC8A | 3 |
| F6WQW2 | Ran-specific GTPase-activating protein | RANBP1 | 3 |
| Q15691 | Microtubule-associated protein RP/EB family member 1 | MAPRE1 | 3 |
| A0A0A0MR50 | Cullin-4A | CUL4A | 3 |

| | | | |
|---|---|---|---|
| Q96IU4 | Alpha/beta hydrolase domain-containing protein 14B | ABHD14B | 3 |
| Q9P0L0 | Vesicle-associated membrane protein-associated protein A | VAPA | 3 |
| E9PRY8 | Elongation factor 1-delta | EEF1D | 3 |
| Q16543 | Hsp90 co-chaperone Cdc37 | CDC37 | 3 |
| P06702 | Protein S100-A9 | S100A9 | 3 |
| P13639 | Elongation factor 2 | EEF2 | 3 |
| E9PJC7 | Tetraspanin;CD82 antigen | CD82 | 3 |
| Q01432 | AMP deaminase 3 | AMPD3 | 3 |
| B1AUU8 | Epidermal growth factor receptor substrate 15 | EPS15 | 3 |
| P54709 | Sodium/potassium-transporting ATPase subunit beta-3 | ATP1B3 | 3 |
| P54727 | UV excision repair protein RAD23 homolog B | RAD23B | 3 |
| P36507 | Dual specificity mitogen-activated protein kinase kinase 2 | MAP2K2 | 3 |
| Q9Y2V2 | Calcium-regulated heat stable protein 1 | CARHSP1 | 3 |
| P31146 | Coronin-1A;Coronin | CORO1A | 3 |
| Q8IY17 | Neuropathy target esterase | PNPLA6 | 3 |
| E7EQR4 | Ezrin | EZR | 3 |
| F8WDS9 | LanC-like protein 1 | LANCL1 | 3 |
| X6RJP6 | Transgelin-2 | TAGLN2 | 3 |
| A0A0J9YXM6 | WD repeat-containing protein 81 | WDR81 | 3 |
| P62140 | Serine/threonine-protein phosphatase PP1-beta catalytic subunit;Serine/threonine-protein phosphatase | PPP1CB | 3 |
| H0YLJ3 | Mortality factor 4-like protein 1 | MORF4L1 | 3 |
| E7EPV7 | Alpha-synuclein | SNCA | 3 |
| K7EK07 | Histone H3 | H3F3B | 3 |
| P05109 | Protein S100-A8;Protein S100-A8, N-terminally processed | S100A8 | 3 |
| I3L0A0 | Ubiquitin-conjugating enzyme E2 variant 1;Ubiquitin-conjugating enzyme E2 variant 2 | TMEM189-UBE2V1;UBE2V1;UBE2V2 | 3 |
| Q6B0K9 | Hemoglobin subunit mu | HBM | 3 |
| O75368 | SH3 domain-binding glutamic acid-rich-like protein | SH3BGRL | 3 |
| A0A0J9YXB3 | Ras-related protein Rap-1b;Ras-related protein Rap-1A;Ras-related protein Rap-1b-like protein | RAP1B;RAP1A | 3 |
| P60953 | Cell division control protein 42 homolog | CDC42 | 3 |
| A0A087WTI1 | Ras-related protein Rab-1B;Ras-related protein Rab-1A | RAB1B;RAB1A | 3 |
| B5MDF5 | GTP-binding nuclear protein Ran | RAN | 3 |
| P61088 | Ubiquitin-conjugating enzyme E2 N | UBE2N | 3 |
| Q00013 | 55 kDa erythrocyte membrane protein | MPP1 | 3 |
| B1AKQ8 | Guanine nucleotide-binding protein G(I)/G(S)/G(T) subunit beta-1;Guanine nucleotide-binding protein G(I)/G(S)/G(T) subunit beta-3;Guanine nucleotide-binding protein G(I)/G(S)/G(T) subunit beta-2 | GNB1;GNB2;GNB3 | 3 |
| P04406 | Glyceraldehyde-3-phosphate dehydrogenase | GAPDH | 3 |
| Q9UJC5 | SH3 domain-binding glutamic acid-rich-like protein 2 | SH3BGRL2 | 3 |
| P04921 | Glycophorin-C | GYPC | 2 |
| Q9NP59 | Solute carrier family 40 member 1 | SLC40A1 | 2 |
| K7EKH5 | Fructose-bisphosphate aldolase;Fructose-bisphosphate aldolase C | ALDOC | 2 |
| P11233 | Ras-related protein Ral-A | RALA | 2 |
| F8WBR5 | Calmodulin | CALM2;CALM3;CALM1 | 2 |

| | | | |
|---|---|---|---|
| P00441 | Superoxide dismutase [Cu-Zn] | SOD1 | 2 |
| H0YDI1 | Lymphocyte function-associated antigen 3 | CD58 | 2 |
| H0YNE9 | Ras-related protein Rab-8B | RAB8B | 2 |
| J3KN67 | | TPM3 | 2 |
| P20160 | Azurocidin | AZU1 | 2 |
| A0A087WZZ4 | Ammonium transporter Rh type A | RHAG | 2 |
| F5GXS0 | Complement C4-A;Complement C4-B | C4B;C4A | 2 |
| Q8ND76 | Cyclin-Y | CCNY | 2 |
| Q14739 | Lamin-B receptor | LBR | 2 |
| Q15181 | Inorganic pyrophosphatase | PPA1 | 2 |
| J3QS92 | Galectin-9 | LGALS9 | 2 |
| I3L471 | Phosphatidylinositol transfer protein alpha isoform | PITPNA | 2 |
| P01111 | GTPase NRas | NRAS;KRAS | 2 |
| F5H4Q5 | Vacuolar protein sorting-associated protein 37C | VPS37C | 2 |
| A0A0A0MSW4 | Phosphatidylinositol transfer protein beta isoform | PITPNB | 2 |
| P67775 | Serine/threonine-protein phosphatase 2A catalytic subunit alpha isoform;Serine/threonine-protein phosphatase | PPP2CA;PPP2CB | 2 |
| P41091 | Eukaryotic translation initiation factor 2 subunit 3;Putative eukaryotic translation initiation factor 2 subunit 3-like protein | EIF2S3;EIF2S3L | 2 |
| A0A087WWS7 | Syntaxin-binding protein 2 | STXBP2 | 2 |
| F8VQX6 | Methyltransferase-like protein 7A | METTL7A | 2 |
| B3KT28 | FAS-associated factor 1 | FAF1 | 2 |
| K7EIJ8 | Katanin p60 ATPase-containing subunit A-like 2 | KATNAL2 | 2 |
| P20339 | Ras-related protein Rab-5A | RAB5A | 2 |
| O95456 | Proteasome assembly chaperone 1 | PSMG1 | 2 |
| K7EK45 | Polypyrimidine tract-binding protein 1 | PTBP1 | 2 |
| Q15365 | Poly(rC)-binding protein 1;Poly(rC)-binding protein 3 | PCBP1;PCBP3 | 2 |
| Q9BSJ8 | Extended synaptotagmin-1 | ESYT1 | 2 |
| H3BP35 | Diphosphomevalonate decarboxylase | MVD | 2 |
| H0Y8C4 | Serine/threonine-protein phosphatase 2A 56 kDa regulatory subunit delta isoform | PPP2R5D | 2 |
| K7EP09 | Bifunctional coenzyme A synthase;Phosphopantetheine adenylyltransferase;Dephospho-CoA kinase | COASY | 2 |
| F8VNT9 | Tetraspanin;CD63 antigen | CD63 | 2 |
| Q8NEV1 | Casein kinase II subunit alpha 3;Casein kinase II subunit alpha | CSNK2A3;CSNK2A1 | 2 |
| F8VTQ5 | Heterogeneous nuclear ribonucleoprotein A1 | HNRNPA1 | 2 |
| A0A087X2E2 | Carcinoembryonic antigen-related cell adhesion molecule 8;Carcinoembryonic antigen-related cell adhesion molecule 1;Carcinoembryonic antigen-related cell adhesion molecule 5 | CEACAM8;CEACAM5;CEACAM1 | 2 |
| H0YAS8 | Clusterin;Clusterin beta chain;Clusterin alpha chain;Clusterin | CLU | 2 |
| E9PP54 | Tubulin-specific chaperone cofactor E-like protein | TBCEL | 2 |
| P43034 | Platelet-activating factor acetylhydrolase IB subunit alpha | PAFAH1B1 | 2 |
| Q9NT62 | Ubiquitin-like-conjugating enzyme ATG3 | ATG3 | 2 |
| K7ERZ3 | Perilipin-3 | PLIN3 | 2 |
| Q6DD88 | Atlastin-3 | ATL3 | 2 |
| Q15084-3 | Protein disulfide-isomerase A6 | PDIA6 | 2 |
| K7EQH4 | ATP synthase subunit alpha, mitochondrial | ATP5A1 | 2 |

| | | | |
|---|---|---|---|
| G3V1U5 | Vesicle transport protein GOT1B | GOLT1B | 2 |
| O00186 | Syntaxin-binding protein 3 | STXBP3 | 2 |
| Q5T6W2 | Heterogeneous nuclear ribonucleoprotein K | HNRNPK | 2 |
| H0YEY4 | ADP-sugar pyrophosphatase | NUDT5 | 2 |
| P35580 | Myosin-10 | MYH10 | 2 |
| F5H081 | Solute carrier family 2, facilitated glucose transporter member 4 | SLC2A4 | 2 |
| Q9H1C7 | Cysteine-rich and transmembrane domain-containing protein 1 | CYSTM1 | 2 |
| K7EJ83 | Cyclin-dependent kinase 2;Cyclin-dependent kinase 3 | CDK3;CDK2 | 2 |
| C9J352 | Importin subunit alpha-5;Importin subunit alpha-5, N-terminally processed | KPNA1 | 2 |
| H9KV75 | Alpha-actinin-1;Alpha-actinin-4;Alpha-actinin-2;Alpha-actinin-3 | ACTN1;ACTN4;ACTN3;ACTN2 | 2 |
| A0A0A0MQS1 | Pyrroline-5-carboxylate reductase;Pyrroline-5-carboxylate reductase 3 | PYCRL | 2 |
| D6RBY0 | Rieske domain-containing protein | RFESD | 2 |
| C9JC71 | Low affinity immunoglobulin gamma Fc region receptor III-A | FCGR3A | 2 |
| P51811 | Membrane transport protein XK | XK | 2 |
| C9J1G2 | DnaJ homolog subfamily B member 2 | DNAJB2 | 2 |
| Q9UN37 | Vacuolar protein sorting-associated protein 4A;Vacuolar protein sorting-associated protein 4B;Fidgetin-like protein 1 | VPS4A;VPS4B;FIGNL1 | 2 |
| P61160 | Actin-related protein 2 | ACTR2 | 2 |
| P16930 | Fumarylacetoacetase | FAH | 2 |
| A0A087X0K4 | CUB and sushi domain-containing protein 2 | CSMD2 | 2 |
| P10746 | Uroporphyrinogen-III synthase | UROS | 2 |
| K7EQ02 | DAZ-associated protein 1 | DAZAP1 | 2 |
| F5GYN4 | Ubiquitin thioesterase OTUB1 | OTUB1 | 2 |
| P10599 | Thioredoxin | TXN | 2 |
| O95197 | Reticulon-3 | RTN3 | 2 |
| E7ETB3 | Aspartyl aminopeptidase | DNPEP | 2 |
| P14868 | Aspartate--tRNA ligase, cytoplasmic | DARS | 2 |
| Q08AM6 | Protein VAC14 homolog | VAC14 | 2 |
| Q93034 | Cullin-5 | CUL5 | 2 |
| Q9BQA1 | Methylosome protein 50 | WDR77 | 2 |
| A0A0B4J2G9 | Ubiquitin-conjugating enzyme E2 L3 | UBE2L3 | 2 |
| Q04446 | 1,4-alpha-glucan-branching enzyme | GBE1 | 2 |
| Q96NA2 | Rab-interacting lysosomal protein | RILP | 2 |
| Q92539 | Phosphatidate phosphatase LPIN2 | LPIN2 | 2 |
| P28482 | Mitogen-activated protein kinase 1 | MAPK1 | 2 |
| Q7Z406 | Myosin-14;Myosin-11 | MYH14;MYH11 | 2 |
| Q8IU68 | Transmembrane channel-like protein 8 | TMC8 | 2 |
| Q96BJ3 | Axin interactor, dorsalization-associated protein | AIDA | 2 |
| P20042 | Eukaryotic translation initiation factor 2 subunit 2 | EIF2S2 | 2 |
| A0A0A0MQR0 | Docosahexaenoic acid omega-hydroxylase CYP4F3;Phylloquinone omega-hydroxylase CYP4F2;Cytochrome P450 4F12;Phylloquinone omega-hydroxylase CYP4F11 | CYP4F2;CYP4F3;CYP4F11;CYP4F12 | 2 |
| Q9BS26 | Endoplasmic reticulum resident protein 44 | ERP44 | 2 |
| O00178 | GTP-binding protein 1 | GTPBP1 | 2 |
| P27797 | Calreticulin | CALR | 2 |

| | | | |
|---|---|---|---|
| G3V0E5 | Transferrin receptor protein 1;Transferrin receptor protein 1, serum form | TFRC | 2 |
| P48147 | Prolyl endopeptidase | PREP | 2 |
| H7BZC1 | Hippocalcin-like protein 1;Neuron-specific calcium-binding protein hippocalcin;Neurocalcin-delta | HPCAL1;NCALD;HPCA | 2 |
| F8VPD4 | CAD protein;Glutamine-dependent carbamoyl-phosphate synthase;Aspartate carbamoyltransferase;Dihydroorotase | CAD | 2 |
| Q9NTJ5 | Phosphatidylinositide phosphatase SAC1 | SACM1L | 2 |
| P26447 | Protein S100-A4 | S100A4 | 2 |
| Q9UIW2 | Plexin-A1 | PLXNA1 | 2 |
| H0YJS0 | V-type proton ATPase subunit D | ATP6V1D | 2 |
| P25445 | Tumor necrosis factor receptor superfamily member 6 | FAS | 2 |
| C9JEU5 | Fibrinogen gamma chain | FGG | 2 |
| F5H562 | Copper-transporting ATPase 2;WND/140 kDa | ATP7B | 2 |
| B5MCF3 | Protein GUCD1 | GUCD1 | 2 |
| Q96TA1 | Niban-like protein 1 | FAM129B | 2 |
| F5GWT4 | Serine/threonine-protein kinase WNK1 | WNK1 | 2 |
| E9PLT1 | Platelet glycoprotein 4 | CD36 | 2 |
| Q8TDB8 | Solute carrier family 2, facilitated glucose transporter member 14;Solute carrier family 2, facilitated glucose transporter member 3 | SLC2A14;SLC2A3 | 2 |
| B4DDD6 | Drebrin-like protein | DBNL | 2 |
| E9PII3 | Band 4.1-like protein 2 | EPB41L2 | 2 |
| E9PNF5 | Glutamine-dependent NAD(+) synthetase | NADSYN1 | 2 |
| K7ELL7 | Glucosidase 2 subunit beta | PRKCSH | 2 |
| Q9BV20 | Methylthioribose-1-phosphate isomerase | MRI1 | 2 |
| J3KNB4 | Cathelicidin antimicrobial peptide;Antibacterial protein FALL-39;Antibacterial protein LL-37 | CAMP | 2 |
| Q5T1Z0 | Phospholysine phosphohistidine inorganic pyrophosphate phosphatase | LHPP | 2 |
| H3BLV0 | Complement decay-accelerating factor | CD55 | 2 |
| Q9Y3E7 | Charged multivesicular body protein 3 | CHMP3 | 2 |
| Q5T6H7 | Xaa-Pro aminopeptidase 1 | XPNPEP1 | 2 |
| O94779 | Contactin-5 | CNTN5 | 2 |
| E9PNR2 | Ras and Rab interactor 1 | RIN1 | 2 |
| E7ESJ7 | Protein FAM114A2 | FAM114A2 | 2 |
| A0A0A0MS99 | Multidrug resistance-associated protein 1 | ABCC1 | 2 |
| A0A0G2JM15 | Large neutral amino acids transporter small subunit 4 | SLC43A2 | 2 |
| H0YBF7 | Arf-GAP with SH3 domain, ANK repeat and PH domain-containing protein 1;Arf-GAP with SH3 domain, ANK repeat and PH domain-containing protein 2 | ASAP1;ASAP2 | 2 |
| P29992 | Guanine nucleotide-binding protein subunit alpha-11 | GNA11 | 2 |
| F8WF69 | Clathrin light chain A | CLTA | 2 |
| B5MCN0 | Atlastin-2 | ATL2 | 2 |
| F8W9F9 | Serine/threonine-protein kinase WNK2;Serine/threonine-protein kinase WNK3 | WNK2;WNK3 | 2 |
| A2A3F3 | Transient receptor potential cation channel subfamily M member 3 | TRPM3 | 2 |
| Q5KU26 | Collectin-12 | COLEC12 | 2 |
| O14523 | C2 domain-containing protein 2-like | C2CD2L | 2 |
| Q96DG6 | Carboxymethylenebutenolidase homolog | CMBL | 2 |
| Q5THJ4 | Vacuolar protein sorting-associated protein 13D | VPS13D | 2 |
| Q02790 | Peptidyl-prolyl cis-trans isomerase FKBP4;Peptidyl-prolyl cis-trans isomerase FKBP4, N-terminally processed | FKBP4 | 2 |
| A0A0G2JQD | Glutathione S-transferase theta-1 | GSTT1 | 2 |

| | | | |
|---|---|---|---|
| 2 | | | |
| Q9NV96 | Cell cycle control protein 50A;Cell cycle control protein 50B | TMEM30A;TMEM30B | 2 |
| P62330 | ADP-ribosylation factor 6 | ARF6 | 2 |
| Q9UPU5 | Ubiquitin carboxyl-terminal hydrolase 24 | USP24 | 2 |
| B2R4S9 | Histone H2B | HIST1H2BI | 2 |
| P10599 | Thioredoxin | TXN | 2 |
| R4GN98 | Protein S100;Protein S100-A6 | S100A6 | 2 |
| H3BS66 | Small integral membrane protein 1 | SMIM1 | 2 |
| Q8NHG7 | Small VCP/p97-interacting protein | SVIP | 2 |
| C9JIG9 | Serine/threonine-protein kinase OSR1;STE20/SPS1-related proline-alanine-rich protein kinase | OXSR1;STK39 | 2 |
| Q5VZR0 | Golgi-associated plant pathogenesis-related protein 1 | GLIPR2 | 2 |
| F8WD49 | Anion exchange protein 3;Anion exchange protein;Anion exchange protein 2 | SLC4A3;SLC4A2 | 2 |
| P61626 | Lysozyme C;Lysozyme | LYZ | 2 |
| Q5T123 | SH3 domain-binding glutamic acid-rich-like protein 3 | SH3BGRL3 | 2 |
| F5H571 | Ubiquitin carboxyl-terminal hydrolase 5 | USP5 | 2 |
| Q9H3K6 | BolA-like protein 2 | BOLA2;BOLA2B | 2 |
| P05164 | Myeloperoxidase;Myeloperoxidase;89 kDa myeloperoxidase;84 kDa myeloperoxidase;Myeloperoxidase light chain;Myeloperoxidase heavy chain | MPO | 2 |
| P50395 | Rab GDP dissociation inhibitor beta | GDI2 | 2 |
| G3V2U7 | Acylphosphatase;Acylphosphatase-1 | ACYP1 | 2 |
| J3KNB4 | Cathelicidin antimicrobial peptide;Antibacterial protein FALL-39;Antibacterial protein LL-37 | CAMP | 2 |
| H0Y9X3 | Programmed cell death protein 6 | PDCD6 | 2 |
| A6NJA2 | Ubiquitin carboxyl-terminal hydrolase;Ubiquitin carboxyl-terminal hydrolase 14 | USP14 | 2 |
| P35998 | 26S protease regulatory subunit 7 | PSMC2 | 2 |
| P30041 | Peroxiredoxin-6 | PRDX6 | 2 |
| P35612 | Beta-adducin | ADD2 | 2 |
| P00918 | Carbonic anhydrase 2 | CA2 | 2 |
| A0A0C4DGH5 | Cullin-associated NEDD8-dissociated protein 1 | CAND1 | 2 |
| C9JZN1 | Guanine nucleotide-binding protein G(I)/G(S)/G(T) subunit beta-2;Guanine nucleotide-binding protein subunit beta-4 | GNB2;GNB4 | 1 |
| I3L4X8 | Integrin beta;Integrin beta-3 | ITGB3 | 1 |
| H7BZJ3 | | PDIA3 | 1 |
| P17066 | Heat shock 70 kDa protein 6;Putative heat shock 70 kDa protein 7 | HSPA6;HSPA7 | 1 |
| J3KT70 | Arf-GAP with dual PH domain-containing protein 2 | ADAP2;CENTA2 | 1 |
| Q9Y6M5 | Zinc transporter 1 | SLC30A1 | 1 |
| P54725 | UV excision repair protein RAD23 homolog A | RAD23A | 1 |
| F8WD59 | 40S ribosomal protein SA | RPSA;RPSAP58 | 1 |
| P06753 | | | 1 |
| E9PMI6 | Methylosome subunit pICln | CLNS1A | 1 |
| Q9BVK6 | Transmembrane emp24 domain-containing protein 9 | TMED9 | 1 |
| C9JJV6 | Myeloid-associated differentiation marker | MYADM | 1 |
| Q8IXQ3 | Uncharacterized protein C9orf40 | C9orf40 | 1 |
| Q8NDC0 | MAPK-interacting and spindle-stabilizing protein-like | MAPK1IP1L | 1 |
| Q99747 | Gamma-soluble NSF attachment protein | NAPG | 1 |

| | | | |
|---|---|---|---|
| E7EWE1 | Ubiquitin-like modifier-activating enzyme 5 | UBA5 | 1 |
| J3KNE3 | Platelet-activating factor acetylhydrolase IB subunit beta | PAFAH1B2 | 1 |
| Q8IUI8 | Cytokine receptor-like factor 3 | CRLF3 | 1 |
| Q9BTX7 | Alpha-tocopherol transfer protein-like | TTPAL | 1 |
| P63261 | Actin, cytoplasmic 2;Actin, cytoplasmic 2, N-terminally processed | ACTG1 | 1 |
| P31153 | S-adenosylmethionine synthase isoform type-2 | MAT2A | 1 |
| O00560 | Syntenin-1 | SDCBP | 1 |
| Q4VB86 | Protein 4.1 | EPB41 | 1 |
| Q8WUD1 | Ras-related protein Rab-2B | RAB2B;DKFZ p313C1541 | 1 |
| Q9NWV4 | UPF0587 protein C1orf123 | C1orf123 | 1 |
| Q9Y2Z0 | Suppressor of G2 allele of SKP1 homolog | SUGT1 | 1 |
| H0YK48 | Tropomyosin alpha-1 chain | TPM1 | 1 |
| H3BS66 | Small integral membrane protein 1 | SMIM1 | 1 |
| Q5VTS0 | Neurensin-1 | NRSN1 | 1 |
| H0Y904 | Multidrug resistance-associated protein 7 | ABCC10 | 1 |
| P08F94 | Fibrocystin | PKHD1 | 1 |
| G3V5X4 | Nesprin-2 | SYNE2 | 1 |
| P48507 | Glutamate--cysteine ligase regulatory subunit | GCLM | 1 |
| H3BUF4 | Cyclin-D1-binding protein 1 | CCNDBP1 | 1 |
| F8WB30 | Target of Myb protein 1 | TOM1 | 1 |
| E5RJI8 | | CA1 | 1 |
| S4R3E5 | Importin subunit alpha-7 | KPNA6 | 1 |
| E7EVS6 | | ACTB | 1 |
| P04206 | Ig kappa chain V-III region GOL;Ig kappa chain V-III region WOL;Ig kappa chain V-III region Ti;Ig kappa chain V-III region SIE | 1 | |
| Q5SSV3 | N(G),N(G)-dimethylarginine dimethylaminohydrolase 2 | DDAH2 | 1 |
| H0YG54 | Oligoribonuclease, mitochondrial | REXO2 | 1 |
| P08246 | Neutrophil elastase | ELANE | 1 |
| P40926 | Malate dehydrogenase, mitochondrial | MDH2 | 1 |
| P98172 | Ephrin-B1 | EFNB1 | 1 |
| Q96DD7 | Protein shisa-4 | SHISA4 | 1 |
| Q71RC9 | Small integral membrane protein 5 | SMIM5 | 1 |
| P68133 | Actin, alpha skeletal muscle;Actin, alpha cardiac muscle 1;Actin, gamma-enteric smooth muscle;Actin, aortic smooth muscle | ACTA1;ACTC 1;ACTG2;AC TA2 | 1 |
| H0Y9Q6 | Clathrin light chain B | CLTB | 1 |
| G3V5P0 | | KTN1 | 1 |
| Q9NWX6 | Probable tRNA(His) guanylyltransferase | THG1L | 1 |
| Q15404 | Ras suppressor protein 1 | RSU1 | 1 |
| B2R4S9 | Histone H2B | HIST1H2B | 1 |
| K7EK06 | Phenylalanine--tRNA ligase alpha subunit | FARSA | 1 |
| H7C3S9 | COP9 signalosome complex subunit 8 | COPS8 | 1 |
| J3KRV4 | Dual specificity mitogen-activated protein kinase kinase 3 | MAP2K3 | 1 |
| Q15042 | Rab3 GTPase-activating protein catalytic subunit | RAB3GAP1 | 1 |
| P01893 | Putative HLA class I histocompatibility antigen, alpha chain H;HLA class I histocompatibility antigen, Cw-6 alpha chain;HLA class I histocompatibility antigen, B-38 alpha chain;HLA class I histocompatibility antigen, B-67 alpha chain;HLA class I histocompatibility antigen, B-82 alpha chain;HLA class I histocompatibility antigen, B-39 alpha chain;HLA class I | HLA-H;HLA-C;HLA-B | 1 |

| | | | |
|---|---|---|---|
| | histocompatibility antigen, Cw-18 alpha chain;HLA class I histocompatibility antigen, Cw-7 alpha chain;HLA class I histocompatibility antigen, B-42 alpha chain;HLA class I histocompatibility antigen, B-14 alpha chain;HLA class I histocompatibility antigen, B-8 alpha chain;HLA class I histocompatibility antigen, B-7 alpha chain | | |
| Q9UNW1 | Multiple inositol polyphosphate phosphatase 1 | MINPP1 | 1 |
| Q6B0K9 | Hemoglobin subunit mu | HBM | 1 |
| O75915 | PRA1 family protein 3 | ARL6IP5 | 1 |
| O95376 | E3 ubiquitin-protein ligase ARIH2 | ARIH2 | 1 |
| E9PBW4 | Hemoglobin subunit gamma-2 | HBG2 | 1 |
| C9J1X0 | WD repeat-containing protein 91 | WDR91 | 1 |
| Q8NCV1 | | | 1 |
| Q9Y4P8 | WD repeat domain phosphoinositide-interacting protein 2 | WIPI2 | 1 |
| A0A087WUX6 | Proteasomal ubiquitin receptor ADRM1 | ADRM1 | 1 |
| Q9NQS7 | Inner centromere protein | INCENP | 1 |
| P62805 | Histone H4 | HIST1H4A | 1 |
| Q8TDY2 | RB1-inducible coiled-coil protein 1 | RB1CC1 | 1 |
| C9JFM5 | Syntaxin-4 | STX4 | 1 |
| B0QZ43 | Erlin-2;Erlin-1 | ERLIN1;ERLIN2 | 1 |
| C9J8T0 | Selenocysteine-specific elongation factor | EEFSEC | 1 |
| P61224 | Ras-related protein Rap-1b;Ras-related protein Rap-1b-like protein | RAP1B | 1 |
| Q99828 | Calcium and integrin-binding protein 1 | CIB1 | 1 |
| Q53GQ0 | Very-long-chain 3-oxoacyl-CoA reductase | HSD17B12 | 1 |
| H0Y9Q9 | ADP-ribosyl cyclase/cyclic ADP-ribose hydrolase 2 | BST1 | 1 |
| R4GN98 | Protein S100;Protein S100-A6 | S100A6 | 1 |
| Q8TB73 | Protein NDNF | NDNF | 1 |
| Q6P1A2 | Lysophospholipid acyltransferase 5 | LPCAT3 | 1 |
| F2Z2Y4 | Pyridoxal kinase | PDXK | 1 |
| Q9HA65 | TBC1 domain family member 17 | TBC1D17 | 1 |
| G3V126 | V-type proton ATPase subunit H | ATP6V1H | 1 |
| D6RGE2 | Isochorismatase domain-containing protein 1 | ISOC1 | 1 |
| A0A0B4J222 | ADP-ribosylation factor-like protein 15 | ARL15 | 1 |
| F8W7W4 | Androglobin | ADGB | 1 |
| Q9GZR7 | | | 1 |
| A0A087WVC4 | cAMP-dependent protein kinase catalytic subunit beta | PRKACB | 1 |
| A8MU39 | Serine/threonine-protein phosphatase;Serine/threonine-protein phosphatase 5 | PPP5C | 1 |
| G3V1N2 | | HBA2 | 1 |
| P69892 | Hemoglobin subunit gamma-2 | HBG2 | 1 |
| F8WEZ0 | 1-phosphatidylinositol 3-phosphate 5-kinase | PIKFYVE | 1 |
| A0A087WZZ4 | Ammonium transporter Rh type A | RHAG | 1 |
| Q1JUQ3 | Peptidyl-prolyl cis-trans isomerase;Peptidyl-prolyl cis-trans isomerase FKBP1A | FKBP12-Exin;FKBP1A | 1 |
| F8VWZ5 | H2.0-like homeobox protein | HLX | 1 |
| P62877 | E3 ubiquitin-protein ligase RBX1;E3 ubiquitin-protein ligase RBX1, N-terminally processed | RBX1 | 1 |
| Q7Z5P9 | Mucin-19 | MUC19 | 1 |
| F8VPB3 | | TPK1 | 1 |
| F8WBF4 | Transmembrane protein 50B | TMEM50B | 1 |

| | | | |
|---|---|---|---|
| C9JL85 | Myotrophin | MTPN | 1 |
| Q53EQ6 | Tigger transposable element-derived protein 5 | TIGD5 | 1 |
| E3W974 | | DNPEP | 1 |
| H7BYV1 | Interferon-induced transmembrane protein 1;Interferon-induced transmembrane protein 2;Interferon-induced transmembrane protein 3 | IFITM2;IFITM3;IFITM1 | 1 |
| D6RC06 | Histidine triad nucleotide-binding protein 1 | HINT1 | 1 |
| E9PNW4 | CD59 glycoprotein | CD59 | 1 |
| H7C2Z6 | Grancalcin | GCA | 1 |
| Q9H1C7 | Cysteine-rich and transmembrane domain-containing protein 1 | CYSTM1 | 1 |
| H0YK07 | ATP-dependent Clp protease ATP-binding subunit clpX-like, mitochondrial | CLPX | 1 |
| E9PG15 | 14-3-3 protein theta | YWHAQ | 1 |
| K7ENK9 | Vesicle-associated membrane protein 3;Vesicle-associated membrane protein 2 | VAMP2;VAMP3 | 1 |
| F8WDD6 | Cation channel sperm-associated protein subunit gamma | CATSPERG | 1 |
| P35754 | Glutaredoxin-1 | GLRX | 1 |
| Q5THJ4 | Vacuolar protein sorting-associated protein 13D | VPS13D | 1 |
| B4E3H6 | Transforming acidic coiled-coil-containing protein 1 | TACC1 | 1 |
| B0YJC4 | Vimentin | VIM | 1 |
| H7C5R6 | AT-rich interactive domain-containing protein 4B | ARID4B | 1 |
| P49755 | Transmembrane emp24 domain-containing protein 10 | TMED10 | 1 |
| E9PMJ3 | Ribonuclease inhibitor | RNH1 | 1 |
| B1AHA9 | DNA replication licensing factor MCM5 | MCM5 | 1 |
| P23634 | Plasma membrane calcium-transporting ATPase 4 | ATP2B4 | 1 |
| Q14152 | Eukaryotic translation initiation factor 3 subunit A | EIF3A | 1 |
| C9IY70 | 60S ribosomal export protein NMD3 | NMD3 | 1 |
| A0A087WUS7 | Ig delta chain C region | IGHD | 1 |
| P07384 | Calpain-1 catalytic subunit | CAPN1 | 1 |
| G3V2C9 | Guanine nucleotide-binding protein subunit gamma;Guanine nucleotide-binding protein G(I)/G(S)/G(O) subunit gamma-2 | GNG2 | 1 |
| Q9Y2Y8 | Proteoglycan 3 | PRG3 | 1 |
| V9GY70 | | DNAJB12 | 1 |
| U5GXS0 | MAM and LDL-receptor class A domain-containing protein 1 | MALRD1 | 1 |
| Q92625 | Ankyrin repeat and SAM domain-containing protein 1A | ANKS1A | 1 |

**Table S3. Complete list of proteins identified in the EEV proteome**. Lists of the protein groups identified by LC-MS/MS analysis using Andromeda/MaxQuant search engine in the Uniprot Complete Proteome *Homo sapiens* database for the non-depleted sample (356 proteins) (**A**) or when hemoglobin was analyzed separately (818 proteins) (**B**). The lists were filtered at 1% False Discovery Rate using a target/decoy database search.